M-AM-SymI-1

COLICIN E1 AND THE STRUCTURAL PUZZLE OF THE CHANNEL-FORMING TOXINS. ((Cynthia Stauffacher, Patricia Elkins, and William Cramer)) Department of Biological Sciences, Purdue University, West Lafayette, IN 47907.

The colicins are a group of bacterial toxins secreted by *E. coli* which kill rival strains of bacteria by blocking a number of biological pathways. The channel-forming colicins, which kill cells by depolarizing the membrane, consist of three functional domains that are involved in receptor binding, translocation across the outer membrane and channel-formation in the inner membrane. Crystal structures of the channel-forming polypeptide have been solved at 2.5Å resolution for two of the colicins, colicin A (Parker, *et al.*, *Nature* 337:93-96) and E1 (Elkins, *et al.*, in prep). In both cases the channel-forming domains of these toxins consist of a sandwich of ten helices arranged in three layers, with a central hydrophobic hairpin known to be important in the mechanism of insertion into the membrane. The structure puzzle is this - how can soluble proteins such as the colicins translocate the outer membrane and convert into voltage-gated channel proteins? Clues can be derived from a comparison of features of colicin E1 to the known structures for the other colicins. These include an apparent hinge formed by the first two helices of the channel-forming domain and a flexible helix which may change conformation or unwind with the exposure of the hydrophobic helices. Analysis of specific charge distributions and side chain bonding patterns provide the basis for evaluating insertion models. Interesting questions also arise about the nature of the interactions of the three domains brought up by the low resolution intact Ia structure (Ghosh, *et al.*, *Nature Struct. Biol.* 1:597-604), where a number of upstream helices appear to be in contact with the ten helices of the channel-forming domain.

M-AM-SymI-2

STRUCTURE AND FUNCTION OF APLHA-HEMOLYSIN: A HEPTAMERIC TRANSMEMBRANE PORE. ((E. Gouaux)) Univ. of Chicago.

M-AM-SymI-3

THE STRUCTURE OF BOVINE MITOCHONDRIAL F1-ATPASE - AN INSIGHT INTO ATP SYNTHESIS ((J.P. Abrahams, A.G.W. Leslie, R. Lutter, J.E. Walker)). MRC Laboratory of Molecular Biology, Hills Road, Cambridge CB2 2QH, UK

ATP synthase is an oligomeric assembly found in the cytoplasmic membranes of eubacteria, the thylakoid membranes of chloroplasts and the inner membranes of mitochondria, and is responsible for the synthesis of ATP from ADP and Pi using the transmembrane proton electrochemical gradient. There is a high level of sequence homology between the enzymes from these various sources and it is likely that they share a common tertiary structure and catalytic mechanism.

The enzyme from bovine mitochondria is a complex of 16 different polypeptides and is composed of three morphologically distinct components: a membrane bound segment (Fo), a soluble segment (F1) and a connecting stalk. The soluble segment F1 is made up of five different chains with a stoichiometry 3α, 3β, γ, δ, ϵ, and displays ATPase activity. The crystal structure of F1-ATPase has been determined at 2.8Å resolution. The α and β subunits are arranged like the segments of an orange around a central spindle made up of two alpha helices from the γ subunit. The structure is strikingly asymmetric, and the asymmetry is associated with the nucleotide content of the catalytic β subunits and the position of the γ subunit. The structure supports the binding change mechanism of catalysis as proposed by P. Boyer, in which the three catalytic sites alternate cyclically between three different states. Several aspects of the structure suggest the intriguing possibility that the $\alpha 3$-$\beta 3$ assembly rotates relative to the γ subunit during catalysis.

M-AM-SymI-4

CRYSTALLIZATION, STRUCTURE AND POSSIBLE MECHANISMS OF ACTION OF CYTOCHROME *C* OXIDASE (H. Michel, C. Ostermeier und S. Iwata) Max-Planck-Institut für Biophysik, Heinrich-Hoffmann-Straße 7, D-60528 Frankfurt/Main, Germany.

The cytochrome *c* Oxidase from the soil bacterium *Paracoccus denitrificans* could be crystallized with the help of antibody F_v-fragments (*Nature Struct. Biol.* 2, 842-846 (1995)). The subsequent X-ray structure analysis revealed the structure of the four protein subunits, and the position and mode of binding of the prosthetic groups as well as the contacts with the antibody fragment. In addition, two possible pathways for proton transfer, one for these being consumed upon reduction of dioxygen and one for those being pumped across the membrane could be identified (*Nature*, 376, 660-669 (1995)). The absence of electron density in the azide inhibited enzyme for a histidine side chain, which was postulated by site-directed mutagenesis and spectroscopy to be a ligand to Cu_B of the oxygen binding site, was used to propose a histidine shuttle/cycle mechanism for proton pumping. Recent preliminary X-ray crystallographic experiments show that this histidine in the azide-free enzyme is a Cu_B ligand in the oxidized form, but not in the reduced one. This observation is in full agreement with a histidine shuttle mechanism.

K CHANNEL PORE

M-AM-A1

PROBING THE MOLECULAR ARCHITECTURE OF A K^+-CHANNEL PORE. ((Rama Ranganathan, John H. Lewis, Roderick MacKinnon)) Department of Neurobiology, Harvard Medical School, 220 Longwood Ave., Boston, MA 02115.

The structurally well-characterized scorpion toxin Agitoxin 2 (AgTx2) blocks ion permeation through Shaker K^+ channels by direct, high-affinity binding to the external pore region. Alanine-scanning mutagenesis of the putative toxin interaction surface reveals a set of residues critical for making energetic contacts with the channel, and suggests a binding orientation for the toxin molecule. To probe the molecular architecture of the K^+-channel pore, we have used thermodynamic mutant cycle analysis to energetically map channel residues relative to the known toxin structure. This study has resulted in a number of spatial constraints for channel residues within the pore forming P-region; in one stretch, we have been able to map six out of eight contiguous residues to the toxin interaction surface. The analysis of these novel spatial constraints, given the probable four-fold symmetry of the K^+ channel, may allow us to significantly constrain the structure of this central catalytic region. One interaction in particular, that of K27M on the toxin with Y445F on the channel, is unique in that the interaction energy depends on the external K^+ ion concentration. This result suggests that Y445 is at or very near to an ion binding site within the pore. These experiments begin the task of assigning functional meaning to the structural interpretations of our data, and provides a method for studying the process of ion permeation through characterizing toxin-channel interactions.

M-AM-A2

INTERACTIONS OF KALIOTOXIN K27 WITH RESIDUES IN THE PORE OF THE Kv1.3 POTASSIUM CHANNEL. ((J. Aiyar, J.P. Rizzi$^+$, J. Boyd$^+$, G.A. Gutman*, and K.G. Chandy)). Depts. of Physiol. & Biophys., and Microbiol. & Mol. Genet.*, Univ. California, Irvine, CA., and Pfizer Central Research, Groton, CT$^+$.

Kv1.3, a voltage-gated K^+ channel expressed in lymphocytes, is blocked with high affinity by several scorpion toxins, including kaliotoxin (KTX). Lysine-27 (K27) of KTX is critical for toxin block, and its neutralization (by replacement with Ala, Asp or Norleucine) results in a 150-fold reduction in toxin potency. K27 is thought to protrude into the pore, and has been proposed to interact with a negatively charged residue within the pore, possibly D402. In order to study the nature of this interaction and to probe the structure of the pore, we replaced K27 with a series of lysine analogs whose side chains varied in length from 2.5-7.7 Å, compared with 6.3 Å for lysine. Surprisingly, all these analogs resulted in toxins with potencies very close to that of wild-type KTX, arguing against the interaction of K27 with a localized charge associated with D402. Our results could be explained by the presence in the channel pore of a *column* of negative charge formed by the asymmetric disposition of the four D402's in the homotetramer; alternatively, the shorter and longer amine-bearing side chains might be interacting with distinct residues in the channel. In support of the latter hypothesis, the potency of KTX with the shorter analogs (2.5-5.0 Å) was dramatically reduced (>200-fold) when tested on the Kv1.3 H404V mutant, while KTX with the longer side chains (6.3-7.7 Å) showed little change on this target. We are continuing to investigate the nature of these interactions and to estimate distances between H404 and D402.

M-AM-A3

DYNAMIC REARRANGEMENT OF THE OUTER MOUTH OF A K^+ CHANNEL DURING GATING ((Y. Liu, M. E. Jurman and G. Yellen)) Dept. of Neurobiology, Harvard Medical School and Massachusetts General Hospital, Boston, MA 02114

The outer mouth of voltage-gated K^+ channels is intimately involved in C-type inactivation gating[1,2]. To learn more about the conformational change accompanying this transition, we made cysteine substitutions at amino acid positions 448-450 near the outer mouth of the Shaker (H4:Δ6-46) K^+ channel, and modified the mutants with various methanethiosulfonate reagents. Reaction rates at all 3 positions were 100-1000 fold faster in the C-type inactivated state than in the closed and open states of the channel. The cysteine at position 448 can also form inter-subunit disulfide bonds, as seen by the presence of dimers on non-reducing immunoblots. Dimerization results in non-functional channels and does not depend on the presence of other cysteines in the membrane-spanning region of the protein. Dimers form spontaneously upon channel expression, but function can be restored by reducing the disulfide bond with DTT. Re-oxidation of M448C by Cu^{2+}-phenanthroline (2 μM) is also state-dependent, occurring 70 fold faster in the C-type inactivated state than in the closed state.

These observations support the idea that, during C-type inactivation, the side chains of 448, 449 and 450 residues become more exposed to the aqueous solution and (at least in the case of the 448 residue), come closer together. Despite these substantial changes that occur during C-type inactivation, this conformational rearrangement may be fairly local: the scorpion toxin agitoxin-2, whose binding is quite sensitive to the identity of individual amino acids at the positions we study[3], binds almost equally rapidly to the inactivated and closed states of wild type or T449C channels.

(1) K.L.Choi *et al.*, PNAS 88:5092, 1991. (2) G.Yellen *et al.*, Biophys.J. 66:1068, 1994. (3) A.Gross and R. MacKinnon, *personal communication.* Supported by NIH grants NS29693 and NS09774.

M-AM-A4

EXPLORING THE PORE OF A K^+ CHANNEL WITH THIOL-SPECIFIC REAGENTS OF DIFFERENT SIZE AND CHARGE. ((R.H. Joho, Y. Liu and L.L. Kürz)) Department of Cell Biology and Neuroscience, The University of Texas Southwestern Medical Center, Dallas, Texas 75235.

Using cysteine-scanning mutagenesis or interaction-analysis of mutated channels and toxins (Kürz et al. 1994 & 1995; Lü & Miller 1995; Pascual el al. 1995; Hidalgo & MacKinnon 1995), work in several laboratories led to a picture of the K^+ channel pore inconsistent with models based on theoretical considerations which predicted an eight-stranded β barrel. In our previous work, we proposed that proline 361 and isoleucine 379, both in the S5-S6 linker region of Kv2.1, line the outer entryway to the narrow part of the pore and are relatively close to the central axis of the ion conduction pathway (Kürz et al. 1994 & 1995). Recently, two groups reported that proline 430 in the Shaker K^+ channel, equivalent to proline 361 in Kv2.1, is located at a distance from the central axis in the outer vestibule not near the beginning of the narrow entryway to the deep pore (Hidalgo & MacKinnon 1995; Lü & Miller 1995). These findings for Shaker channel do not agree with our original proposal for Kv2.1. The discrepancy may reflect structural differences between closely related voltage-gated K^+ channels like Kv2.1 and Shaker, or it may point out the inherent difficulties of interpreting functional data in a structural model, as long as the real three-dimensional structure is unknown. We probed the Kv2.1 mutants P361C and I379C with a series of thiol-specific reagents that differ in size and charge: MTSET, MTSEA, MTSES, Zn^{2+}, Cd^{2+}, Hg^{2+}, and Ag^+. For all reagents used, both mutants behaved identically. If similar reactivities resulted from a common microenvironment, then these findings are best understood in light of our original model where both P361 and I379 in Kv2.1 mark the beginning of the narrow part of the ion conduction pathway. (Supported by grants from the NIH and MDA to RHJ).

M-AM-A5

INTERACTION BETWEEN THE PORE OF A K^+ CHANNEL AND RESIDUES IN S6 REVEALED BY *IN SITU* OXIDATION OF AN ENGINEERED CYSTEINE. ((H.-J. Zhang, Y. Liu, R.D. Zühlke, and R.H. Joho)) Department of Cell Biology and Neuroscience, The University of Texas Southwestern Medical Center, Dallas, Texas 75235.

A major part of the ion conduction pathway of voltage-gated potassium (K^+) channels is formed by the linker region between S5 and S6. We showed previously that an invariant cysteine in S6 (C393) of the K^+ channel Kv2.1 is involved in gating and ion permeation (Zühlke, Zhang & Joho; *Receptors & Channels* 2:237-248 [1994]). The chemical nature not the side-chain volume governs the rate constants of deactivation and inactivation; in contrast, side chain volume influences the Rb^+/K^+ conductance ratio. We postulated that the side chain at position 393 is in a region of tight protein packing, is involved in conformational changes during open-closed-state transitions, and also contributes to the control of ion permeation. Here, we report the use of cysteine-scanning mutagenesis followed by *in situ* oxidation to determine the physical proximity of the S6 region to the pore. We demonstrate that I379, a residue near the outer end of the ion conduction pathway, is within the sphere of influence of C394, which is adjacent to the residue involved in channel gating and ion permeation. Patch-clamp recordings after *in situ* oxidation of mutant I379C indicate that NxPo not unit conductance is affected. This implies that the channel becomes locked in a closed state, presumably by preventing conformational transitions for opening after formation of a disulfide bridge. (Supported by grants from the NIH and MDA [RHJ], and the American Heart Association Texas-Affiliate [HJZ].)

M-AM-A6

THE DWELL TIME OF THE LAST ION IN THE MULTI-ION PORE OF A K^+ CHANNEL ((Thomas Baukrowitz and Gary Yellen)) Dept. of Neurobiology, Harvard Med. Sch. and Mass. General Hospital, Boston, MA 02114

We studied the effect of quaternary ammonium blockers on the C-type inactivation process in Shaker K^+ channels (using the Δ6-46 mutation to remove N-type inactivation). These blockers applied from the intracellular side greatly accelerate the rate of C-type inactivation (a process that principally involves the external mouth of the channel). By blocking the outward flow of K^+ ions, they deplete a specific ion site in the channel pore that controls C-type inactivation. Blockers with a short dwell time are relatively ineffective, apparently because they do not block K^+ flux long enough to allow the ion site to empty. This effect titrates with blocker dwell time, with a half maximal effect at 150 μs. We propose that this characteristic dwell time reflects the average dissociation time of a K^+ ion from the control site in the blocked channel. This dwell time is surprisingly long compared to the average dwell time of a K^+ ion during active permeation, about 0.1 μs. The difference can be explained by a multi-ion permeation mechanism. During permeation, the channel fluctuates between high and low occupancy states, but is rarely empty; the electrostatic repulsion between multiple ions in the pore causes fast ion dissociation. When the channel is blocked, the channel empties but the last ion remains for a relatively long time, because it no longer experiences repulsion. Supported by NIH grant NS29693 (G.Y.) and by a stipend from the Gottlieb Daimler - Karl Benz foundation (T.B.).

M-AM-A7

THE INTERNAL MOUTH OF THE *SHAKER* K^+ CHANNEL EXAMINED THROUGH CYSTEINE MUTAGENESIS AND CHEMICAL MODIFICATION ((M. Holmgren, M. E. Jurman and G. Yellen)) MGH, Boston MA 02114.

The intracellular segment of the *Shaker* K^+ channel lying between transmembrane domains S4 and S5 has been proposed to form at least part of the receptor for the tethered inactivation "ball" (Isacoff *et al.*, Nature 353:86, 1991) . We have introduced (one at a time) 15 cysteines in this region using a background channel lacking the N-type inactivation process. We have studied the biophysical properties of the channel, and the block by the "ball" peptide before and after chemical modification by thiosulfonate derivatives. Chemical modification of position 391 alters specifically the kinetics of "ball" peptide binding without altering other biophysical properties of the channel. Results with chemical reagents that add moieties of different charges and sizes suggest both electrostatic and steric interactions between the site of modification and the "ball" peptide. At 6 of the other positions studied, chemical modification by trimethylammonium ethyl methanethiosulfonate (MTSET) resulted in a substantial current reduction (> 80%). These residues, G381-L382, T388-L389, and E395-L396 describe a characteristic heptad pattern coincident with the leucine zipper motif recognized by McCormack *et al.* (Nature 340:103, 1989). In all residues in which we could measure modification, it occurred 2 to 5 times faster in the open and/or C-inactivated states than in the closed state, with apparent second order reaction rates between ~200 and ~20000 $M^{-1}s^{-1}$. Supported by a NIH grant NS29693 (GY) and a MDA postdoctoral fellowship (MH).

M-AM-A8

VOLTAGE-DEPENDENT Ba^{2+} BLOCK OF APAMIN-SENSITIVE Ca^{2+}-ACTIVATED POTASSIUM CHANNELS IN JURKAT T CELLS. ((S. Grissmer and C. Hanselmann)). Department of Applied Physiology, University of Ulm, 89081 Ulm, Germany. (Spon. by R. J. Mather)

The human leukemic T cell line Jurkat expresses K^+ channels (K_{Ca}) that are activated by an increase in the intracellular Ca^{2+} concentration. The majority of these channels are activated independent of the applied membrane potential and are highly sensitive to block by apamin (Grissmer *et al., J. Gen. Physiol.* 99:63, 1992), a peptide component of bee venom. Here we report the blocking effect of divalent cations on this type of K_{Ca} channel. Activation of the channels was achieved by dialyzing the cytoplasm during whole-cell recording with pipette solutions containing 1 or 10 μM free Ca^{2+}. Five minutes after the transition from the cell-attached to the whole-cell recording mode, sufficiently long enough to get maximal and stable activation, current was recorded in response to voltage ramps from -160 to 40 mV within 400 ms every 10 s. With a bath solution containing 160 mM K^+, current through those K_{Ca} channels exhibit an almost linear current-voltage relationship at potentials between -150 to -50 mV with an extrapolated reversal potential ~0 mV. Addition of 0.1, 1, and 10 mM Ba^{2+} to the bath solution resulted in a voltage-dependent current reduction, the block of Ba^{2+} being strongest at more negative potentials with $V_{1/2}$, the voltage where half the channels are being blocked, of -160 ± 10 mV (mean ± SD, n = 2), -90 ± 25 mV (n = 3), and -35 ± 6 mV (n = 3), respectively. The steepness, k ,of the voltage-dependence of the Ba^{2+} block (millivolts per *e*-fold change) was independent of the Ba^{2+} concentration and estimated using a fit of the data to a Boltzmann equation to be 20 ± 1 mV (n = 8). Ba^{2+} block of Jurkat K_{Ca} channels is therefore as steep as expected from the movement of a single divalent cation about half way into the electric field of the membrane (δ = 0.62 ± 0.04, n = 8). Mg^{2+} and Ca^{2+} did not show any significant block at concentrations up to 10 mM at the potentials tested. 10 mM Sr^{2+}, however, was able to reduce the current through K_{Ca} channels in Jurkat cells similar to the block by Ba^{2+}. From the similarity in the steepness of the Ba^{2+} and Sr^{2+} block we conclude that both, Ba^{2+} and Sr^{2+}, can reach the same blocking site within this channel, while Mg^{2+} and Ca^{2+} are unable to reach the site. (Supported by a grant from Pfizer Inc, CT)

M-AM-A9

STRUCTURAL MODELS OF THE S5-P-S6 PORTION OF THE *SHAKER* K^+ CHANNEL. ((H. Robert Guy and Stewart.R. Durell)) Lab. of Mathematical Biology, DCBDC, NCI, NIH, Bethesda, MD 20892.

We have recently modified our models of *Shaker* channel pores to make them more consistent with results of mutagenesis experiments and to include the S5 and S6 segments. The first part of P, P1, is postulated to be an α helix (A432- T441). The lining of the narrow portion of the pore is formed by the segment TVGYGD and carbonyl oxygens from T442, V443, and G444 form K^+ binding sites in the pore. A β turn is formed by the GDMT segment. Additional α helices are formed by S5 (E395-A419), L5-P (S424-S428), LP-6 (P450-W454) and S6 (I457-A471). The inner part of the pore is formed primarily by S6. Relationships between our 96 model and the following types of data will be discussed: multiple occupancy of the pore by K^+ ions, locations of TEA and 4-aminopyridine binding sites, interactions between K^+ channels and scorpion toxins, and results of cysteine mutagenesis on the P segment.

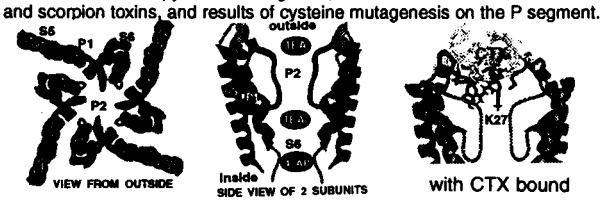

Ca2+ CHANNELS AND Ca2+ RELEASE

M-AM-B1

IP3 TRANSIENTS IN NORMAL AND DYSTROPHIC SKELETAL MUSCLE CELLS ARE ASSOCIATED TO MEMBRANE POTENTIAL, MUSCARINIC RECEPTORS AND SLOW CALCIUM WAVES. (E. Jaimovich, R.Reyes, J.L.Liberona, R. Caviedes, M. Pinçon-Raymond and J.A. Powell.) Dept. Fisiología y Biofísica, Fac. de Medicina, Universidad de Chile, casilla 70005, Santiago, Chile; Centro de Estudios Científicos de Santiago; INSERM, Paris and Smith College, Massachussets.

We have reported the presence of both IP3 receptors and slow calcium waves in cultured rat myotubes; suggesting a role for IP3 in the regulation of intracellular calcium. We measured the mass of IP3 using a radioreceptor assay in various cell lines including rat myotubes, human normal (RCMH) and Duchenne muscular dystrophy (RCDMD), mice normal (CB319), dysgenic mdg (DA322) and dystrophic mdx (XLT-4). Basal IP3 ranged between 10 and 60 pmol/mg prot. in all but dystrophic cells, where levels were 2-3 fold higher than their normal counterpart; more IP3 receptors were also evident (5 vs 1 pmol/mg prot. in XLT-4 vs CB319). Potassium depolarization induced a transient 2-3 fold rise in the mass of IP3 in all but mdg cells; this rise is independent of extracellular calcium and can be seen in calcium depleted cells. The time course of the IP3 signal parallels slow calcium waves in rat myotubes and slow calcium transients in cell lines. Muscarinic agonists induced both an increase in IP3 and a slow calcium rise in rat myotubes; binding of ^{3}H-QNB (40 fmol/mg prot., Kd=.7 nM) supports the presence of muscarinic receptors in these cells.

The level of IP3 in cultured muscle cells appears to be regulated both by membrane potential, trough the α-1 subunit of the DHP receptor, and by muscarinic ACh receptors; regulation seems somehow altered in dystrophic cells. The causal relationship between IP3 signals and calcium transients remains to be studied.

Funded by MDA, FONDECYT 1931089 and DTI B-3390.

M-AM-B2

ACTIVATION OF CARDIAC RYANODINE RECEPTORS BY FAST AND SLOW Ca^{2+} STIMULI. MODULATION BY Mg^{2+} AND ATP. ((Andrew J. Lokuta and Hector H. Valdivia)) Department of Physiology, University of Wisconsin Medical School, Madison, WI 53706. (Sponsored by M. Kirby).

The steady-state activity of single cardiac ryanodine receptors (RyR) reconstituted in lipid bilayers is a monotonic function of increasing $[Ca^{2+}]$ *if the rate of* Ca^{2+} *application is slow* (≥ 0.25 μM s^{-1}). However, a fast increment of cytosolic Ca^{2+} evokes a transient burst of channel activity well above the steady-state level (Valdivia, et al. *Science* 267:1997, 1995). This confirms that the *rate* of Ca^{2+} application ($d[Ca^{2+}]/dt$) is critical to control both the RyR response to Ca^{2+} and SR Ca^{2+} release during CICR (Fabiato, *J. Gen. Physiol.* 85:247, 1985). Mg^{2+} and ATP are important modulators of the steady-state activity of RyR but their effect on the *transient* RyR response to fast Ca^{2+} stimuli has not been determined. We used NP-EGTA, a caged Ca^{2+} with low affinity for Mg^{2+} (Ellis-Davies and Kaplan, *PNAS* 91:187, 1994) to apply "Ca^{2+} ramps" (slow increases in cytosolic $[Ca^{2+}]$) and "Ca^{2+} steps" (essentially instantaneous $[Ca^{2+}]$ increases) and determined the effects of Mg^{2+} and ATP on the transient and steady response of RyR to Ca^{2+}. In the absence of Mg^{2+} and ATP, a Ca^{2+} step from 0.1 to 10 μM increased P_o from <0.01 to ~1.0. However, P_o spontaneously decayed to a steady ~0.5 even though the Ca^{2+} stimulus was sustained. Mg^{2+} inhibited both the transient and the steady component of RyR activity with a half-maximal effective concentration (ED_{50}) = 0.1 mM and ~1 mM, respectively. ATP antagonized the effect of Mg^{2+} and shifted ED_{50}'s to 0.3 and 10 mM, respectively. The ED_{50} for Mg^{2+}-inhibition of $[^3H]$ryanodine binding was similar to that for the steady component of RyR activity but was ~10-fold higher than that for the transient component. The results will be discussed in the context of a model that considers two different Ca^{2+} binding sites with different sensitivity to Mg^{2+}. Supported by AHA and NIH.

M-AM-B3

PEPTIDE PROBE OF RYANODINE RECEPTOR FUNCTION. Imperatoxin A is a selective activator of skeletal-type ryanodine receptor isoforms. ((Carolina Arévalo, Andrew J. Lokuta and Hector H. Valdivia)) Department of Physiology, University of Wisconsin, Madison, WI 53706.

We used $[^3H]$ryanodine binding experiments and single channel recordings to provide convergent descriptions of the effect of Imperatoxin A ($IpTx_a$), a ~5 KDa peptide from the venom of the scorpion *Pandinus imperator* (Valdivia, et al, *Proc. Ntl. Acad. Sc. U.S.A.* **89**:12185, 1992) on Ca^{2+} release channels/ryanodine receptors (RyR) of sarcoplasmic reticulum (SR). At nanomolar concentrations, $IpTx_a$ increased the binding of $[^3H]$ryanodine to skeletal SR and, to a lesser extent, to cerebellum microsomes. The activating effect of $IpTx_a$ on skeletal SR was Ca^{2+}-dependent, synergized by caffeine, and independent of other modulators of RyRs. However, $IpTx_a$ had negligible effects on tissues where the expression of skeletal-type RyR isoforms (RyR1) is small or altogether absent, i.e. cardiac, cerebrum and liver microsomes. Thus, $IpTx_a$ may be used as a ligand capable of discriminating between RyR isoforms with nanomolar affinity. $IpTx_a$ increased the open probability (P_o) of rabbit skeletal muscle RyRs by increasing the frequency of open events and decreasing the duration of the closed lifetimes. This activating effect was dose-dependent (ED_{50} = 10 nM), had a fast onset, and was fully reversible. Purified RyR from CHAPS-solubilized skeletal SR displayed high affinity for $[^3H]$ryanodine with a K_D of 6.1 nM and B_{max} of ~30 pmols/mg protein. $IpTx_a$ increased $[^3H]$ryanodine binding noncompetitively by increasing B_{max} to ~60 pmols/mg protein. These results suggested the presence of an $IpTx_a$-binding site on the RyR or a closely associated regulatory protein. This site appears to be distinct from the caffeine- and the adenine nucleotide-regulatory sites. $IpTx_a$ may prove a useful tool to identify regulatory domains critical for channel gating and to dissect the contribution of skeletal-type RyRs to intracellular Ca^{2+} waveforms generated by stimulation of different RyR isoforms. Supported by AHA and NIH.

M-AM-B4

REGULATION OF INTRACELLULAR CALCIUM RELEASE CHANNEL EXPRESSION DURING MURINE EMBRYOGENESIS. ((M.C. Moschella, E. Ondriasova, K. Ondrias and A.R. Marks)). Department of Medicine, Mount Sinai School of Medicine, New York, NY, 10029

Inositol 1,4,5-trisphosphate (IP3R) and ryanodine receptors (RyR) comprise a family of calcium (Ca^{2+}) release channels located on the endo- and sarcoplasmic reticuli. These channels control intracellular Ca^{2+} release that has been linked to cell growth and differentiation. IP3R1, RyR1 (skeletal) and RyR2 (cardiac) mRNA expression was examined using *in situ* hybridization at the following murine embryonic stages: E5.5, E6.5, E7.5, E8.5, E9.5, E10.5, E11.5, E14.5 and E16.5. IP3R1 mRNA was observed at all stages. At E5.5 IP3R1 mRNA was present in the inner cell mass, at E6.5 and E7.5 highest levels of IP3R1 mRNA were in the mesoderm of the primitive streak. At E8.5, E9.5 and E10.5 IP3R1 mRNA was in the mesenchyme, dermatome, sclerotome, neural tube and heart. RyR2 mRNA was first detected at E8.5 in the heart and at E9.5 in the myotome. RyR1 mRNA was first detected at E9.5 and only in the myotome. At later stages (E10.5-E16.5) highest mRNA level were detected as follows: 1) IP3R1 in brain (cerebellum) and olfactory tissues; 2) RyR1 in skeletal muscle; and 3) RyR2 in cardiac muscle. To correlate gene expression with function, intracellular Ca^{2+} release was examined in fluo-3 loaded embryos. IP3 induced intracellular Ca^{2+} release in embryonic tissues at all stages examined. Caffeine induced Ca^{2+} release (via RyR) was not detected until E9.5 in the heart, and at later stages in skeletal muscle. These data suggest that IP3 mediated intracellular Ca^{2+} release may dominate during early embryogenesis and that RyR channels become more important as cell differentiation leads to organogenesis.

M-AM-B5

EXPRESSED RYANODINE RECEPTOR (RYR) CAN SUBSTITUTE FOR THE INOSITOL 1,4,5-TRISPHOSPHATE RECEPTOR (IP3R) IN *XENOPUS LAEVIS* OOCYTES DURING PROGESTERONE INDUCED MATURATION.

((E. Kobrinsky, K. Ondrias and A.R. Marks)) Mount Sinai School of Medicine, New York, NY 10029.

Xenopus laevis oocytes do not express an RyR and intracellular calcium release is regulated via the IP3R. Although the role of intracellular calcium release during oocyte fertilization is well accepted, measurements of cytosolic calcium levels during oocyte maturation have yielded conflicting results. Thus, a role for calcium during oocyte maturation has not been established. We examined the role of intracellular calcium release channels during oocyte maturation and the effect of replacing the IP3R with the skeletal muscle form of RyR (RyR1). IP3R expression was inhibited in *Xenopus laevis* oocytes using antisense oligonucleotides. IP3R deficient oocytes demonstrated a marked delay (3.7±0.6 hr, n=6, p<0.01) in the time required for progesterone induced maturation. Recombinant RyR1 was expressed in IP3R deficient oocytes by injecting in vitro transcribed RyR1 mRNA. IP3R deficient *Xenopus laevis* oocytes that expressed RyR1 were able to undergo progesterone induced maturation with a time course comparable to that of wild type oocytes when caffeine (10 mM) was used to activate RyR1 mediated intracellular calcium release (n=3). These studies show that intracellular calcium release channels may be important for controlling the rate of progesterone induced maturation and that RyR1 can substitute for the IP3R as the intracellular calcium release channel required for *Xenopus* oocyte maturation.

M-AM-B6

VOLTAGE-DEPENDENT RECTIFICATION OF THE RECOMBINANT RABBIT SKELETAL MUSCLE RYANODINE RECEPTOR EXPRESSED IN HEK293 CELLS

((John P. Imredy, Wayne Chen, Lin Zhang, Claire Bartlett, and David H. MacLennan)) Charles H. Best Institute, University of Toronto, Toronto, Ontario, Canada M5G1L6

Recent studies have shown that the native rabbit skeletal muscle ryanodine receptor may display inward (lumenal to cytoplasmic) rectification (1,2). In our characterization of the recombinant skeletal muscle ryanodine receptor expressed in the human embryonal kidney cell line HEK293 from the full length cDNA clone we observe a similar rectification of the channel. In order to characterize the voltage- and/or current-dependence of this rectification, we apply a series of voltage steps across a PE:PS (5:3) bilayer harboring a single purified and reconstituted recombinant receptor. In the presence of only background Ca^{2+} (no EGTA, ATP,or Mg^{2+}), with symmetrical 250 mM K^+ serving as charge carrier, receptor deactivation is voltage-dependent and occurs with time constants on the order of seconds (Po below, V = -40 mV) (V = Vlumen-Vcytoplasm). The channel deactivates more rapidly with increasingly negative potentials. Recovery from deactivation, or reactivation, is accelerated with more positive potentials (Po below, V= -10mV vs. +10 mV). The rate of deactivation remains insensitive to the magnitude of current flow as the kinetics of deactivation do not change when 250 mM K is replaced by 125 mM K on the lumenal side.

(1. Chen, S.R.W. et al. PNAS 91:11953-11957; 2. Ma, J. Biophy.J. 68:893-899).

Supported by MRC and Heart and Stroke Foundation of Canada .

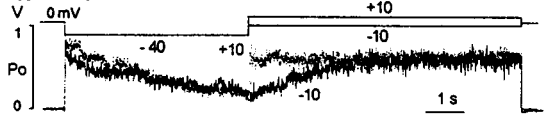

M-AM-B7

DIFFERENTIAL DISTRIBUTION OF RYANODINE RECEPTOR TYPE 3 (RYR3) GENE PRODUCT IN MAMMALIAN SKELETAL MUSCLES

((Antonio Conti[1] and Vincenzo Sorrentino[1,2]))[1]DIBIT, San Raffaele Scientific Institute, via Olgettina 58, 20132 Milano, and [2]Institute of Histology, University of Siena, Italy. (Spon. by M. Mazzanti).

Activation of intracellular calcium release channels/ryanodine receptors (RyRs) is a fundamental step in the regulation of muscle contraction. In mammalian skeletal muscle the skeletal isoform of RyR (RyR1) opens to release calcium from the sarcoplasmic reticulum upon stimulation by the voltage-activated dihydropyridine receptor (DHPR) on the T-tubule/plasmamembrane. Whether the DHPRs activate all RyRs in one step, or whether a calcium-induced calcium release mechanism participates in activating some of the RyRs of skeletal muscle fiber is a debated issue. Western blot analysis of fractions of sarcoplasmic reticulum revealed that in the terminal cisternae of mammalian skeletal muscle, in addition to RyR1, another calcium release isoform, RyR3, is present. At variance with the even distribution of the RyR1, the RyR3 content is sensibly higher in some muscles than in others. Differential utilisation of the RyR3 isoform in skeletal muscle may be relevant to modulate calcium release with respect to specific muscle contraction properties.

M-AM-B8

POSSIBLE ROLE OF DHP RECEPTOR β_1 SUBUNIT IN EXCITATION-CONTRACTION COUPLING.

((C. Strube, R.G. Gregg*, P.A. Powers*, R. Coronado)) Department of Physiology and *Waisman Center, University of Wisconsin, Madison, WI 53706, USA.

The dihydropyridine receptor complex (α_1, β_1, α_2/δ, γ) is responsible for L-type calcium current (I_{Ca}) and is involved in excitation-contraction coupling. We used skeletal muscle cells from mice carrying a null mutation in the β_1 gene (cchb1) to study the role of the β_1 subunit in both processes. Skeletal muscles from cchb1$^-$ homozygotes are excitation-contraction uncoupled despite the presence of normal action potentials. In mutant myotubes, I_{Ca} is reduced ~10-fold and the I_{Ca}-V curve is shifted ~5 mV towards positive potentials. Nifedipine sensitive charge movement (Q_{ns}) is reduced ~2.5 fold and the Q_{ns}-V curve is shifted ~10 mV towards negatives potentials. The shift between the Q_{ns}-V and G_{Ba}-V curves was much more prominent in mutants (20 mV) than in normal cells (2.3 mV). These results show that in skeletal muscle the β_1 subunit is essential for a correct expression of I_{Ca} and charge movement. β_1 could be directly implicated in excitation-contraction coupling or could modulate α_1 subunit.

(Supported by NSF, NIH, MDA and Philippe Foundation).

SUPRAMOLECULAR SYSTEMS: CHAPERONINS AND CYTOSKELETAL PROTEINS

M-AM-C1

NESTED ALLOSTERY AND SUBSTRATE INHIBITION IN ASPARTATE TRANSCARBAMYLASE (ATCase) AND THE GroEL CHAPERONIN

((Vince J. LiCata and Norma M. Allewell)) Department of Biochemistry, University of Minnesota, St. Paul, MN 55108

Both ATCase and GroEL exhibit strong substrate inhibition: the reduction of enzyme activity at high substrate concentrations. Substrate inhibition of ATPase activity in GroEL was recently discovered and a nested allosteric model was proposed to explain the effect (Yifrach & Horovitz (1995) *Biochemistry 34*: 5303). The GroEL oligomer consists of 14 subunits, each of which binds ATP, arranged as two stacked seven-membered rings. Yifrach and Horovitz show that ATPase activity data are fit by a model incorporating concerted positive cooperativity of ATP binding to the seven monomers within each ring, combined with sequential negative cooperativity between the two rings.

Substrate inhibition of ATCase by aspartate has been recognized for decades, but never analyzed. We recently began using a Michaelis-Menten based rate equation which incorporates a Hill coefficient into partial uncompetitive substrate inhibition to analyze the enzyme kinetics of ATCase. This equation fits the data and returns physically meaningful values for all parameters. However, the catalytic subunits within the ATCase holoenzyme are arranged as two stacked three-membered rings: suggesting that the nested allosteric model might also apply in this system.

We find that both the steady-state rate equation and the nested allosteric model fit the data for both ATCase and GroEL. Several statistical indicators show that the fit to the steady-state rate equation is slightly better for both systems. Moreover, the isolated catalytic trimers of ATCase exhibit substrate inhibition which can be fit with the nested allosteric model. This is not a physically realistic model for the catalytic trimers, however, suggesting that the nested allosteric model may merely fit the curve shapes generated by substrate inhibition, and pointing out the need to test the nested allosteric model experimentally for both GroEL and the ATCase holoenzyme. This work was supported by NIH grant DK-17335.

M-AM-C2

THE MOLECULAR CHAPERONE HSC70 BLOCKS AGGREGATION OF BOTH WILD-TYPE AND A CYSTIC FIBROSIS CAUSING MUTANT FORM OF A NUCLEOTIDE-BINDING DOMAIN OF CFTR.

((E.H. Strickland, B.-H. Qu and P.J. Thomas)) Graduate Program in Molecular Biophysics and Department of Physiology, The University of Texas Southwestern Medical Center at Dallas, Dallas, TX 75235-9040. (Spon. by E.J. Goldsmith)

Molecular chaperones assist in protein folding, presumably by protecting the nascent polypeptide chain from inappropriate interactions which might lead the not yet completely folded protein off the folding pathway. Previously our laboratory has shown that the most prevelant disease causing mutation of the cystic fibrosis transmembrane conductance regulator (CFTR), deletion of a phenylalanine (ΔF508) in the amino terminal nucleotide-binding domain (NBD1), is a temperature-sensitive folding mutant, and thus, alters the folding pathway. In this study we investigate possible interactions between CFTR and the molecular chaperone Hsc70. Wild-type and ΔF NBD1 were expressed with a recombinant *E. coli* expression system and purified from inclusion bodies. The recombinant proteins can be refolded with high yield *in vitro*; however, under conditions of temperature and concentration that favor intermolecular interactions the folding yield is low, and NBD1 aggregates are formed as indicated by light scattering. The ΔF508 mutation increases the rate of formation of these off-pathway species. Significantly, substoichiometric amounts of Hsc70 inhibit off-pathway aggregation of both NBD1 and NBD1-ΔF *in vitro*, causing the mutant to closely resemble the wild type. The observation that steps off the folding pathway are blocked by Hsc70 *in vitro* provides valuable insight into both the mechanisms of chaperone action and possible therapies for cystic fibrosis.

M-AM-C3

BIOPHYSICAL PROPERTIES OF REFINED ALPHA CRYSTALLIN MODELS. ((K. Singh[1], T. F. Kumosinski[2], B. Groth-Vasselli[1] and P. Farnsworth[1,3])) [1]Ophthalmology and [3]Physiology, UMD-NJ Med. Sch., Newark, NJ 07103, [2]USDA-ARS, Philadelphia PA 19118.

Our previously reported 3D models for α-crystallin subunits, αA and αB, have been refined to accommodate recent experimental and theoretical observations. These models are elongate, amphipathic and contain about 18-20% α-helix, 20-24% β-structure and 55-60% turns and coils. The 2° structure distribution of the models is in agreement with our previously reported FTIR data and our far UV-CD spectra evaluated by two algorithms (K2D and SELCON). The relative orientation of sidechains was dictated by the PHD secondary structure prediction method. The C-terminal domain refinement is in accord with the experimental observations that ATP binds α-crystallin and a recent hypothesis that ATP binding proteins possess a "catalytic triad". This consists of Lys, Asp and Asp/Glu spaced ~22-25 residue apart and are located in a structural motif containing four β-sheets and one α-helix. Our models match well with the experimental data on α-crystallin electrostatic properties, such as, dipole moment, net charge and electrostatic potential. Orientation of dipole moment favors the formation of our predicted "open" micellar quaternary structure. Also the maximum value of the net charge (~48) on the aggregate of ~800 kDa, at physiological ionic strength supports the credibility of our models. The chaperone activity of α-crystallin can also be explained by these models at molecular level. Supported by UMDNJ foundation and Lions Eye Research Foundation of New Jersey.

M-AM-C4

THYMOSIN β_4 CROSSLINKS TO THE BARBED END OF THE ACTIN MONOMER. ((D. Safer and M. Elzinga*)) Dept. of Cell and Developmental Biology, University of Pennsylvania, Phila, PA 19104-6058, and *Dept. of Pharmacology, Institute for Basic Research in Developmental Disabilities, Staten Island, NY 10314-6399.

To identify inter-residue contacts between actin and thymosin β_4, the product from zero-length crosslinking was cleaved with trypsin after reversible blocking of lysine residues, and the digest was fractionated by gel filtration and reverse-phase HPLC. Crosslinked peptides were identified by immunoblotting with anti-Tβ_4 and by mass spectroscopy. A peptide of mass 7262 gave a single amino acid sequence, corresponding to actin residues 148-169, a region on the barbed end of the actin monomer on subdomain 3. Possible sites of crosslinking within this sequence are D154, D157, and E167. No Tβ_4 sequence was observed because its N-terminus is blocked, but the observed mass and amino acid analysis are in good agreement with the calculated mass (7253) and composition of actin residues 148-169 plus Tβ_4. The crosslink is located at an inter-monomer contact, indicating that Tβ_4 sterically blocks actin polymerization. Preliminary data on other crosslinked peptides suggest another site of crosslinking near the N-terminus of actin. (Supported by NIH Grant AR40840 and the New York State OMRDD)

M-AM-C5

APPARENT HYDROLYSIS OF GTP AT TUBULIN'S N-SITE. ((Rick B. Dye, Susan Pedigo and Robley C. Williams, Jr.)) Dept. of Molecular Biology, Vanderbilt Univ., Nashville, TN 37235. (Spon. Paula F. Flicker)

When microtubules (MT) are assembled from tubulin (Tb) with 2 molecules of bound GTP per dimer, one, at the exchangeable site (E-site), is hydrolyzed to GDP. The other remains GTP, bound to the nonexchangeable site (N-site) on the alpha-chain. To explore the behavior of Tb with its E-site otherwise occupied, Tb was treated with immobilized alkaline phosphatase (AP) in the presence of GMP-PCP. HPLC showed that this Tb bore, on average, 0.99 (±0.17) GTP and <0.01 GDP per dimer (n = 15), confirming quantitative removal of GTP from the E-site. When 100 μM taxol was added at 37°, about 75% of this tubulin assembled into microtubules. (Structure confirmed by electron microscopy.) Analysis of the nucleotides extracted from the pelleted MTs yielded 0.60 ±0.1 GTP and 0.56 ±0.09 GDP per dimer (n = 3). The GDP must have arisen from hydrolysis of the GTP that initially occupied the N-site. The Tb must also have been native, since it formed MTs. AP-treatment of these MTs hydrolyzed neither GTP nor GDP. But when they were subsequently dissociated, GDP (but not GTP) could be hydrolyzed by AP. Assembly and hydrolysis of about half the GTP initially bound to the N-site was also seen when the following were added to empty-E-site-Tb: 2 mM GMP-PCP, 100 μM taxol; 2 mM GMP-PCP, 4 M glycerol; 2 mM GMP-CPP, 100 μM taxol. We conclude that when assembly occurs without a hydrolyzable nucleotide bound at the E-site, GTP initially bound to the N-site is hydrolyzed. Whether hydrolysis occurs directly at the N-site, or whether the N- and E-sites first exchange GTP is not yet clear. Supported by NIH Grant GM25638.

M-AM-C6

VISUALIZATION OF TAU BINDING TO TUBULIN ZINC SHEETS BY ELECTRON CRYSTALLOGRAPHY ((S.G. Wolf*, E. Nogales*, B.L. Goode§, S.C. Feinstein§, and K.H. Downing*)) *Life Sciences Div., Lawrence Berkeley National Laboratory, Berkeley Ca. 94720; §Neuroscience Research Institute, Univ. of California, Santa Barbara Ca. 93106.

We have obtained a 3-D model of tubulin at 6.5 Å resolution by electron crystallography of zinc-induced, two-dimensional crystalline sheets of tubulin embedded in tannin (1). In addition, we decorated tubulin sheets with the anti-mitotic drug taxol, and identified its binding site in projection, using projection density difference maps at 4 Å resolution (1). In the present work, we have decorated the tubulin zinc-sheets with recombinantly expressed full-length rat tau protein. Gel electrophoresis suggests that the tau binds to the tubulin zinc-sheets with close to saturating stoichiometry. This binding occurs despite the fact that the grooves between neighboring protofilaments are entirely different in the zinc-sheets (where protofilaments are arranged in an anti-parallel fashion), than they are in microtubules (where protofilaments are parallel). Tau binding is speculated to occur in these microtubule grooves. A projection density difference map of tau binding to zinc sheets at 15 Å resolution shows increased density at the site of the β-monomer of tubulin, near the protofilament interface.

Tau protein contains multiple 18-amino acid repeats (R1, R2....) that bind microtubules and are separated by 13-14 amino acid inter-repeat (IR) regions. The R1-R2 IR region was recently found to have high microtubule binding affinity (2). We are currently constructing a difference map at high resolution of zinc-sheets decorated with a 26 amino acid synthetic peptide which contains the R1 region, and the R1-R2 IR region.

We have compared the structures of the tubulin in zinc sheets to their structure in microtubules by comparing the electron diffraction patterns of both, and by fitting the tubulin protofilament model from zinc-sheets into a 25 Å resolution helical reconstruction of microtubules (3). Both comparisons show the structure in the two polymers to be very similar, even at high resolution. Therefore, the structural information derived from tau decoration of zinc-sheets may be correlated to tau interactions with microtubules.

References
(1) Nogales E, Wolf SG, Khan IA, Luduena, RF, Downing KH (1995) *Nature* 375, 424-427.
(2) Goode BL and Feinstein SC (1994) *J.Cell Biol.* 124, 769-782.
(3) Wolf SG, Nogales E, Gratzinger D, Kikkawa M, Hirokawa N, Downing KH, in preparation.

M-AM-C7

THE BIREFRINGENCE OF MICROTUBULES MEASURED AT DIFFERENT FOCUS POSITIONS WITH THE NEW POLARIZED LIGHT MICROSCOPE. ((R. Oldenbourg, P.T. Tran, E.D. Salmon)) Marine Biological Laboratory, Woods Hole, MA 02543.

To measure the three dimensional imaging properties of the polarizing microscope we have imaged submicroscopic filaments of single microtubules (dia. 25 nm) and bundles of microtubules polymerized *in vitro*. We used a new polarizing microscope[1] to measure complete retardance profiles along a line perpendicular to the filament axes. A retardance profile shows the highest retardance in the center of the filament with rapidly decreasing retardance at either side of the diffraction limited image. We found that the central retardance of a single microtubule (MT) imaged in focus with a 60x/1.4 NA Plan Apo objective is 0.07±0.02 nm. The retardance of a bundle of two or three MTs increased linearly with the number of MTs in the bundle. When a filament was moved slightly out of focus, its image broadened and the measured central retardance decreased. While the peak retardance in the profile decreased, the retardance integrated over the whole profile remained constant and was independend of focus position.
This study is part of a project with the aim to measure live cell architecture, without the need of staining or labeling, at high resolution in all three spatial dimensions and in time, using the new polarized light microscope. Supported by a NIH grant awarded to R.O.

1 R. Oldenbourg and G. Mei. 1995. New polarized light microscope with precision universal compensator. J. Microscopy (November issue)

M-AM-C8

CENTERING OF MICROTUBULE ASTERS BY POLYMERIZATION FORCES IN MICRO-FABRICATED GLASS WELLS. ((M. Dogterom, A.N. Pargellis and B. Yurke)) AT&T Bell Laboratories, Murray Hill, NJ 07974.

Individual microtubules can exert forces through polymerization. Here we show how such forces can lead to the symmetrical positioning of microtubule asters in micron sized three-dimensional structures. Using photolithography techniques we constructed, in glass coverslips, wells of typical dimensions: 15 x 15 x 4 μm. Centrosomes (which nucleate microtubules in a radial fashion), tubulin and GTP were confined to the geometry of the wells. Microtubule polymerization was initiated by a raise in temperature and we followed the subsequent motions of single centrosomes using video-enhanced DIC microscopy and automated tracking routines. An initially "naked" centrosome performs Brownian motion that becomes more and more damped as microtubules polymerize. With time the centrosome invariably moves to the center of the well, where it finds a stable position. Detailed analysis of the shape of the trajectory reveals rapid excursions in different directions during early times that can be interpreted as one or several microtubules pushing the centrosome away from the edges of the well.

M-AM-D1

MOLECULAR FORCES INVOLVED IN FORCE GENERATION DURING MUSCLE CONTRACTION ((Y. Zhao*, K.P. Murphy**, M. Kawai*)). Departments of Anatomy* and Biochemistry**, The University of Iowa, Iowa City, Iowa 52242, U.S.A.

The effect of temperature on elementary steps of the cross-bridge cycle was investigated with sinusoidal analysis technique in skinned rabbit psoas fibers. The effects of MgATP, MgADP, and Pi on exponential processes at six different temperatures in the 5°C to 30°C range were studied. From these studies, we deduced the temperature dependence of the kinetic constants and thermodynamic properties of the elementary steps of the cross-bridge cycle. We found that the cross-bridge isomerization step which generates force is the most temperature sensitive step, and the rate constant of this step has a high Q_{10} (6.8) and a large activation energy (135 kJ mol^{-1}). Because the rate constant of its reversal reaction does not change much with temperature, the overall effect is a significant increase in the equilibrium constant of the force generation step with temperature. We found that this is an endothermic reaction (ΔH° = 124 kJ mol^{-1}), and it accompanies a large entropy increase (430 J $K^{-1}mol^{-1}$), hence this step is an entropy driven reaction. Our analysis indicates that the heat capacity change (ΔC_P) with this step is large (-6.4 kJ $K^{-1}mol^{-1}$). Based on ΔH° and ΔC_p, we deduced that a change in accessible surface area associated with apolar amino acid residues is -51 nm^2, and that associated with polar amino acid residues is -29 nm^2. These observations are consistent with the hypothesis that the stereospecific and hydrophobic interaction between residues of actin and myosin and residues within the cleft of the myosin head is involved in the mechanism of force generation.

M-AM-D2

PHOSPHATE RELEASE AND LENGTH-STEP TRANSIENTS IN RABBIT SKINNED PSOAS MUSCLE FIBERS ((Perry L. Sun, Yale E. Goldman, and Henry Shuman)) Pennsylvania Muscle Inst., Univ. of Pennsylvania, Philadelphia, PA 19104.

The dependence of tension in skinned muscle fibers on $[P_i]$ suggests that release of P_i in the AM.ADP.P_i (low force) to AM.ADP (high force) transition of the actomyosin ATPase cycle is linked to cross-bridge force generation (Hibberd et. al., *Science*, **228**:1317, 1985). A quick stretch or sudden release of P_i by caged-P_i photolysis during isometric contraction should therefore shift the population of cross-bridges from high force toward low force states. The declining phase of the tension transients after a quick stretch (phase 2) and after sudden release of P_i during active contraction have similar rates. We tested whether these two events are the same process by sequentially imposing a step stretch (ΔL, amplitude 4-5 nm/half sarcomere (h.s.)), a step increase of $[P_i]$ by photolysis of caged-P_i ($\Delta[P_i]$, 1.5-2 mM), and another step stretch (ΔL, arrows in Fig.) on a steady-state isometrically contracting muscle fiber at 10°C. The tension decline following $\Delta[P_i]$ and following the second ΔL can be directly compared because they occur at the same $[P_i]$. The sum of two exponentials for the two quick recovery components (phase 2) and an asymptote to phase 3 was fitted to the length step transient. The sum of a single exponential and an asymptote was fitted to the caged-P_i transient. Both rates increase with $[P_i]$ but phase 2 after ΔL is ~two-fold faster. This suggests that the biochemical and mechanical steps in the force generating transition are kinetically separated. Supported by NIH grant AR42333 and the MDA.

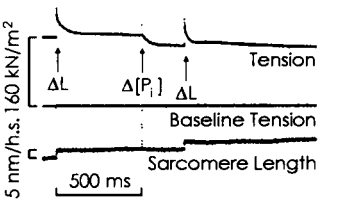

M-AM-D3

THE TWO MYOSIN HEADS FUNCTION SEQUENTIALLY IN NON-TENSION AND TENSION GENERATING MODES DURING ISOMETRIC CONTRACTION. ((J.S. Davis and M.E. Rodgers)) Department of Biology, The Johns Hopkins University, 34th and Charles Streets, Baltimore, MD 21218.

A key question in muscle contraction is whether the two heads of myosin function independently or not. We present laser temperature-jump kinetic data to show a nearly equal partitioning of crossbridges between a group involved in tension generation and a second group held in an earlier, non-tension generating, part of the cycle. Our interpretation is based on the observation that the rise in fiber tension following small-perturbation laser temperature-jumps has two phases with very similar amplitudes. We recently showed [Davis & Rodgers (1995) *Biophys. J.* 68:2032 & *Proc. Natl. Acad. Sci. USA.* 92:(in press)] that the slow kinetic phase ($1/\tau_3$) corresponds to ATP binding and hydrolysis, while the fast phase ($1/\tau_2$) arises from *de novo* tension generation. The tension increase of the slow phase results from a flux of crossbridges through to *de novo* tension generation, while tension from the fast phase arises directly from a perturbation of the temperature-sensitive equilibrium associated with *de novo* tension generation. These data appear to fit a model in which one of a pair of myosin heads generates force, while the second is poised to function once the power stroke of the first has occurred.
Supported by NIH grant AR-04349 to JSD.

M-AM-D4

THE EFFECTS OF CTP ON KINETICS OF CONTRACTION IN SKINNED FAST AND SLOW SKELETAL MUSCLE FIBERS. ((Philip A. Wahr and Joseph M. Metzger)) Department of Physiology, University of Michigan, Ann Arbor, MI 48109.

Mechanical measurements of single glycerinated rat soleus and rabbit psoas fibers were performed at 15 °C using ATP and the ATP analogue cytidine 5'-triphosphate (CTP) to examine the kinetics of the crossbridge cycle in skeletal muscle fibers. The replacement of ATP with CTP caused dramatic changes in the mechanical responses of single fibers. At pCa 4.5 CTP produced 76 ± 3 % (mean ± S.D., N = 9) of the force relative to ATP in rat soleus and 89 ± 7% (N = 5) of the force in rabbit psoas. CTP also produced a rightward shift in the force-pCa curve of 0.20 ± 0.04 pCa units (N = 6) in soleus with an increase in the Hill coefficient from 1.7 ± 0.1 to 2.1 ± 0.1 (N = 6) relative to ATP results from the same fiber. In psoas there was also a rightward shift in the force-pCa curve, however the Hill coefficient decreased slightly (N = 2). The differential effect of CTP on the Hill coefficient is evidence of a difference among fiber types in the ability of crossbridge binding to produce cooperative activation. V_{max}, as measured by the slack test method, was reduced from 1.4 ± 0.2 to 0.8 ± 0.1 ML/s (N = 8) in soleus and from 3.2 ± 0.4 to 1.1 ± 0.1 ML/s (N = 5) in psoas at pCa 4.5. In the presence of ATP the slack test plots became biphasic in both fiber types as the thin filament activation was reduced through decreased $[Ca^{2+}]$, with a fast phase in response to small length changes and a slow phase at longer step sizes. With CTP the plots remained monophasic at reduced Ca^{2+} activation in both fiber types with a slope in psoas fibers that was less than that observed for either phase of the ATP plot. In soleus the slope of the CTP slack test plot was similar to the slow phase of the ATP plot at a similar submaximum force level. In contrast, the rate of tension redevelopment, k_{tr}, increased from 3.9 ± 0.5/s to 8.0 ± 0.8/s (N = 6) at maximum Ca^{2+} activation in rat soleus when CTP replaced ATP. A similar doubling of k_{tr} was also observed at submaximal force levels. These results are interpreted as an increase in the crossbridge rate of transition into the force producing state followed by a decreased crossbridge detachment rate when CTP replaces ATP as the substrate for cycling crossbridges.

M-AM-D5

PARA-PHENYLENEDIMALEIMIDE AFFECTS BOTH ACTIVE AND PASSIVE SKELETAL MUSCLE MECHANICS. ((Cheryl A. Miller and Vincent A. Barnett)) Department of Physiology, University of Minnesota.

We have previously shown that extended treatment of relaxed skinned rabbit psoas fibers with para-phenylenediamaleimide (pPDM) traps myosin heads in an ATP-independent weakly-binding rapid-equilibrium crossbridge state (Barnett et al., Biophys. J. 61:358-367, 1992) that cannot be calcium activated (Barnett & Schoenberg, Adv. Exp. Med. Biol. 332:133-140, 1993). We have also shown that under the same conditions titin is crosslinked by pPDM in a manner that increases the resistance to stretch of relaxed muscle cells (Barnett et al., 1992). These reports focused on the effect of pPDM when the modification was sufficient to trap all the myosin heads in the weakly-bound state. We have recently reinvestigated the dual nature of pPDM's effects on muscle fiber mechanics and have observed that in single rabbit psoas fibers, the time course of the change in active force and resistance to stretch are similar and saturable. The time course of the change in active force generation is similar to the decline of rigor stiffness in pPDM-treated fibers (Barnett et al., 1992), and the modification of titin by pPDM is the likely explanation for the increase in resting stiffness (*ibid.*) The implication of the time course of the change in resistance to stretch is that the sites on titin must be accessable and have reactivity that is similar to SH-1 and SH-2 on myosin *under our labeling conditions.* It also suggests that the effects of pPDM are due to the modification of a finite population of sites as opposed to indiscrimanant crosslinking. We are pursuing both of the paths provided by these data. On one hand, the sequential modification of myosin heads by pPDM continues to provide a model system for the study of possible cooperativity of myosin crossbridges. On the other, the modification of sites on titin that change its resistance to stretch provide a convenient handle for examining the elastic nature of this giant myofibrillar protein.

M-AM-D6

INORGANIC PHOSPHATE ALTERS THE CROSS-BRIDGE DETACHMENT RATE FOLLOWING RAPID STEP STRETCHES IN CONTRACTING SKINNED FIBERS OF RABBIT PSOAS MUSCLE. ((*Jody A. Dantzig, *Yale E. Goldman, †Vincenzo Lombardi)) *Pennsylvania Muscle Institute, University of Penna., Phila., PA, 19104, †Dipartimento di Scienze Fisiologiche, Universita di Firenze, Italy. (Spon. by A. Weber)

Sinusoidal analysis of active tension transients obtained during ramp stretches indicates that inorganic phosphate (P_i) increases the rate of cross-bridge detachment (Dantzig et al., *J. Physiol.*, **426**:39*P*, 1990). In the present study, we measured the kinetics of cross-bridge detachment and reattachment following a rapid (<150 μs) step stretch in contractions at 10 °C (5 mM ATP, 200 mM ionic strength, pCa 4.5, pH 7.1). Evidence from structural (Lombardi et al., *Nature*, **374**:553, 1995) and mechanical studies (Lombardi et al., *J. Physiol.*, abstr. in press) suggests that strained cross-bridges, after a stretch, detach fully and are replaced by freshly attached and force generating cross-bridges during the slower part of phase 2 and phase 3. Using complete replacement as a constraint, we fit a multiple exponential equation to the tension transients. For a 4 nm / half sarcomere stretch, the exponential time constant for detachment (τ_D) decreases from 40 to 12 ms, while the time constant for reattachment and force generation (τ_3) decreases from 49 to 17 ms with increasing P_i (0 - 25 mM). If the detaching and reattaching cross-bridges are distinct populations, then detachment as well as reattachment and force generation depend on $[P_i]$.
Support: NIH grant AR42333 & Italian CNR.

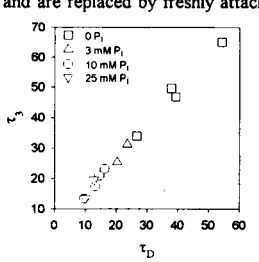

M-AM-D7

SMOOTH MUSCLE MYOSIN WITH AN ELONGATED NECK REGION PRODUCES GREATER UNITARY DISPLACEMENTS IN VITRO

((William H. Guilford, Matthew J. Tyska, Yelena Freyzon*, David M. Warshaw and Kathleen M. Trybus*)) University of Vermont, Burlington, VT 05405 and *Brandeis University, Waltham, MA 02254

A simple model for myosin force and motion generation has been proposed, based on the myosin S1 crystal structure (Rayment et al., 1993, Fisher et al., 1995). In this model, a substantial portion of the myosin head maintains a fixed orientation relative to actin, while the neck region pivots about a fulcrum at a point where the essential light chain (ELC) and motor domain abut one another. The neck region may therefore act as a rigid lever to transmit force and to amplify smaller conformational changes that originate within the motor domain. The simplest lever arm model predicts that myosin with a longer neck should generate larger unitary displacements and smaller unitary forces. To test this model, we utilized a dual laser optical trap to measure unitary displacements and forces from wild type smooth muscle HMM and a mutant with an elongated neck, expressed in an insect cell line (Trybus, 1994). The long-necked HMM had an additional ELC binding region thus elongating the neck by ≈50%. As predicted by the lever model, the long-necked HMM produced significantly higher displacements of 13-14 nm compared to 10-11 nm displacements from wild type HMM. In contrast, unitary forces were not significantly different, and were in the range of 3-4 pN. These data suggest that although myosin's neck region may act as a lever, its role may be more complex thus requiring further structure-function analysis.

CARDIAC ELECTROPHYSIOLOGY

M-AM-E1

SYNCHRONIZATION OF RABBIT SINOATRIAL NODE CELLS STUDIED WITH COUPLING CLAMP.

((1,2E. Etienne Verheijck, 1,2Ronald Wilders, 3Ronald W. Joyner, 1Antoni C. G. van Ginneken, and 2Habo J. Jongsma)) 1Department of Physiology, University of Amsterdam, 1105 AZ Amsterdam, The Netherlands, 2Department of Medical Physiology and Sports Medicine, Utrecht University, 3584 CG Utrecht, The Netherlands, and 3Department of Pediatrics, Emory University, Atlanta, GA 30322, USA.

We have investigated the effects of gap junctional conductance on the synchronization of rabbit sinoatrial node cells using a computer-controlled version of the "coupling clamp" technique introduced by Tan and Joyner (*Circ. Res.* 67:1071–1081, 1990). With this digital coupling clamp technique, the membrane potentials of two single isolated cells not in physical contact with each other are recorded using the amphotericin-perforated patch technique. These cells can be electrically coupled at any desired value of intercellular conductance by means of a computer-controlled circuit that continuously supplies time-varying currents to each cell with a sign and magnitude that would have been present if the cells would have been physically coupled. This allows the rapid independent measurement of the intrinsic cellular properties and then the analysis of the effects of a wide range of intercellular conductance values on the electrical behavior of the coupled cells. In our coupling clamp experiments we consistently found that an ohmic intercellular conductance of ~150 pS was sufficient for frequency entrainment, and that waveform entrainment occurred at intercellular conductance values ≥2 nS. Recalling that the conductance of a single cardiac gap junctional channel is ~70 pS, we conclude that very few gap junctional channels are required for synchronous firing of sinoatrial node cells.

M-AM-E2

EXPRESSION AND REGULATION OF CARDIAC (EXON 5-) CFTR CHLORIDE CHANNELS IN *XENOPUS* OOCYTES BY PKA AND PKC.

((M.L. Collier, J.D. Warth, Y. Geary, P. Hart, B. Horowitz and J.R. Hume)) Department of Physiology and Cell Biology, University of Nevada, Reno, NV 89557-0046.

A cDNA from rabbit ventricle was isolated and sequenced, which encodes an exon 5 spliced variant (exon 5-) of CFTR. Outside of this region, cardiac CFTR shows greater than 90% homology compared with epithelial CFTR and contains all putative phosphorylation sites for protein kinase A (PKA) and protein kinase C (PKC). We injected *Xenopus* oocytes with cRNA encoding rabbit cardiac CFTR and tested on day 4/5 for functional expression of Cl^- conductance by activation of either PKA or PKC. All Cl^- current recordings were made in Ca^{2+}-free Ringer solution and contained (in mM): NaCl, 96; KCl, 2; $MgCl_2$, 2.8; EGTA, 1; HEPES, 5; pH 7.5. In some experiments Cl^- gradient was changed by substituting Cl^- with aspartate. Time-independent membrane currents were activated when external solution contained either 8-bromo-cAMP (100μM), forskolin (1μM) and 3-isobutyl-1-methylxanthine (500μM) or phorbol 12,13-dibutyrate (100nM) and 1,2-dioctanoyl-sn-glycerol (120μM). Mean current amplitudes in the presence of elevated cAMP or by PKC activation were 4377 ± 447 nA (n=20; +70mV) and 1041 ± 167 nA (n=3; +70mV), respectively. With external Cl^- = 28mM, current amplitudes were reduced and the shift in reversal potentials were close to predicted E_{Cl}. Currents were reduced in a voltage-dependent manner in the presence of 4,4'-diisothiocyanatostilbene-2,2'-disulphonic acid (DPC 200μM; n=5). Activation of PKA or PKC failed to elicit Cl^- sensitive currents in water injected control oocytes. We conclude that an exon 5 splice variant of CFTR encodes the cAMP-dependent Cl^- channel in native rabbit cardiac cells and these channels can also be activated by PKC. (supported by NIH HL 52803, AHA grant-in-aid and AHA Nevada Affiliate).

M-AM-E3

INHIBITION OF CFTR GENE EXPRESSION REDUCES cAMP-DEPENDENT Cl^- CURRENTS IN CULTURED GUINEA-PIG VENTRICULAR MYOCYTES.

((J.D. Warth, P. Hart, B. Horowitz, and J.R. Hume.)) Department of Physiology and Cell Biology, University of Nevada, Reno, NV 89557-0046.

In heart, a variety of indirect and circumstantial evidence suggests that the cystic fibrosis transmembrane conductance regulator (CFTR) gene product may be responsible for cAMP-dependent Cl^- currents (*Ann. Rev. Physiol.* 57:387, 1995). We tested the hypothesis that cAMP-dependent Cl^- currents in native guinea-pig ventricular cells are due to cardiac expression of CFTR by using antisense probes directed against the first 23 base pairs of the CFTR gene product beginning with the start codon. Acutely cultured guinea-pig ventricular cells exhibited cAMP-dependent Cl^- currents that were of comparable density compared to those observed from freshly dispersed myocytes for time periods up to 24 hours. Three groups of cultured guinea-pig ventricular myocytes were examined in a blinded study: group one was exposed to sterilized distilled water, group two was exposed to 8 μM sense oligodeoxynucleotides (ODN), and group three was exposed to 8 μM antisense ODNs. Following exposure for 24 hours, the maximal forskolin (FSK, 1μM)-activated Cl^- current density was determined in each cell. At +40 mV, mean current density for cells in group one and two were 4.24 ± 0.83 $pApF^{-1}$ (n=10) and 4.11 ± 0.56 $pApF^{-1}$ (n=10), respectively, whereas cells in group three (antisense) exhibited a significantly smaller mean current density of 2.45 ± 0.34 $pApF^{-1}$ (n=9). Since FSK-induced augmentation of L-type Ca^{2+} currents was not significantly different among the three groups, alterations of the second messenger pathway were not responsible for the observed antisense induced attenuation of I_{Cl}. These results provide direct evidence that the CFTR gene encodes a channel responsible for the cAMP-dependent Cl^- current in native cardiac cells. (Supported by HL52803, AHA and AHA Nevada Affiliate).

M-AM-E4

$[Mg^{2+}]$ GOVERNS CFTR Cl^- CHANNEL OPENING AND CLOSING RATES, CONFIRMING HYDROLYSIS OF TWO ATP MOLECULES PER GATING CYCLE.

((A.G. Dousmanis, A.C. Nairn, and D.C. Gadsby)) The Rockefeller University, New York, NY, 10021.

Protein kinase A (PKA)-phosphorylated CFTR Cl^- channels in patches from guinea-pig ventricular myocytes require hydrolyzable nucleoside triphosphate to open and close normally. At 1.2 mM free $[Mg^{2+}]$, channel open probability (P_o) increases hyperbolically with [ATP] ($K_{0.5}$ ~35 μM [ATP]), largely due to an increase in opening rate. That ATP hydrolysis governs channel opening is almost certain, since all ATPases require Mg^{2+}, and Mg^{2+} ions are needed for channel opening by ATP. Thus, at 2 mM [ATP], the mean opening rate at 20-22 °C is ~0 at ~0 $[Mg^{2+}]$ (Mg^{2+}-free with ≥ 1 mM CDTA), ~0.03 s^{-1} at 5 μM $[Mg^{2+}]$, and ~0.22 s^{-1} at 1.2 mM $[Mg^{2+}]$. This suggests that both ATP and Mg^{2+} must be bound before a channel can open. Free $[Mg^{2+}]$ levels also regulate closing. At 5 μM $[Mg^{2+}]$, channels can stay open for tens of sec, even after rapid (~1 s) ATP washout, but close promptly on raising $[Mg^{2+}]$: the mean closing rate rises with $[Mg^{2+}]$, from ~0.05 s^{-1} at 0 or 5 μM $[Mg^{2+}]$, to ~0.3 s^{-1} at 1.2 mM $[Mg^{2+}]$. This confirms (PNAS, 1994, **91**:4698) that hydrolysis of a second ATP prompts channel closure. Evidently, that second ATP stays tightly bound, stabilizing the open conformation, without Mg^{2+}. The closing rate on Mg^{2+} readdition then reflects the probability that a Mg^{2+} ion will bind and catalyze hydrolysis of that ATP, leading to channel closure. This stabilization of the open state by binding of a nucleotide barred from hydrolysis resembles the locking open by AMP-PNP of channels opened by ATP. The slowing of channel closure by low $[Mg^{2+}]$ seems linked to phosphorylation level. In 4 patches, closing of ≥ 1 channel was unaffected by lowering $[Mg^{2+}]$ to 5 μM, but, just after reapplying PKA, low $[Mg^{2+}]$ prolonged the open time of all channels. *NIH HL49907*

M-AM-E5

DEVELOPMENT AND PROPAGATION OF SPHERICAL CALCIUM WAVES IN RAT CARDIAC MYOCYTES.
((M.H.P. Wussling, H. Salz)) J. B. Institute of Physiology, Martin Luther University, D-06097 Halle , Germany.

Spontaneous calcium waves in isolated rat cardiac myocytes were investigated by confocal laser scanning microscopy using the Ca^{2+}-indicator fluo-3 AM. The wave velocity was low close to the focus and increased with time and propagation length. The maximum velocity amounted to 113 µm/s at room temperature.
It is suggested that the propagation velocity is critically dependent on the curvature of the spreading wave. From the linear relationship of velocity vs. curvature a critical radius of 2.7±1.4 µm (mean ±S.D.) was figured out below which an outward propagation of the wave will not take place. Once released from a sufficiently extended cluster of SR release channels, Ca diffuses ($D=3*10^{-4}$ mm^2/s) and activates its neighbors. While travelling away the volume into which calcium diffuses becomes effectively smaller than at low radii. Thus, the time taken to reach a critical threshold of $[Ca^{2+}]_i$ at the neighboring calcium release site decreases and the wave propagates faster.

M-AM-E6

NA-CA EXCHANGE CURRENTS AND SR CA CONTENT WERE REDUCE IN POST-INFARCTION MYOCYTES. ((X.Q. Zhang and J.Y Cheung)) Dept. of Medicine, Penn State Univ., Hershey PA 17033. We have shown cytosolic Ca ($[Ca]_i$) an peak cell shortening in single rat myocytes isolate from 3 weeks infarcted (MI) hearts were lower. W have also shown Ca current (I_{Ca}) was not differen between Sham and MI myocytes. Reverse Na-Ca exchang current (I_{NaCa}) has been recognized to mediate Ca entr during depolarization and trigger SR Ca release Under conditions that favored Ca influx (revers mode), I_{NaCa} measured with whole cell patch clamp wa significantly lower in MI myocytes ($p<0.0007$; 2-wa ANOVA of repeated measures). For example, at +70mV I_{NaCa} was 3.22±0.23 pA/pF in Sham and 1.72±0.34 pA/p in MI myocytes. Depolarization to more positiv voltages increased I_{NaCa} more in Sham than MI myocyte ($p<0.0001$). SR Ca content estimated by caffeine induced Ca release and measured as forward I_{NaCa} wa 2.99±0.20 fmol/cell in Sham and 1.70±0.28 fmol/cell i MI myocytes ($p=0.0017$). We conclude that Na-C exchange activity is depressed in MI myocytes an suggest that it is causally related to decreased SR C content. This in turn leads to less SR Ca release pe beat, accounting for lower peak $[Ca]_i$ and reduced cel shortening in MI myocytes.

M-AM-E7

Il-1β Protects Against Hypoxia Induced Nuclear Calcium Overload and TNF Protects Against Chemically Induced Nuclear Calcium Overload in Neonatal Rat Cardiac Myocytes ((L.Nutt, R.Bick, L.Max.Buja))Department of Molecular Pathology, UTHSC, Houston, Texas

This study tested the effects of the cytokines, Tumor Necrosis Factor (TNF) and Interleukin 1-β (Il-1β), on changes in subcellular calcium distribution in cardiac myocytes induced by adriamycin and hypoxia. Cultured cardiac myocytes were loaded with Fluo-3AM for 15 min. and examined by scanning laser confocal microscopy (SLCM). Treatment of the cardiac myocytes with .04mg/ml of adriamycin was for 2 or 18 hours. After two hours, adriamycin caused a dramatically increased intranuclear calcium level as determined by SLCM. However, TNF (9ng/ml), added with adriamycin, reduced nuclear calcium, compared to other cytokines (2hr:160nM± 40 vs. 500nM ± 100, and 18hr: 50nM ± 10 vs. 500nM ± 100). Il-1β (10ng/ml), added prior to 2hrs of hypoxia, reduced intranuclear calcium as well as preserving the contractility of the cardiac myocytes (50nM ± 10 vs. 150nM ± 20). Hypoxic conditions were met via incubation of the cells in a nitrogenous atmosphere. Contractile studies reinforce our findings that TNF has a protective effect during adriamycin treatment (20% ±1% vs. 0% shortening), and Il-1β has a similar result in hypoxia (22%±1.6% vs. 39%±1.9%), where Il-1β acts to preserve contractions similar to control cells (22%+1.6% vs. 23%± 1%). Adriamycin, hypoxia, and TNF treated cells exhibited decreased or noncontractile function, and elevated intranuclear calcium. Myocytes, treated with adriamycin plus TNF, had increased contractility, and increased intracellular calcium compared to untreated cells, but a normal morphology compared to the adriamycin treated cells. Il-1β showed a similar effect in hypoxic myocytes. TNF increases intranuclear calcium in cardiac myocytes, but in adriamycin treated cells, TNF effectively blunted increases in intranuclear calcium. Conversely, Il-1β effectively protected cardiac myocytes from intranuclear calcium loading due to hypoxia.

M-AM-E8

DEVELOPMENTAL CHANGES IN β-ADRENERGIC MODULATION OF L-TYPE CALCIUM CHANNELS IN EMBRYONIC MOUSE HEART. ((R-H. An*, M. P. Davies*, P. A. Doevendans#, S. W. Kubalak#, R. Bangalore*, K. R. Chien#, and R. S Kass*)) Dept. of Physiology, U of Rochester Medical Center, Rochester, NY* and Dept. of Medicine, U of California San Diego, San Diego, CA#.

In the adult mammalian myocardium, L-type calcium channel currents are markedly increased by β-adrenergic (β-A) agonists. In the developing mammalian heart, however, the regulation of calcium entry by this enzyme cascade has not been clearly established. In this study, we systematically investigated the functional activity of distinct steps in the β-A signaling cascade in murine embryonic myocytes at different stages of gestation. Our data indicate that L-type Ca^{2+} channels in early stage (day 11-13) myocytes are unresponsive to either isoproterenol or cAMP. L-type Ca^{2+} channels in late stage (day 17-19) murine myocytes, however, exhibit responses to isoproterenol and cAMP similar to adult cells, providing evidence that the β-A cascade becomes functionally active during this period of embryonic development. We found that L-type Ca^{2+} channel activity in early stage cells is increased by cell dialysis with the catalytic subunit of cAMP-dependent protein kinase (CS-cA-PK) and that dialysis of early stage cells with the holoenzyme of cA-PK (holo-cA-PK) restores functional responses to forskolin and cAMP, but not to isoproterenol. Our results provide strong evidence that a key factor in the early stage insensitivity of L-type Ca^{2+} channels to cAMP is the absence, or low expression level, of holo-cA-PK, but that, in addition, another element in the signaling cascade upstream from adenylate cyclase (AC) is expressed at a non-functional level or is uncoupled from the cascade contributing to L-channel insensitivity to β-A agonists in early stages of the developing murine heart.

TRANSMEMBRANE SIGNALING - ALTERED CALCIUM CHANNELS

M-AM-F1

IVS4 MUTATIONS WHICH ALTER INACTIVATION OF THE SKELETAL L-TYPE CALCIUM CHANNEL WITHOUT AFFECTING ACTIVATION ((A. Gonzalez, and K. Beam)) Dept. Anatomy and Neurobiology, Colorado State University, Fort Collins, CO 80523.

PCR was used to mutate arginines in S4 segments of the rabbit skeletal muscle dihydropyridine receptor cDNA (CAC6). The mutated cDNAs were expressed in dysgenic myotubes and characterized with standard whole-cell recording methods. Voltage-dependence of steady-state inactivation was studied with a 10 s conditioning pulse to different membrane potentials. The mutations R1236E and R1249E in repeat IV altered both the rate of inactivation (τ_{decay} at +50mV) and voltage dependence ($V_{1/2}$, k) of steady-state inactivation (wild-type CAC6 had a τ_{decay} of 533 ± 148 ms, $V_{1/2}$= -5.2 ± 1.9 mV and k= 7.3 ± 0.5 mV.; R1236E had a τ_{decay} =2122 ± 365 ms, $V_{1/2}$= 3.2 ± 0.9 mV and k= 11.1± 0.8 mV; R1249E had a τ_{decay} =2627 ± 506 ms, $V_{1/2}$= 6.8 ± 1.9 mV and k= 13.1± 0.6 mV). Neither the voltage-dependence nor kinetics of activation were noticeably affected by these mutations. Thus, charged amino acids of the fourth repeat appear to be more important for inactivation of the skeletal L-type calcium channel than activation. Because inactivation of L-type current has been reported to be altered in myotubes from humans with a mutation causing hypokalemic periodic paralysis (R528H), this mutation and two others (R1239G and R1239H) were introduced into CAC6. None of the mutations appreciably affected either activation or inactivation. The discrepancy with human myotubes bearing the R528H mutation may reflect differences between the rabbit and human DHPRs or the cellular environment of human and mouse myotubes . Supported by NIH grant NS24444 to KB.

M-AM-F2

A SMALL G PROTEIN OF THE *RHO-RAC* FAMILY MEDIATES INHIBITIOI OF NEURONAL CALCIUM CURRENTS BY BRADYKININ. ((M.A. Wilk Blaszczak, W.D. Singer, P.C. Sternweis, F. Belardetti)) Dept Pharmacology, UT Southwestern, Dallas, TX 75235.

In NG108-15 cells, the slow inhibition of the voltage-dependent calciun current ($I_{Ca,V}$) by bradykinin (BK) is transduced by the heterotrimeric G protein G_{13}. We now find that intracellular application of recombinant *Rho* GDI (a guanine nucleotide-dissociation inhibitor specific for the small G proteins of the *Rho-Rac* family) attenuates the response to BK (9 ± 129 inhibition, n = 8 treated; 16 ± 8% n = 8 control). This action of *Rho*-GDI i selective, because in the same cells it does not affect the inhibition of I_{Ca} by Leu-enkephalin (Leu-Enk), and in separate cells it is not replicated b intracellular application of a blocking anti-*Ras* IgG (n = 4 treated; n = control). These data suggest that a small G protein of the *Rho-Rac* famil couples G_{13} to a pathway leading to inhibition of $I_{Ca,V}$. Because intracellula perfusion of brain purified $G_{\beta\gamma}$ subunits neither mimics (n = 11), nor block (n = 5) the effect of BK (or Leu-Enk), signaling between G_{13} and *Rho-Ra* is not likely to be mediated by $G_{\beta\gamma}$ subunits released from activated G_{13} Similarly, a $G_{\beta\gamma}$-scavenger peptide (*Science* 268, 1166) does not block th response to BK (n = 9 treated; n = 10 controls) or Leu-Enk. We find instea that intracellular perfusion of GTPγS-bound $G_{\alpha 13}$ suppresses the inhibitio of $I_{Ca,V}$ by BK (6 ± 11%, n = 12 treated; 19 ± 17%, n = 10 control) but no Leu-Enk, and it does not directly mimic the inhibition of $I_{Ca,V}$ by BK. Thes observations suggest that $G_{\alpha 13}$ is responsible for the downstream signaling via a pathway that rapidly desensitizes.

M-AM-F3

MOLECULAR DETERMINANTS INVOLVED IN THE MODULATION OF N-TYPE CALCIUM CHANNELS BY G-PROTEINS. ((J.F. Zhang, P.T. Ellinor, R.W. Aldrich and R.W. Tsien)) Dept Mol & Cell Physiol, HHMI, Stanford Univ, Stanford, CA 94305

To study the molecular mechanisms of the modulation of Ca^{2+} channels by G-proteins, cloned Ca^{2+} channels were co-expressed in *Xenopus* oocytes along with subunits of G-proteins and a seven-transmembrane receptor (somatostatin or α_2). Of the three wild type channels (α_{1A}=BI, α_{1B}=N-type, α_{1C}=L-type), N-type Ca^{2+} channels stood out in that application of 1 μM somatostatin solution caused a robust inhibition (20±1.7% reduction). α_{1A} was much less responsive and the L-type was insensitive. As expected for G-protein dependent inhibition of the N-type channel, the inhibition was sensitive to pertussis toxin and a strong depolarization (+150 mV) prior to the test pulse reversed the inhibitory effect.

To delineate the structural determinants involved in the inhibition, we constructed a series of mutant channels and expressed them in *Xenopus* oocytes. The results show that all four repeats of the α_{1B} subunit are involved in the inhibition by G-proteins. However, the effects of swapping portions of individual repeats were not equal, with repeats I and IV showing larger differences than repeats II and III. A combination of mutations in multiple regions of the channel molecule completely eliminated both the inhibitory effect of somatostatin or α_2-receptor stimulation and the relief of inhibition by strong prepulses.

M-AM-F4

MAKING A CLASS A (BI) CALCIUM CHANNEL SENSITIVE FOR PHENYLALKYLAMINES (PAA) ((S. Hering, F. Döring, V.E. Degtiar, M. Grabner, J. Striessnig, H. Glossmann)) Institut für Biochemische Pharmakologie, Peter Mayr Straße 1, A-6020 Innsbruck, Austria (Spon. by H. Glossmann)

To identify the structural elements of the PAA-receptor of L-type calcium channels we implanted sequence stretches of the PAA-sensitive carp skeletal muscle α_{1S} subunit into the α_{1A} subunit. cRNA encoding for $\alpha_{1C\text{-}a}$, α_{1A} and chimeric α_{1A}/α_{1S} channels with equimolar ratios of β_{1a} and α_2/δ subunit cRNA were injected into *Xenopus laevis* oocytes. Barium currents (I_{Ba} in 40 mM barium solution) were tested for sensitivity to PAAs (50 μM (-) devapamil). We estimated the conditioned I_{Ba}-block (± S.E.M.) by (-) devapamil as cumulative peak I_{Ba}-inhibition during a 100 ms test pulses train (pulse frequency of 0.1 Hz). I_{Ba} of $\alpha_{1C\text{-}a}$ were sensitive to (-) devapamil (30±4%) whereas I_{Ba} of α_{1A} were only slightly affected by the drug (10±1.5%). Implantation of the α_{1S} transmembrane segment S6 of repeat IV (IVS6) into α_{1A} resulted in transfer of PAA sensitivity to α_{1A}. I_{Ba} of the subsequent chimera measured during a pulse train of 100 ms test pulses from -80 mV to 20 mV was substantially inhibited in the presence of (-) devapamil (58±6%) compared to 21±5% inhibition caused by incomplete recovery from inactivation (see figure). Our results demonstrate that the seven amino acid difference between the IVS6 segments of α_{1A} and α_{1S} carry the key elements of the L-type calcium channel PAA receptor.

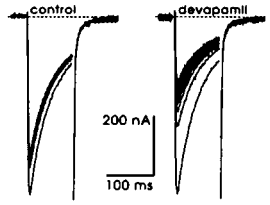

Supported by FWF grants S6601-MED (H.G.), S6602-MED (J.S.) and S6603-MED (S.H.)

M-AM-F5

EXPRESSION OF G-PROTEIN βγ SUBUNITS IN RAT SYMPATHETIC NEURONS PRODUCES VOLTAGE-DEPENDENT CALCIUM CHANNEL MODULATION. ((S.R. Ikeda)) Department of Pharmacology & Toxicology, Medical College of Georgia, Augusta, GA 30912-2300.

Components of the heterotrimeric G-protein signaling pathway were expressed in dissociated adult rat sympathetic neurons by nuclear micro-injection of plasmids containing a CMV promoter. Calcium currents were recorded 14–24 hours following injection with the whole-cell variant of the patch-clamp technique from neurons expressing a co-injected reporter gene, the S65T mutant of the jellyfish GFP (Heim et al., *Nature* **373**:663, 1995). Expression of wild-type and mutant (Q205L and G204A) GoA α-subunits resulted in calcium currents which inactivated slightly following a depolarizing voltage prepulse (+80 mV for 50 ms) but otherwise appeared similar to control neurons (uninjected or injected with S65T GFP alone). However, calcium channel modulation resulting from application of norepinephrine (NE) was greatly attenuated in these neurons. In contrast, the expression of several different G-protein βγ-subunit combinations (β1γ2, β1γ3, β1γ7) resulted in calcium currents which displayed profoundly slowed activation kinetics and large prepulse facilitation—characteristics which mimic those of neurotransmitter-mediated modulation. Application of NE to βγ-subunit expressing neurons produced little further modulation. Taken together, these data suggest that the βγ-subunit, and not the α-subunit, of heterotrimeric G-proteins mediates the voltage-dependent modulation of N-type calcium channels in rat sympathetic neurons. (Supported by a grant from the American Heart Association-Georgia Affiliate)

M-AM-F6

PROTON BINDING IN THE PORE-LINING SEGMENT (P-LOOP) OF THE HUMAN CARDIAC CALCIUM CHANNEL. ((U. Klöckner[1], G. Mikala[2], J. Eisfeld[1], A. Schwartz[2] and G. Varadi[2])) [1]Department of Physiology, University of Cologne, 50931 Cologne, Germany and [2]Institute of Molecular Pharmacology and Biophysics, University of Cincinnati, OH 45267-0828, USA.

High-selectivity calcium filtration sites have recently been identified for cardiac (α_{1C}) and neuronal (α_{1A}) calcium channels. These reside on the P-loop structures in each motif. The filtration machinery involves at least one glutamic acid residue in each loop as revealed by Ca^{2+} and Cd^{2+} block of ionic currents carried by monovalent cations. In order to probe the functional role of the glutamic acid residues in the ion permeation process, we studied the effect of protons on the permeation of monovalent cations through the human cardiac L-type calcium channel. The wild type channel, with sodium as charge carrier, exhibited single channel function that can be resolved into two conductance levels, probably corresponding to two different protonation states of the channel. Point mutations for E^{667} did not alter the two single channel conductance levels, suggesting that protons do not bind at this glutamic acid residue. In contrast, mutations for E^{1387}, when protonated, produced a marked increase at the conductance level, while the conductance of the unprotonated form remained unchanged. Mutations of conserved glutamic and aspartic acid residues located more extracellular from the entryway showed two conductance levels. Similarly to the behavior of the wild type, this suggests that these residues are not targets for proton binding.

M-AM-F7

PROTEASE PERFUSION REVEALS INHIBITORY DOMAINS ON THE CARBOXYL TERMINUS OF THE α_1 SUBUNIT OF A HUMAN CARDIAC L-TYPE Ca^{2+} CHANNEL. ((G. Mikala[1], U. Klöckner[2], M. Varadi[1], G. Varadi[1] and A. Schwartz[1])) [1]Institute of Molecular Pharmacology and Biophysics, University of Cincinnati, OH 45267 and [2]Department of Physiology, University of Cologne, 50931 Cologne, Germany

Previously, we have shown that intracellular application of proteases increases Ca^{2+} channel availability by a partial removal of the C-terminus of the α_1 subunit (till Leu^{1673}; Klöckner et al., J. Biol. Chem., 270, 17306-17310, 1995). In order to identify the inhibitory domain(s) removed by the proteases, we studied the effects of protease perfusion on C-terminal deletion mutants of the α_{1C} subunit expressed in HEK293 cells. Mutants Δ1935 and rΔ1935 (a mutant based on an α_1 splice variant that lacks the fragment 1785-1855) behaved in a manner indistinguishable from the wild type α_1 subunit (≈3-fold enhancement). This indicates that residues 1674-1784 or 1856-1935 may harbor the critical domain(s) for this effect. Mutant Δ1784 responded to trypsin perfusion by an ≈2-fold increase in peak current, showing that a portion of the inhibitory region was already removed by the deletion. Surprisingly, currents carried by the internal deletion mutant Δ(1674-1935) were found to be significantly more enhanced by trypsin than the wild type currents. Our data suggest the presence of multiple intertwined inhibitory domains illustrating the profound complexity of the functional domain structure of the C-terminus of the α_{1C} subunit.

M-AM-F8

THE SUBSTITUTED DIPHENYLUREA NS 1608 ACTIVATES THE α-SUBUNIT OF THE HUMAN BK CHANNEL (hSlo). ((S.-P. Olesen, D. Mathiasen, P. Christophersen, P.K. Ahring and T.E. Johansen)) NeuroSearch A/S, 26B Smedeland, DK-2600 Glostrup, Denmark. (Spon. by S. Dissing).

The molecular constituents of the human BK channel is an α- and a ß-subunit. The human α-subunit has been reported to exist in at least 9 differently spliced isoforms. We have generated stable HEK 293 cell lines expressing the α-subunit bearing no sequence in the known splice sites. The effects of the novel BK channel activator NS 1608 on the human BK channel was studied in these stable cell lines. The expression level was very high, in the range of 300-600 single BK channels per patch, resulting in currents up to 20 nA in an IO patch. The Ca^{2+} sensitivity of the channels was comparable to that reported in many smooth muscle cells with a $V_{½}$ of 90 and 23 mV in 0.3 and 1 μM free internal Ca^{2+}, respectively. NS 1608 increased the BK current, when measured either as voltage-activated plateau currents or as tail currents, and the maximal effect was a 70 mV leftward shift of the activation curve. The lowest active concentration of NS 1608 was 100 nM, and the EC_{50} was 2.1 μM. The compound delayed the relaxation of the tail currents similarly to the effect of internal Ca^{2+} at high concentrations, suggesting an interaction with the binding of Ca^{2+} to the channel. The compound hyperpolarized the transfected cells by up to -50 mV.

M-AM-F9

TRANSFER OF DIHYDROPYRIDINE-SENSITIVITY TO THE CLASS A (BI) Ca^{2+} CHANNEL. ((M. Grabner, Z. Wang, M.J. Sinnegger, J. Mitterdorfer, S. Hering, J. Striessnig, and H. Glossmann)) Institut für Biochemische Pharmakologie, Universität Innsbruck, Peter Mayrstraße 1, A-6020 Innsbruck, Austria.

Sensitivity to organic Ca^{2+} channel modulators like the 1,4-dihydropyridines (DHPs) is characteristic for L-type Ca^{2+} channels and is missing in all other types of Ca^{2+} channels. To identify molecular motifs responsible for the formation of the DHP-receptor domain we transferred DHP-sensitivity from 2 classes of L-type Ca^{2+} channels to the DHP-insensitive class A (α_{1A}) brain Ca^{2+} channel, BI-2. Expression of class A / L-type channel constructs in oocytes of *Xenopus laevis* revealed minimum sequence stretches conferring DHP-sensitivity located within the putative pore forming regions of repeats III and IV. These include segments IIIS5, IIIS6 and the connecting linker, as well as the IVS5-IVS6 linker plus segment IVS6. DHP agonist and antagonist effects are determined by different regions within the repeat IV motif. Sequence regions responsible for the transfer of DHP-sensitivity to α_{1A} comprise only 9.4% of the overall primary structure of a DHP-sensitive α_{1A}/α_{1S} construct (AL12s). Chimera AL12s (see figure) fully exhibits the DHP agonist and antagonist sensitivity of channels formed by L-type α_1 subunits. In addition, AL12s displays the electrophysiological properties of α_{1A} as well as its sensitivity towards the peptide toxins ω-agatoxin IVA and ω-conotoxin MVIIC, indicating that regions responsible for DHP-sensitivity do not disrupt the toxin interaction site(s). Amino acid substitutions were performed to elucidate the degree of contribution of distinct residues in transmembrane segments IIIS5, IVS6 and in the IVS5-IVS6 linker to DHP-antagonist and/or agonist sensitivity. (Supported by FWF grants S6601-MED (H.G.), S6602-MED (J.S.) and S6603-MED (S.H.))

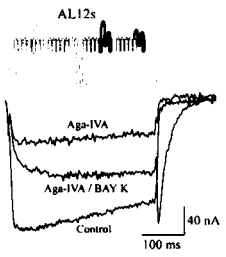

PHOTOSYNTHESIS

M-AM-G1

DISCOVERY OF A NEW PHOTOSYNTHETIC PATHWAY: PHOTOSYSTEM II LIGHT REACTION CAN SUPPORT COMPLETE PHOTOSYNTHESIS ((James W. Lee and Elias Greenbaum)) Chemical Technology Division, Oak Ridge National Laboratory, P. O. Box 2008, Oak Ridge, TN 37831-6194.

Recently, we have observed that Photosystem I (PSI)-deficient green algae were capable of growing photoautotrophically by Photosystem II (PSII) light reaction alone using atmospheric CO_2 as the sole source of carbon and water as the source of electrons. Experimental demonstration for photoassimilation of CO_2 and evolution of H_2 and O_2 by the PSII light reaction has been reported and discussed in *Nature* [376, 438 (1995)]. This "PSII photosynthesis" clearly challenges the textbook model of electron transport in oxygenic photosynthesis, the "Z-scheme," which requires both PSII and PSI working together in series. Although sequential transfer of electrons through PSII and PSI acting in series may be the major route of light-activated electron flow from H_2O to CO_2 in intact oxygenic photosynthesis, our work clearly demonstrated that PSI is not a necessary component as the Z-scheme would require. In this presentation, we report our elucidation of the electron transport pathway for the newly discovered PSII photosynthesis, using chemical inhibitors and algal genetic mutants. Our experiments demonstrated that the electrons from PSII did not directly go to Fd/NADP$^+$ as reported by Allakhverdiev and Klimov [*Z. Naturforsch.* 47c, 57 (1992)] and speculated by Barber [*Nature*, 376, 388 (1995)], but followed a rather energetically surprising path through the plastoquinone pool and Cyt b/f complex:

$$H_2O \rightarrow P680 \rightarrow Phe \rightarrow Q_A \rightarrow Q_B \rightarrow PQH?/PQH_2 \rightarrow cyt\ b_l \rightarrow cyt\ b_h \rightarrow Fd.$$

Important features and implications of the new pathway will also be discussed.

M-AM-G2

FUNCTIONAL ANALYSIS OF SITE-DIRECTED N-TERMINAL MUTANTS OF CHLOROPLAST CYTOCHROME *f* IN *CHLAMYDOMONAS* ((J.G. Fernandez-Velasco, J. Zhou and R. Malkin)) Dept. Plant Biology, 461 Koshland Hall and University of California. Berkeley, CA 94720.

The N-terminal Tyr of cyt f, which provides the sixth ligand to the heme group, has been changed, by side-directed mutagenesis in *Chlamydomonas*, to Pro, Phe, Trp or Ser in order to test its role in cytochrome assembly and redox activity. The second residue, a highly conserved Pro, and the third one, Val, have been changed to Val and Pro, respectively. Y1P is the only strain that lacks the cytochrome b6f complex and is incapable of photoautotrophic growth. All the other strains show wild type b6f complex/P700 ratio, PSI unit size and Chla+b/cell. The rate of cyt f photooxidation in the wt and all photosynthetic mutants are comparable (t1/2 ca. 300 μs) whereas the re-reduction sensitive to stigmatellin at Eh 0 mV for wt, Y1W, Y1F, Y1S, P2V and V3P has a t1/2 of 3, 4, 5, 9, 65 and 2 ms, respectively. Intact cell oxygen evolution is different only for P2V (35% inhib.) andY1F or Y1S (20% inhib.). At low light, all competent strains have the same growth rate, whereas at saturating intensities, only P2V shows a significant inhibition (40%). We conclude that: 1) The N-terminal primary amine is essential for the assembly of cyt f, but an N-terminal aromatic side chain has no critical role in the electron transfer into or out of the heme. 2) The presence of a Pro in the 2nd or 3rd position contributes to an adequate configuration for electron transfer from the Rieske center. 3) In the mutant P2V, the b6f complex (specifically the re-reduction of cyt f) is, probably, the rate limiting step of photoautotrophic growth.

M-AM-G3

CIRCULAR DICHROISM and the ORGANIZATION of INTERACTIONS in the LIGHT HARVESTING II PROTEIN of *RHODOPSEUDOMONA ACIDOPHILA*.

O.J.G. Somsen, R.W. Visschers, M. Wendling, R.J. Cogdell$^+$ and R. van Grondelle. Dept. of Physics and Astronomy, Free University, Amsterdam, The Netherlands, and $^+$Department of Botany, University of Glasgow, UK.

The light harvesting systems from photosynthetic purple bacteria form an interesting category of pigment-protein complexes. The organization of small units (two- or three pigments) in highly symmetric rings, feeds the discussion on the amount and nature of exciton delocalization. The first crystal structure has recently been obtained for LH2 from *Rhodopseudomonas (Rps.) acidophila*. It shows a ring of 9 pigments, responsible for the B800 band, while 18 B850 pigments are organized in a ring of 9 dimers, which deviates very little from 18-fold symmetry.

However elucidating, the crystal structure leaves many details, such as interaction strengths, unknown. It can be supplemented by polarized absorption spectra. We discuss details of the B850 circular dichroism. The zero-crossing of the S-shaped CD band is considerably (75 cm^{-1}) redshifted with respect to the maximum of the absorption (OD) band. In the simplest model this may be explained by the two allowed transitions. The OD-shift indicates that the dipole strength is concentrated on the blue transition. The CD is explained by two opposite rotational strengths, so that the zero-crossing is in the middle between the two transitions. An exciton splitting of 150 cm^{-1} is required. A dipole-dipole calculation from the crystal structure (in vacuum) yields an interaction strength in the order of 500 cm^{-1} between neighboring pigments. For several models we investigate whether these two values are compatible.

M-AM-G4

STRUCTURE OF THE LIGHT-HARVESTING COMPLEX-II OF *RHODOSPIRILLUM MOLISCHIANUM*

((Xiche Hu[1], Klaus Schulten[1], Juergen Koepke[2] and Hartmut Michel[2])) [1]Beckman Inst., UIUC, Urbana, IL 61801; [2]Max Planck Inst. for Biophys., Frankfurt, Germany (Spon. by Tom Ebrey)

We have determined the structure of the light-harvesting complex-II (LH-II) of *Rhodospirillum molischianum* by means of the molecular replacement method with 2.4 Å resolution X-ray diffraction data. The LH-II of *Rhodospirillum molischianum* is an octameric aggregate of a pair of polypeptides, commonly referred to as the α- and the β-apoprotein, which bind 24 bacteriochlorophyll-a (BCA) molecules and 8-12 lycopenes. The search model for the molecular replacement method was an aggregate of a homologous protein from LH-II of *Rps. acidophila* [(McDermott et al., Nature, 374, 517, (1995)] generated by means of comparative modeling, energy minimization and molecular dynamics simulations. The crystal structure displays two concentric cylinders of helical protein subunits with the α-apoproteins inside and the β-apoproteins outside. Sixteen B850 BCA molecules form a continuous overlapping ring with each BCA oriented perpendicular to the plane of membrane and sandwiched between the helical apoproteins. A ring of eight B800 BCA are parallel to the membrane plane. The binding sites for the B850 BCA are α-His-34 and β-His-35 respectively, while the B800 BCA binds to α-Asp-6. Eight membrane spanning lycopene pigments intertwine between tails of B850 and B800 BCA. The Q_y transition moments of the neighboring B850 and B800 BCA are parallel to each other, which is optimal for efficient Förster exciton transfer.

M-AM-G5

CRYSTALLIZATION OF PHYCOBILIPROTEINS OF THE CRYPTOMONAD ALGAE USING DETERGENTS AND UNUSUAL ADDITIVES ((Michael Becker, Milton T. Stubbs and Robert Huber)), Strukturforschung, Max-Planck-Institut für Biochemie, 82152 Martinsried, Germany. (Spon. by M.G. Rossmann)

Phycobiliproteins from 3 species of cryptomonad algae have been crystallized under a wide variety of conditions. The crystals were typically poorly ordered, or ordered in only 2 dimensions. However, crystals of phycoerythrin 545 of *Rhodomonas lens* that were well-ordered in 3-dimensions could be obtained under 2 different conditions, which included the detergent LDAO, as well as the additive propionamide in one case, and the ions Cs^+/Br^- in the other. The crystals show diffraction to at least 3.0 Å resolution and appear suitable for structural analysis. Both have the space group $P2_12_12_1$, with cell constants ≈ a = 86 Å, b = 108 Å, and c = 131 Å, and contain 2 dimers (ie., 2 x $(\alpha_2\beta_2)$) in the asymmetric unit. They show intense, strongly-polarized fluorescence, which should provide a basis for quantitive investigation of the role of exciton interactions in PE545.

M-AM-G6

ULTRAFAST ENERGY TRANSFER DYNAMICS IN C-PHYCOCYANIN. ((Ruth E. Riter, Maurice D. Edington, William M. Diffey, William J. Doria, and Warren F. Beck)) Department of Chemistry, Vanderbilt University, Nashville, TN 37235.

We have performed a series of femtosecond transient hole-burning studies with a range of pump wavelengths on the cyanobacterial light-harvesting protein C-phycocyanin in order to address the role that exciton-coupled chromophores play in excitation energy transfer. C-phycocyanin contains phycocyanobilin (open-chain tetrapyrrole) chromophores arranged so that dimers are formed across subunit interfaces in the trimeric and hexameric aggregation states. We are exploiting this structural organization in order to distinguish between intra-chromophore and dimer photophysics by comparing the response of a single phycocyanobilin chromophore in isolated α subunits with that of the chromophore dimers present in trimeric or hexameric preparations. We observe transient line broadening and a dynamic Stokes shift in α subunits on the 150-fs time scale; these phenomena report the presence of spectral diffusion processes involving intramolecular vibrational redistribution and protein-matrix solvation. In comparison, the transient spectra observed in preparations of C-phycocyanin trimers and hexamers exhibit a red shift on the <200-fs time scale, which precludes an assignment to Förster energy-transfer processes. The red shift involves interexciton state relaxation, which transfers population between the exciton states of a chromophore dimer. We have previously observed similar photophysics in the dimer systems of allophycocyanin trimers. We are considering how coherent energy-transfer processes involving exciton-coupled chromophores can play a role in directed energy-transfer mechanisms.

M-AM-G7

SPECTRAL VARIATION IN THE KENNARD-STEPANOV TEMPERATURE: A POSSIBLE NEW SIGNATURE OF EXCITED-STATE RELAXATION PROCESSES* ((R. S. Knox and D. A. Sawicki)), University of Rochester, Rochester, NY 14627.

The "universal relation" between fluorescence and absorption spectra developed by Kennard[1] and Stepanov[2] and others predicts that under ideal circumstances the ratio of the fluorescence intensity and absorption cross section will be related to the Boltzmann factor. The theory has been tested extensively and has been found to fail in an interesting way, namely, that an exponential dependence is present but the temperature derived from it experimentally (called T^*) usually differs significantly from the ambient temperature. It can range from $0.9T$ to $2T$ and can be excitation-frequency dependent. There is apparently no satisfactory explanation of T^* despite various modeling attempts. For example, inhomogeneous broadening goes a long way[3] but is not wholly satisfactory. We report a new approach to the problem. The inverse slope of is computed at each frequency, rather than being averaged over the entire data set. With appropriate unit conversion, the resulting quantity can be viewed as a spectral Kennard-Stepanov temperature. In most systems it is not at all constant and contains features such as distinct peaks. These features appear to be reproducible within the data sets we have analyzed and can be modeled in terms of finite relaxation times among manifolds of states. Analyses of several biologically interesting chromophores will be presented.

*Research supported in part by USDA grant 95-37306-2014
[1]E. H. Kennard, Physical Review 11, 29 (1918); 28, 672 (1925)
[2]B. I. Stepanov, Dokl. Akad. Nauk SSSR 112, 839 (1957)
[3]R. L. Van Metter and R. S. Knox, Chem. Phys. 12, 333 (1976)

M-AM-G8

NEAR-FIELD FLUORESCENCE MICROSCOPY AND SPECTROSCOPY OF PHOTOSYNTHETIC MEMBRANES

((Erik Sanchez, Laurens Mets+, Sunney Xie)) Pacific Northwest Laboratory, Environmental Molecular Sciences Laboratory, P. O. Box 999, MS K2-14, Richland WA 99352 and +University of Chicago, Department of Molecular Genetics and Cell Biology, 1101 E. 57th Street, Chicago, IL 60637

Recent advances in near-field optical microscopy offer exciting possibilities for conducting molecular spectroscopy at the nanometer dimension. A few groups, including ours, have recently demonstrated imaging the fluorescence of single dye molecules with sub diffraction resolution. Furthermore, we have completed a study on the fluorescence lifetimes of single dye molecules using time-correlated single photon counting.

In our efforts to study photosynthetic membranes, we have obtained near-field fluorescence and shear force images of intact photosynthetic membrane fragments such as those from the *Chlamydomonas reinhardtii* . The simultaneous images taken under buffer solution allow us to correlate the spectroscopic and topographic information in the native state. Lifetimes were also measured at various points within the membrane fragments. These studies are aimed at a spectroscopic mapping of the photosynthetic membrane and a detailed understanding of energy and electron transfer processes. Further progress along these directions will be presented.

DNA ENZYMES AND THEIR SUBSTRATES: MOTORS, MECHANISMS AND MORE

M-AM-SymII-1

EUKARYOTIC DNA TOPOISOMERASE II AS A MOLECULAR MACHINE AND DRUG TARGET. (J. C. Wang) Department of Molecular and Cellular Biology, Harvard University, 7 Divinity Avenue, Cambridge, MA 02138.

Eukaryotic DNA topoisomerase II is a homodimeric enzyme that catalyzes the ATP-dependent transport of one DNA double helix through an enzyme-mediated gate in a second DNA double helix. The enzyme belongs to the type II subfamily of DNA topoisomerases, which include bacterial DNA gyrase and DNA topoisomerase IV, and phage T2 and T4 DNA topoisomerases. *In vivo* the enzyme serves an indispensable role in chromosomal condensation and decondensation, as well as in the segregation of mitotic and meiotic pairs of entangled chromosomes. Extensive biochemical and structural studies of these enzymes have been carried out in the past two decades. A molecular picture of the intricate ATP-dependent reactions catalyzed by yeast DNA topoisomerase II has emerged from recent studies, including the determination of the three-dimensional structure of a 92-kD fragment of the enzyme. Type II DNA topoisomerases have also been identified as the targets of a large number of natural and synthetic antimicrobial and anticancer therapeutics, and mechanistic studies of the enzymes have provided new insights on the actions of these drugs.

M-AM-SymII-2

Mechanical Manipulation of Single DNA Molecules

by Carlos Bustamante
Institute of Molecular Biology and Howard Hughes Medical Institute,
University of Oregon, Eugene, Oregon

Recent advances in fine spatial control of macrosopic objects have made possible the study of the mechanical properties of individual molecules. The present capabilities and limitations of single-molecule manipulation methods will be reviewed, and applications to the study of the elasticity of single DNA molecules will be described in detail. The elastic behavior of the molecules both within and beyond the entropic elastic response regime will be discussed. Within the entropic regime the elasticity of the molecules can be rationalized by current theories of polymer statistics. Beyond this regime, however, the molecules display a number of novel and interesting features, such as a highly cooperative overstretching transition. Possible models to rationalize this behavior will be discussed.

M-AM-SymII-3

TRANSCRIPTION AGAINST AN APPLIED FORCE. ((H. Yin[1], M.D. Wang[2], K. Svoboda[3], R. Landick[4], S.M. Block[2], and J. Gelles[1])) [1]Dept. Biochemistry, Brandeis Univ., Waltham, MA 02254; [2]Dept. Molecular Biology, Princeton Univ., Princeton, NJ 08544; [3]AT&T Bell Labs, Murray Hill, NJ 07974; [4]Dept. Bacteriology, Univ. of Wisconsin, Madison, WI 53706.

The force produced during transcription by a single molecule of *Escherichia coli* RNA polymerase was measured using an optical trapping interferometer. Stalled ternary transcription complexes, consisting of single molecules of RNA polymerase, each associated with a single DNA template and nascent RNA transcript, were assembled in solution and adsorbed onto the surface of a coverglass inside a microscope flow cell. A polystyrene bead (0.52 mm diameter) was attached to the transcriptionally downstream end of each DNA molecule, so that the bead became tethered to the surface by its connection to the DNA and through the polymerase. Transcriptional elongation was then started by addition of nucleoside triphosphates, and the position of the bead was monitored with sub-nanometer accuracy by interferometry while calibrated, piconewton-sized forces in the direction opposing translocation of the polymerase were applied to the bead using the optical trap. Upon application of a sufficiently high force, movement by the enzyme complex could be mechanically slowed and eventually stalled, in many cases reversibly. At saturating nucleoside triphosphate concentrations, polymerase molecules stalled reversibly at an estimated mean applied force of ~14 pN. This force is substantially larger (by factors of 2-4) than those previously measured for the cytoskeletal motors kinesin and myosin, and it exceeds certain mechanical loads estimated to oppose transcriptional elongation *in vivo*. Raising the pyrophosphate concentration to a level that slowed transcription by a factor of ~2 did not alter the apparent stall force, suggesting that the efficiency of RNA polymerase mechanochemical energy transduction varies with chemical conditions. The results show that this nucleic acid polymerase is a powerful biological motor that can exert considerable force, and may operate with energy-conversion efficiencies comparable to those of prototypical mechanoenzymes.

M-AM-SymII-4

MECHANISMS OF HELICASE-CATALYZED DNA UNWINDING. ((Timothy M. Lohman)) Department of Biochemistry and Molecular Biophysics, Washington University School of Medicine, St. Louis, MO 63110

DNA helicases are ubiquitous motor proteins that couple the binding and hydrolysis of NTP to the unwinding of duplex (ds) DNA to form the single stranded (ss) DNA intermediates that are required for replication, recombination and repair. We are studying the DNA unwinding mechanisms catalyzed by two helicases from *E. coli*: Rep and Helicase II (UvrD) by examining the linkage of DNA binding, protein oligomerization and nucleotide binding using both thermodynamic and kinetic approaches. A dimer of the Rep protein is the active form of the helicase; however, the dimer forms only upon binding either ss or ds DNA. We have shown that nucleotides (ATP, ADP) allosterically control the DNA ligation states of the Rep dimer and based on these studies have proposed an "active, rolling" mechanism for the Rep dimer unwinding of duplex DNA. An essential intermediate is a complex, in which ss- and ds-DNA bind simultaneously to each subunit of a Rep dimer. This model predicts that Rep helicase translocation along DNA is coupled to ATP binding, whereas ATP hydrolysis drives unwinding of multiple DNA base pairs for each catalytic event. Rapid chemical quench-flow and stopped-flow fluorescence studies of Rep and UvrD-catalyzed DNA unwinding of a series of non-natural DNA substrates support the "active, rolling" mechanism and rule out a strictly "passive" mechanism of unwinding. Kinetic studies of DNA and nucleotide binding and ATP hydrolysis by wild type and mutant Rep proteins will be discussed that bear on the coupling of ATP binding and hydrolysis to translocation along DNA and DNA unwinding.

SODIUM CHANNELS II

M-AM-H1

INACTIVATION AND LIDOCAINE BLOCK PHENOTYPES IN WILD TYPE AND CHIMERIC (HEART AND SKELETAL MUSCLE) Na CHANNELS. ((J. C. Makielski, J. Limberis[1], L.-Q. Chen[2], R. G. Kallen[2])) University of Wisconsin, Madison, WI, University of Chicago[1], Chicago, IL, and University of Pennsylvania[2], Philadelphia, PA

Inactivation and lidocaine block phenotypes were investigated for the heart isoform (hH1), skeletal muscle isoform (rSkM1) and 7 chimeric channels that progressively incorporated more hH1 structure by substituting one or more hH1 domains (I-IV) and/or cytoplasmic linkers into rSkM1. Channels expressed in oocytes without a β-subunit were studied by two-micro-electrode voltage clamp. Three phenotypic differences were identified: tonic block by lidocaine (greater for hH1), macroscopic decay rate (more rapid for hH1), and steady-state inactivation midpoint $V_{½}$ (more negative for hH1). Tonic block by lidocaine (Hp=-120 mV) showed a graded response toward the hH1 phenotype as more hH1 domains were added to the chimera, suggesting that the structural determinants for the difference in lidocaine block are distributed over all domains. Chimera decay rates were not graded, but rather were as rapid as hH1 with any hH1 domain substitution, except for those chimera with hH1 III (and II-III linker) or hH1 IV (and III-IV linker) having intermediate decay rates. On the other hand, none of the chimera had $V_{½}$ as negative as hH1. Indeed some were more positive than rSkM1 and only chimera having both heart domains I and IV had $V_{½}$ intermediate between rSkM1 and hH1. Thus the inactivation properties decay rate and $V_{½}$ did not change in parallel over the chimera, and were not graded, suggesting separable and discrete structural requirements for these properties.

M-AM-H2

COMPARISON OF SLOW INACTIVATION IN HYPP-T698M AND F1304Q MUTANT RAT SKELETAL MUSCLE Na^+ CHANNELS ((T.R. Cummins and F.J. Sigworth)) Interdept. Neurosci. Prog. and Dept. of Physiol., Yale Univ. Sch. of Med., New Haven, CT 06510. (Spon. by G.G. Haddad)

We have shown that a mutation (rT698M) in the rat skeletal muscle sodium channel that corresponds to one of the human HYPP mutations (T704M) impairs slow inactivation. In an effort to better understand this impairment, we examined slow inactivation in another mutant, F1304Q, which has impaired fast inactivation. While only about 60% of rT698M current is slow inactivated after 5 min at -20 mV, nearly all of the F1304Q and WT current is slow inactivated. Recovery from prolonged depolarizations (-20 mV) for WT and F1304Q channels was fitted with two slow time constants. In contrast, roughly 40% of T698M channels recover with a much fast time constant that is identical to that for recovery from fast inactivation.

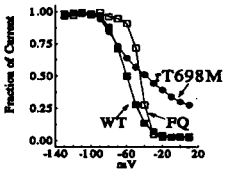

The figure shows s_{∞} curves for WT, F13 04Q and T698M channels. The data were obtained with 50 s prepulses to the voltage indicated, followed by a 30 ms recovery pulse (-100 mV) and 20 ms test pulse (-10 mV).

M-AM-H3

AN EXTERNAL PORE-LINING RESIDUE UNDERLIES SLOW INACTIVATION IN RAT SKELETAL MUSCLE (μ1) NA^+ CHANNELS ((Jeffrey R. Balser, Eduardo Marban, Gordon F. Tomaselli))The Johns Hopkins University School of Medicine, Baltimore, MD 21205.

Fast inactivation in Na channels is mediated by cytoplasmic occlusion of the pore by III-IV linker residues, but the structural features of the slow inactivation process have not been described. When μ1 Na channel α subunits are expressed without β_1 in *Xenopus* oocytes and are briefly depolarized, recovery consists of a rapid component derived from fast-inactivated channels, followed by a prominent slow component reflecting slow-inactivated channels. In potassium channels, external pore-lining residues mediate C-type inactivation. To determine whether similarly-placed residues influence Na channel slow inactivation, site-directed mutagenesis was performed in the external P-segments of all four domains of the μ1 Na channel α subunit. Wild-type and mutant channels were expressed in *Xenopus* oocytes, and whole-cell Na currents were recorded using a two-electrode voltage clamp. Serial cysteine mutagenesis in the domain I P-segment has yielded only one residue, W402, that influences Na channel gating. In addition to hastening the rate of current decay during depolarization, the rate of recovery from inactivation at -100 mV was accelerated through a marked reduction in the magnitude of the slow component of recovery. W402C exhibited no slow inactivation even with 2.5 sec depolarizing pulses, which suffice to slow-inactivate > 70% of wild-type channels. Cysteine substitution of homologous residues in domains II-IV that complete a ring of tryptophans in the external pore do not alter slow inactivation. We conclude that this external, pore-lining residue strongly influences slow inactivation in the μ1 Na channel.

M-AM-H4

SINGLE CHANNEL STUDY OF SLOW INACTIVATION OF Na^+ CHANNELS. ((R.L. Ruff)) Cleveland VAMC, Case Western Reserve Univ., Cleveland, OH 44106

Mammalian skeletal muscle has two distinct inactivation processes. Fast inactivation (FI) closes channels on a msec time scale, whereas slow inactivation (SI) takes seconds to minutes. FI terminates the action potential. SI operates at more negative potentials than FI, so that SI regulates the Na^+ current as a function of the membrane potential. I recorded macroscopic I_{Na} with a loose patch voltage clamp and single channel currents were measured simultaneously on an adjacent region of membrane from the same rat skeletal muscle fiber. The holding potentials of the two clamps were kept the same. This enabled simultaneous monitoring of the impact of SI on macroscopic and single channel currents. Changes in the macroscopic currents due to SI were accompanied by changes in the maximum number of excitable channels within a patch of membrane. The single channel current amplitudes and open-times did not change during the development of and recovery from SI. Therefore, SI resulted from Na^+ channels accumulating in a non-conducting state. Five different Markovian kinetic models have been proposed to describe SI of Na^+ channels. The major distinction among the models is whether the SI state is accessed through only the: open, FI or closed channel states or the open and FI state but not the closed state. Using different pulse protocols I determined that channels are not required to transit through only the open, closed or FI states to access the SI state. In addition, channels can enter the SI state if they are restricted to the closed state. The data was most consistent with a model in which the SI state can be accessed from either the open, closed or FI states. [Supported by the Office of Research and Development, Medical Research Service of the Department of Veterans Affairs]

M-AM-H5

EVIDENCE FOR A ROLE OF AN S4-S5 LINKER IN SODIUM CHANNEL INACTIVATION. ((L. Tang, R.G. Kallen and R. Horn)) Dept of Physiol, Jefferson Medical College, Philadelphia, PA 19107; Dept of Biochem & Biophysiol, Univ. of Penn., Philadelphia, PA 19104.

A pair of conserved methionine residues, located on the cytoplasmic linker between segments S4 and S5 in the fourth domain of human heart Na channels, plays a critical role in the kinetics of inactivation. Substitution of these residues by either glutamine (MM/QQ) or alanine (MM/AA) increases the inactivation time constant at depolarized voltages, shifts steady-state inactivation in a depolarized direction, and decreases the time constants for recovery from inactivation. The inactivation time constant at 0 mV is 3.4-fold (MM/QQ) and 9.4-fold (MM/AA) greater than in wild-type channels. The data indicate that the mutations increase the rate constant for unbinding of a hypothetical inactivation particle from its docking site with little effect on the association rate constant. We examined the block of outward currents by cytoplasmic application of the pentapeptide KIFMK, which has been postulated to restore inactivation to Na channels mutated to remove inactivation (Eaholtz et al., *Neuron* 12:1041, 1994). KIFMK produced a concentration-dependent, voltage-independent block of MM/QQ and MM/AA channels. Although MM/QQ inactivates ~2.5-fold faster than MM/AA, the estimated rate constants for peptide block & unblock do not differ in these mutants, suggesting that either i) KIFMK does not compete with the natural inactivation particle for its site, or ii) the MM/XX mutations do not directly affect the affinity of the inactivation particle for its site.

M-AM-H6

MOLECULAR BASIS OF CHARGE MOVEMENT IN VOLTAGE-GATED SODIUM CHANNELS. ((N. Yang, A.L. George and R. Horn)) Dept of Physiol, Jefferson Medical College, Philadelphia, PA 19107; Dept of Medicine, Vanderbilt School of Medicine, Nashville, TN 37232

The 8 basic residues in the 4th transmembrane segment (S4) of domain 4 (D4) of the human skeletal muscle Na channel (hSkM1) were individually substituted by cysteines. Voltage-dependent exposure of cysteines was revealed by the effects of membrane-impermeant cysteine reagents on gating (Yang and Horn, '95, *Neuron* 15:213). The second and third substituted residues (from the outside: R2C & R3C) can be modified by reagents from the cytoplasmic surface of the channel at hyperpolarized voltages, and from the extracellular surface at depolarized voltages, supporting an outward movement of S4 during depolarization. R4C, however, resides on the cytoplasmic side of the membrane at all voltages. We find no evidence that the bottom 4 basic residues (R5-R8) are accessible extracellularly at any voltage. S4/D4 charge movement can therefore be explained by the movement of a few residues all the way across the membrane field, rather than many residues each moving a short electrical distance. The maximum distance between R3C and R4C cannot be >11 angstroms, suggesting that this S4 segment passes through a short 'channel' containing at most one basic residue at a time. These results show that the energetic problems of moving charged S4 residues across hydrophobic regions of the protein are solved in the same way that many ion channels achieve highly selective and rapid permeation through an open pore, by restricting the contact region between the permion and its channel.

M-AM-H7

ARE THE m_∞ AND h_∞ OF Na CHANNEL COUPLED? POSSIBLE ROLE OF CYTOSKELETON. ((V.A. Maltsev and A. I. Undrovinas)) Henry Ford Heart and Vascular Institute, Detroit, MI 48202.

The midpoint potential of both h_∞ and conductance (V½h and V½G) was monitored in 105 rat ventricular cardiomyocytes during long-lasting recordings (63±5 min, mean±SE) at 22-24°C by the whole-cell patch clamp. In control cells both V½h and V½G shifted with time toward hyperpolarizing potential in exponential manner. The shift of V½G was faster (τ= -13.8±1 min, n=17), but varied in a smaller range (9±1.3 mV) as compared to that for V½h (τ= -35.4±3.3 min and 20.4±1.6 mV; n=24, $p<0.01$). An F-actin disrupter, cytochalasin-D (20 μM) induced a linear shift of V½h with a faster initial rate. In contrast, phalloidin, an F-actin stabilizer, alone or combined with a microtubule stabilizer, taxol (both 100 μM), induced an initial plateau (27±5 min, n=20) in the time course of V½h. The cytoskeleton-related V½h component (20.7±2.7 mV) of the shift was determined as the difference between the plateau level and asymptotic level of exponential shift. The time-dependent shifts of V½G and V½h were not parallel. The best fit for the V½G-V½h relationship (n=817, in 40 control cells, see Figure) was evaluated as a parabolic function with a degree of 1.8. The V½G-V½h relation shifted toward higher and lower V½G values in cells with disrupted and stabilized cytoskeleton, respectively. The cytoskeleton-related component (5.4 mV) of V½G variations was determined as a sum of the shifts. Conclusions: The h_∞ and m_∞ are not coupled in conventional linear manner. The degree of freedom for both h_∞ and m_∞ is determined by the cytoskeleton-related components.

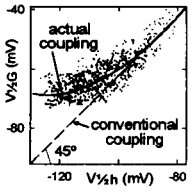

M-AM-H8

MODULATION OF CHIMERICAL SODIUM CHANNELS BY PROTEIN KINASE A ((B. Frohnwieser, J. Chen[1], R.G. Kallen[1] and W. Schreibmayer) Institute for Medical Physics and Biophysics, A-8010 Graz, Austria and [1]: Institute for Biochemistry and Biophysics, Philadelphia PA 19109. (Spon. by H.A. Tritthart)

Stimulation of cyclic AMP dependent protein kinase (PKA) leads to an increase in the activity of the rat cardiac SkM2 sodium channel isoform, expressed in oocytes of *Xenopus laevis*. Site directed mutagenisis of the 'strong' PKA phosphorylation consensus sites on α_{SkM2} did not abolish this effect, indicating that either another, hitherto unknown structural determinant on SkM2 becomes posphorylated by PKA or the effect is mediated by an additional, hitherto unknown protein (Schreibmayer et al. (1994)). In this study, we were able to show that also the human cardiac sodium channel α-subunit (α_{hH1}) is subject to PKA-dependent modulation. Since the skeletal muscle isoform of voltage dependent sodium channels, α_{SkM1}, does not react to PKA activation, we constructed a set of chimerical channels, comprising partially α_{SkM1} and α_{hH1}. Most excitingly, most of these constructs were functional. Whereas some of them exerted the PKA effect, others did not and by engineering four generations of constructs we were able to assign to the cytosolic loop interconnecting the first and the second transmembrane domain of the hH1 sodium channel the role of a PKA substrate or an acceptor for the hypothetical regulatory protein.

Schreibmayer Wolfgang, Bibiane Frohnwieser, Nathan Dascal, Dieter Platzer, Brigitte Spreitzer, Rudolf Zechner, Roland G. Kallen and Henry A. Lester. β-adrenergic modulation of currents produced by rat cardiac Na+ channels expressed in Xenopus laevis oocytes. Receptors and Channels 2: 339-350. (1995)

Supported by the Austrian Research Foundation (P9249).

M-AM-H9

IDENTIFICATION AND PROPERTIES OF FIVE FUNCTIONAL GATING MODES IN SINGLE CARDIAC Na^+ CHANNELS. ((Th. Böhle and K. Benndorf)) Dept. of Physiology, University of Cologne, D-50931 Cologne, Germany. (Spon. by C. Methfessel)

In cell-attached membrane patches of mouse ventricular heart cells, unitary Na^+ currents were recorded at 20 kHz band width and room temperature. Extraordinarily tipped patch pipettes (resistance up to 150 MΩ in 200% Tyrode) with thick walls (ratio of outer to inner diameter 4/1 or 8/1) yielded a seal resistance of up to 1000 GΩ. In patches containing one and only one channel, fast and reversible switches between different modes of Na^+ channel action could be identified by plotting the long-time course of the averaged current per trace, yielding life times of the modes in the range of some seconds to several minutes. Fast back and forth switching between two modes caused a biphasic time course of inactivation in the ensemble-averaged current. Five modes (F, M1, M2, S, and P) were specified, which differ in the time course of macroscopic inactivation, steady-state activation and inactivation, occurrence of fast flickering and heterogenous levels of single channel current, as well as open-time and first-latency distributions.

M-AM-I1

MICROTUBULE-ASSOCIATED PROTEINS AND THE FLEXIBILITY OF MICROTUBULES. ((Jeffrey C. Kurz and Robley C. Williams, Jr.)) Dept. of Molecular Biology, Vanderbilt Univ., Nashville, TN 37235.

Is the flexibility of native microtubules altered by the binding of microtubule-associated proteins (MAPs)? To find out, flexibility was measured *in vitro* by two established techniques: assessment of bending in a flow of buffer (Venier et al. (1994) J.B.C. *269*, 13353) and observation of random thermal fluctuations in the microtubule's shape (Gittes et al. (1993) J.C.B. *120*, 923). Microtubules were assembled from purified tubulin, from tubulin plus saturating concentrations of the naturally occurring mixture of MAPs, and from MAP-containing microtubule protein. Flagellar axonemal pieces were used as nuclei, assembly was carried out in the presence of GTP, and observation was by video-enhanced DIC microscopy. At 37° and pH 6.9, the flow technique yielded persistence lengths of 8.4 (± 2.2 S.D.) mm without MAPs and 9.4 (± 2.7 S.D.) mm with MAPs, corresponding to flexural rigidities of 3.6 (±1.0 S.D.) x 10^{-23} Nm^2 and 4.0 (±1.3 S.D.) x 10^{-23} Nm^2, respectively. Thermal fluctuation measurements gave persistence lengths of 6.2 ± 0.8 without MAPs and 6.5 ± 0.8 mm with MAPs. No significant dependence of flexibility on the length of the microtubules was apparent. We conclude that binding of MAPs to native microtubules *in vitro* has little or no effect on their flexibility. MAP-induced effects on cellular shape *in vivo* are therefore likely to be caused by other factors, such as formation of microtubule bundles. Supported by NIH Grant GM25638.

M-AM-I2

DYNAMICS OF Ca^{2+}-CONTAINING VESICLES IN LEUKOCYTES. ((S.H. Gilbert, R.A. Tuft, D.S. Bowman, K.E. Fogarty, V. Mekagaroon and F.S. Fay)) Biomedical Imaging Group, UMMC, Worcester MA 01605.

Regional differences in cytosolic [Ca^{2+}] are essential in establishing and maintaining polarity in many cells. In newt eosinophils, both $[Ca^{2+}]_i$ and sensitivity to local increases in $InsP_3$ are larger in the perinuclear-centrosomal region than elsewhere. This region also has a high density of $DiOC(6)_3$-labelled structures. To determine which structures are Ca^{2+} stores, live active cells were loaded with the AM esters of several Ca^{2+} probes, including Calcium Green 5N (K_d ~3 μM), and through-focus fluorescence images acquired at 2-10-sec intervals. The fluorophore was excited for 2-5 msec and focus changed in 2-3 msec, to acquire images in 30 focal planes (total thickness 10 μm) in 0.2-0.3 sec. Both CGr5N and $DiOC(6)_3$ labelled vesicular structures ~1-3 μm in diameter whose density was highest near the centrosome, where they seemed to aggregate (or coalesce) and redisperse within a few seconds. A few highly mobile vesicles were present in the nuclear-septal region. Vesicle density in the front of the cell was greater than expected from experiments with spatially uniform photorelease of $InsP_3$, raising the possibility that all Ca^{2+}-containing vesicles may not be sensitive to $InsP_3$. This could account for the observation that the rate of decline in $[Ca^{2+}]_i$ is spatially uniform after photorelease of Ca^{2+}.

M-AM-I3

POLYMERIZATION RATCHET. ((A.Mogilner)) ESPM, U. of California, Berkeley, Ca 94720-3112. (Spon. by G. Oster)

The movement of many types of embryonic cells, as well as certain pathogenic bacteria, is driven by polymerization of actin. I will present a model of how polymerization of actin or microtubules generate forces by rectifying the thermal bending motions of actin filaments. In addition to providing a motive force for movement, the "ratcheted" polymerization generates the spatio-angular pattern observed in the polymer network of lamellipodia of motile cells.

M-AM-I4

Membrane Networks in Large Deformations: . ((D. Discher, S.K. Boey, D.H. Boal.)) Departments of Physics, Simon Fraser Univ.,Univ. of British Columbia. B.C. Canada V5A 1S6 (Spon. by D.H. Boal).

Analyses of cytoskeletal network models in large deformation are motivated in part by the order of magnitude variations observed for both surface density and shear strain in the spectrin-based network of the red cell (*Science* 266:1032). To understand the elasticity of such quasi-ordered molecular nets, discrete element networks in large homogeneous and non-homogeneous deformation have been analysed. The most detailed cytoskeletal model is based on a bead and spring model of filamentous spectrin. Model spectrin chains are tied together at their ends into a triangular network tacked above a hard wall. MC simulations under a fixed, low surface pressure or uniaxial stress show this model behaves as a low-temperature, triangular network of Hookean springs where the ratio of surface bulk modulus to shear modulus is two, agreeing closely with experiments. As deformations become larger, the networks become more ordered and the chains stiffen. Simplified coarse-grained models with these and additional features have also been constructed and analysed or simulated in stress and strain ensembles. The finite length effect of network chains is captured by a square-well potential, integrable exactly in mean field analyses. The exact strain energies of Hookean spring networks at low temperature are shown to be anisotropic, a general feature expected of these models. With small enough elemental spring constant, a crossover occurs from a nearly isotropic and stiff network in small deformation to a softer, entropically-suppressed regime. MC simulations of these simple but discrete element models in a non-homogeneous deformation like micropipette aspiration show results similar to experiments. In sum, discretized models of membrane networks offer novel insights and raise new questions of cytoskeletal mechanics.

M-AM-I5

CRYSTAL STRUCTURE OF THE MOTOR DOMAIN OF NCD, A KINESIN-RELATED MOTOR THAT MOVES ALONG MICROTUBULES WITH THE OPPOSITE POLARITY TO KINESIN ((E. Sablin*, R. D. Vale*#@, R. J. Fletterick*)) Depts. of Biochemistry* and Pharmacology# and the Howard Hughes Medical Institute@, University of California, San Francisco, CA 94143. (Spon. by D. Pierce)

The kinesin superfamily of motor proteins all contain a motor domain of ~340 amino acids that are 30-40% identical in amino acid sequence. Unlike myosin motors which all move in the same direction along actin, some members of the kinesin superfamily, such as the Drosophila motor ncd, move along a microtubule in the opposite direction to kinesin. We have solved the three dimensional structure of the ncd motor domain to 2.5 Å resolution and have compared it to the structure of the kinesin motor domain. The positions of conserved amino acids residues in the kinesin superfamily in the three dimensional structure and the contacts between the nucleotide and the protein will also be reported. The data provides insight into the allosteric coupling between nucleotide hydrolysis and microtubule binding and the possible origin of the polarity difference of these two microtubule motors.

M-AM-I6

TRACTION FORCES DURING CELL DIVISION AND LOCOMOTION. ((K. Burton & D.L. Taylor)). Center for Light Microscope Imaging and Biotechnology, Carnegie Mellon University, Pittsburgh, PA, 15213.

The magnitude and spatial distribution of traction forces produced by Swiss 3T3 fibroblasts have been studied during cytokinesis and daughter cell migration. Traction forces were monitored using an extension of the method introduced by Harris et al. (*Science* 208:177, 1980) in which cells apply traction forces to silicone rubber substrata via sites of adhesion and produce strain which we visualized using video-enhanced Normarski DIC microscopy. The compliance of the substratum can now be altered so that its sensitivity to stress matches the strength of the cells under study. The silicone substrata have been calibrated in terms of compliance by measuring the strain resulting from the application of known forces using calibrated glass microneedles. Stress can cause sheets to bend into wrinkles and elastic moduli calculated for this type of strain have allowed measurements of forces ranging from nanonewtons to micronewtons. The sheets are highly elastic and most wrinkles disappear as soon as an applied stress is removed. The silicone polymer we use also permits high quality interference-reflection and fluorescence microscopy and we have shown a strong dynamic correlation between the location of myosin II in cytoskeletal fibers, sites of membrane-substratum contact, and traction forces at those sites. During formation of the cleavage furrow, wrinkles transiently formed in the sheet at the equator and their orientation indicated that forces were centered on the furrow, presumably arising from myosin II which localizes there. These forces were found to be 1-2 orders of magnitude lower than those produced by spread cells. As daughter cells respread and attempted to disconnect, forces often transiently rose until the cells separated. At the same time, blebs and filopodia applied traction forces on the order of 10-100 nN.

M-AM-I7

CRYSTAL STRUCTURE OF THE MOTOR DOMAIN OF KINESIN REVEALS STRUCTURALHOMOLOGY TO THE CATALYTIC DOMAIN OF MYOSIN. ((F.J. Kull*, R.D. Vale*#@, Robert J. Fletterick*)) Depts. of Biochemistry* and Pharmacology# and the Howard Hughes Medical Institute@, University of California, San Francisco, CA 94143. (Spon. by D. Cherbavaz)

Kinesin is the prototype of a large family of microtubule-based molecular motors that perform of variety of force-generating tasks including axonal transport and chromosome segregation. The crystal structure of the human kinesin motor domain with bound ADP was determined to 1.8 Å resolution. Unexpectedly, the entire motor consists of a single domain. This domain exhibits a striking structural similarity to the core of the catalytic domain of the actin-based motor myosin, which was not previously suspected given the absence of any significant amino acid identity between these proteins. Although kinesin and myosin operate on different cytoskeletal polymers and have different ATPase kinetics, these data suggest that these two classes of mechanochemical enzymes very likely evolved from a common precursor and may share a common force-generating strategy.

M-AM-I8

ELASTICITY OF SEMIFLEXIBLE BIOPOLYMER NETWORKS. ((F.C. MacKintosh#, J. Kas* and P.A. Janmey*)) # Dept. of Physics, Univ. of Michigan, Ann Arbor, MI48109, USA *Div. of Exp. Med., Brigham and Women's Hosp., Harvard Medical School, Boston, MA02115, USA

A major function of the cortex of eukaryotic cells is to provide mechanical stability. This network, which consists of a network of actin filaments, also plays an essential role in cell motion. A basic model for the origin of viscoelasticity of the actin cortex and how individual filament stiffness affects the elastic properties of such a network is essential to understand how nature controls the properties of the cytoskeletal rim. However, to date, little is known about how the specific properties of cytoskeletal filaments lead to the important mechanical properties of the cortex in vivo. The focus of our work is on modeling of the viscoelastic properties of the actin cortex, and especially the relationship of these properties to the mechanical properties of the single filaments. We describe a theoretical model which can provide an appropriate description of the viscoelesticity of actin networks, and which allows us to identify the important factors modulating the elastic response. In particular, our model can account for the large storage modulus observed in actin solutions and gels. Our considerations show that the strength of an actin gel depends strongly on the filament stiffness in contrast to gels of flexible polymers.

NUCLEIC ACID-PROTEIN COMPLEXES I

M-AM-J1

BINDING OF IONIC LIGANDS TO BIOPOLYMERS. ((D. Stigter and K. A. Dill)) Department of Pharmaceutical Chemistry, University of California San Francisco, San Francisco, CA 94143

Ionic ligands can bind to polyelectrolytes such as DNA or charged polysaccharides. We develop a Poisson -Boltzmann treatment to compute binding constants as a function of ligand charge and salt concentration in the limit of low ligand concentration. For flexible chain ligands, such as oligopeptides, we treat their conformations using lattice statistics. The theory predicts well the salt dependence and binding free energies of Mg ions to polynucleotides, of hexammine cobalt(III) to calf thymus DNA, of polyamines to T7 DNA, of oligolysines to poly(U) and poly(A), and of tripeptides to heparin, a charged polysaccharide. One parameter is required to obtain absolute binding constants, the distance of closest separation of the ligand charge to the polyion.

M-AM-J2

Electrostatic Effects of Ligand Charge Distribution and DNA Length on Peptide-DNA Interactions ((Wentao Zhang and M. Thomas Record, Jr.)) Departments of Chemistry and Biochemistry, University of Wisconsin, Madison, WI 53706.

Coulombic and hydrophobic interactions, and coupled folding transitions are important determinants of stability and specificity of binding proteins to DNA. We have investigated the nonspecific binding of 17-residue, tetravalent alanine-lysine peptides with different initial charge distribution to double-stranded DNA using fluorescence spectroscopy. We find the nonspecific DNA-binding of these peptides is determined primarily by the overall positive charge on the peptides, with the binding constants being modulated only to a relatively small extent by the initial charge distribution in these peptides. Effects of DNA length on ligand-DNA interactions are investigated by monitoring the binding of an oligolysine octacation to single-stranded dT-mers of different lengths. At physiological cation concentrations (0.1-0.3 M) the binding to poly(dT) is much stronger per site and significantly more [salt]-dependent than binding to short dT-mers. These large differences are consistent with Poisson-Boltzmann calculations for a model that characterizes the charge distributions with key preaveraged structural parameters. Therefore, our results demonstrate that long-range electrostatic interactions involving phosphate charges that flank the complexation site on a polymeric DNA make large contributions to both the magnitude and the [salt]-dependence of its binding interactions with simple oligocationic ligands.

M-AM-J3

CALCULATION OF DNA BASE-AMINO ACID INTERACTION ENERGIES FOR STRUCTURES AND SEQUENCES ((Brooke Lustig and Robert L. Jernigan*)) Chemistry Department, San Jose State University, San Jose, CA, 95112. *Laboratory of Mathematical Biology, NCI, NIH, Bethesda, MD, 20892.

We derive normalized relative interaction energies for each of the four bases interacting with a specific amino acid, using data from combinatorial multiplex DNA binding of zinc finger domains [Desjarlais, J. R. & Berg, J. M. (1994) Proc. Natl. Acad. Sci. USA **91**, 11099]. The five strongest interactions are observed for lysine-guanine, lysine-thymine, arginine-guanine, aspartic acid-cytosine and asparagine-adenine. The rankings for interactions with the four bases appear to be related to base-amino acid charges. Also, similar normalized relative interaction energies are derived by using DNA binding data for Cro and λ repressors and the R2R3 c-Myb protein domain [Takeda, Y., Sarai, A. & Rivera, V. M. (1989) Proc. Natl. Acad. Sci. USA **86**, 439; Sarai, A. & Takeda, Y. (1989) Proc. Natl. Acad. Sci. USA **86**, 6513; Sarai, A. (personal communication)]. These energies correlate well with the combinatorial multiplex energies, and the strongest cases are similar between the two sets. They also correlate well with similar relative interaction energies derived directly from frequencies of bases in the bacteriophage λ operator sequences. These results suggest that such potentials are general and that extensive combinatorial binding studies can be used to derive potential energies for DNA-protein interactions.

M-AM-J4

CHARACTERIZATION OF PEPTIDE/DNA COMPLEXES FOR GENE DELIVERY. ((John G. Duguid[1], Cynthia Li[1], Mark J. Logan[1], Jenna Claspell[1], James T. Sparrow[2], Louis C. Smith[2] and Alain Rolland[1])) [1]GENEMEDICINE, INC., 8301 New Trails Drive, The Woodlands, TX 77381[2]Department of Medicine, Baylor College of Medicine, One Baylor Plaza, Houston, TX 77030

Novel synthetic peptide-based gene delivery systems have been prepared by formulating plasmid DNA with carrier peptide analogs and an amphipathic peptide shown to be lytically active at pH 5.0 but not pH 7.4. The carrier peptides are synthesized as novel analogs of poly-L-lysine and used to condense DNA into nanoparticles with a hydrodynamic diameter below 100 nm. Size characteristics of the carrier peptide/DNA complexes have been determined as a function of peptide/DNA charge ratio, number of lysines per peptide, DNA concentration, and time. Particle sizing data reveal complex instability near 1/1 charge ratios and in the presence of carriers containing less than 5 lysine residues. As the DNA concentration is raised from 20-100 μg/ml, a simultaneous increase in particle size is observed. Above 100 μg/ml, a size plateau is reached and is constant out to 400 μg/ml. For most complexes, the particle size was stable for over 100 hours. The gene delivery system was activated by incorporating an amphipathic peptide into the carrier/DNA complex. Transfection data on C_2C_{12} myotubes reveal that both carrier and amphipathic peptides are necessary for effective gene delivery. A comparison between carrier peptide analogs that vary in the number of lysine residues indicates an optimal number of core lysines (6-8) necessary for effective myotube transfection. Analysis of the sizing data suggests that a lower number of lysine residues (<5) fails to hold the peptide/DNA complex together in a condensed particle. At relatively larger numbers of lysine residues (~40), the gene delivery complex becomes cytotoxic. A comparison of transfection data with a variety of physical characterization methodologies has revealed that there is a strong correlation *in vitro* between transfection efficiency and several physical properties of the complex, including DNA dose, zeta potential, and peptide lytic activity.

M-AM-J5

DNA STRUCTURES IN FILAMENTOUS BACTERIOPHAGES.

((Loren A. Day)) Public Health Research Institute, New York, NY 10016

The genus *Inovirus* encompasses the slender filamentous single-stranded circular DNA viruses that infect bacteria. In each of these viruses the DNA is a helix of two anti-parallel strands held in the core of a cylindrical shell of thousands of copies of a small helical protein. At the ends of the virus the circular DNA folds back on itself. The part of the small protein subunit in contact with the DNA is highly basic and its local α-helix axis is almost parallel to the DNA axis. These basic features are common to all species of the genus, but there are dramatic differences in the actual DNA structures present. For example, in Pf1 there is exactly one nucleotide per protein subunit (n/s = 1), the DNA and the shell have the same helical symmetry (two subunits and two nucleotides comprise the asymmetric unit), and the DNA phosphates are in at the center and the bases are unstacked and out, interacting with protein (1, 2). Yet in C2 n/s = 2, the DNA has a pitch near +30 Å, and the bases are stacked at the center (3). Exact integer stoichiometry allows the protein shell and DNA to have the same helical symmetry, but whether they are the same in C2 has not been established. Finally, in Ff (M13, fd, f1) n/s = 2.4, the DNA has +28 Å pitch, and the bases are stacked at the center, yet the protein shell and DNA do not have the same helical symmetry (2 and references therein). Some of the structural data for this group of viruses and the DNA-protein symmetry matching problems defined by these data will be presented.

(1) D.J. Liu and L.A. Day, *Science* **265,** 671 (1994); (2) C.J. Marzec and L.A. Day, *Biophys. J.* **67,** 2205 (1994); (3) L.G. Kostrikis *et al., Biochemistry* **34,** 4077 (1995).

M-AM-J6

NUCLEIC ACID-INTERACTIVE PROPERTIES OF BACTERIOPHAGE T4 GENE 32 PROTEIN AND ITS SUBSTITUENT DOMAINS

((R.L. Karpel, L.A. Waidner, E.K. Flynn and H.I. Ziserman)) Department of Chemistry and Biochemistry, University of Maryland Baltimore County, Baltimore, MD 21228.

We are studying the nucleic acid binding, helix-destabilizing, and renaturing activities of full-length and truncated bacteriophage T4 gene 32 protein, a single-strand specific binding protein. We have cloned and overexpressed variants lacking the C-terminal domain ('I) or the N-terminal domain ('II). Although intact 32 protein does not lower the T_m of natural double-stranded DNA, 'I readily brings about both ds DNA denaturation (above T_m) and renaturation (below T_m). The T_m-depressing activity is possibly related to an increased affinity of the truncated product for ds DNA, but preliminary binding experiments show no major differences between 'I and full-length protein. Conditions under which oligonucleotides hybridize to ss DNA in the presence of 'I have been established, and there are indications that this protein can overcome secondary structural impediments in sequencing reactions. We have developed an assay employing DNA amplification which is being used to determine the effect of 'I and other binding proteins on the fidelity of hybridization reactions. The presence of the C-terminal domain confers resistance to the action of endoproteinase Arg-C on the central (core) domain, which contains the nucleic acid binding surface. Oligonucleotides selectively protect the internal *LAST* ($[Lys/Arg]_3[Ser/Thr]_2$) sequence, which we have previously proposed to be within this surface. The presence of the C-domain in the protein also reduces the affinity for oligonucleotides. The dependence of binding on oligonucleotide length provides further insights into the protein's structure-function relationships.

M-AM-J7

INTERACTIONS OF HIV-1 NUCLEOCAPSID PROTEIN WITH SINGLE-STRANDED NUCLEIC ACIDS.

((M. A. Urbaneja, R. J. Fisher, M. Fivash, S. Bladen, A. Rein, L. O. Arthur, L. E. Henderson, and J. R. Casas-Finet)) AIDS Vaccine Program and Lab. of Cellular Biochemistry, SAIC; ABL-BRP, and Data Management Services, NCI-FCRDC, Frederick, MD 21702. (Spon. by A. Wallqvist)

Nucleocapsid (NC) and *gag* precursor proteins from all known strains of lenti- and oncoretroviruses contain one or two copies of an absolutely invariant Zn-binding motif, **Cys-X_2-Cys-X_4-His-X_4-Cys**, that are essential for RNA genome packaging and infectivity. Non-specific nucleic acid binding by NC is significant in retroviral replication. We have studied HIV-1 NC p7 binding to $(dT)_n$ oligonucleotides (n = 4, 8, 16, 64) and poly(dT) monitoring its Trp fluorescence. wt p7 and a finger replacement mutant, p7(2.2), bound $(dT)_{n>8}$ in 13 mM Na^+ with *ca.* 10^8 M^{-1} affinity, which was markedly reduced by increasing [NaCl]. 1, 2 and 7-8 p7 molecules were bound to $(dT)_8$, $(dT)_{16}$, and $(dT)_{64}$, resp. Binding to poly(dT) occurred with an occluded site size of ~ 6 nucleotide bases and marginal cooperativity. Real-time BIAcore measurements of the binding of wt p7, p7(1.1), p7(2.1) and p7(2.2) to immobilized $(dT)_n$ homopolymers (n = 8, 16, 32, 64), and to heteropolymeric DNA lattices with succesive truncations from the 5' terminus (n = 52, 40, 28, 20, 13) were carried out at 150 mM NaCl using surface plasmon resonance detection. wt p7 binding was observed to the 52-mer with a 3:1 stoichiometry, whereas it was 2:1 for the 40- and 28-base sequences, and 1:1 for the shorter DNAs. Equilibrium binding isotherms with p7 and p7(2.2) detect 2 sites of dissimilar affinities in the 28-mer oligo. Computer-assisted base pairing predictions point to G/T- and T/C-rich sequences as the high and low affinity sites, in agreement with p7 base preferences: G > T > C > A. Both BIAcore and fluorimetric results suggest that the binding sites recognized by p7 mutants are not identical to those to which wt p7 binds. No interaction was detected with peptides spanning the 1st (res. 13-30) or 2nd (res. 34-51) zinc fingers or the N- or C-terminal halves of p7, alone or in combination, nor with the half-site oligo $(dT)_4$, indicating that both structural units contribute to the binding free energy. A peptide containing both zinc fingers (res. 13-51) exhibited lower affinity than full-length p7, suggesting that charged sequences flanking the fingers also interact. $(dT)_8$ labelled with fluorescein at both the 3' and 5' terminii exhibited quenching of the extrinsic probe in the presence of myristylated HIV-1 *gag* precursor, indicative of binding.

M-AM-J8

THE STRUCTURE AND ACTIVITIES OF THE MOBILE LOOP L2 OF RECA, THE HOMOLOGOUS PAIRING DOMAIN.

((L. Wang, O.N. Voloshin, H. Kinal and R.D. Camerini-Otero)) NIDDK, NIH, Bethesda MD 20892

Binding of E.coli RecA protein to both DNA substrates is essential for its critical role in homologous recombination. Previous work from our lab. has shown that the region of RecA that binds to ssDNA and dsDNA is a 20 amino acid spanning mobile loop L2. This 20 amino acid peptide is also capable of carrying out the hallmark reactions mediated by the whole RecA protein: pairing (targeting) of a single-stranded DNA to its homologous site on a duplex DNA and the formation of homology-dependent stable joint molecules. Surprisingly, the F203W mutant peptide showed much better binding and pairng activities than the wild type peptide. In the course of this reaction, the DNA binding peptides adopt a β structure as monitord by CD. Their ability to form both inter- and intrapeptide β-structures seems to be an intrinsic property of the peptide that can be stimulated by DNA as well as by changes in pH, concentration, and solvent. While both CD and filter binding assay gave consistent results in probing the peptide binding ability, the latter seems to be associated more with the aggregation of the peptide-DNA complex. Fluorescence and equilibrium ultracentrifugation experiments are being conducted to determine the binding stoichiometry and the self-association of the peptides. In addition, all possible mutants of this 20 amino acid stretch in the whole RecA protein are being constructed in order to elucidate the functional role of each residue both *in vitro* and in *E. coli* cells.

M-AM-J9

RNA POLYMERASE-PROMOTER KINETICS AND THERMODYNAMICS: RESULTS OF AN ANALYTICAL METHOD

Oleg V. Tsodikov‡, Peter E. Schlax Jr.‡, Kristi L. McQuade† and M. Thomas Record Jr.‡†*, Biophysics Program‡ and Departments of Biochemistry† and Chemistry*, University of Wisconsin, Madison, WI 53706 (Spon. by Jeff P. Bond)

The mechanism of formation of RNA-polymerase (R) - promoter (P) open complexes is

$$R + P \underset{k_{-1}}{\overset{k_1}{\rightleftarrows}} RP_{c1} \underset{k_{-2}}{\overset{k_2}{\rightleftarrows}} RP_{c2} \underset{k_{-3}}{\overset{k_3}{\rightleftarrows}} RP_o$$

where the equilibrium constants (K_1, K_2 and K_3) are equal to the ratios of the forward and reverse rate constants of each step. An analytical approach to solving equations of kinetics for first- and pseudo-first order mechanisms was implemented to determine the rate and equilibrium constants of this reaction as a function of temperature. The method allowed us to resolve kinetic and thermodynamic quantities involved in this process, which is the primary level of regulation in transcription initiation. The solution is exact and not based on steady-state approximations, making it applicable to a broad variety of systems.
Using this analysis, we have determined K_1, K_2, K_3, k_2 and k_{-2} from kinetic data in the temperature range 7-37°C. We find that large negative heat capacity changes are associated with the first two steps of this process, consistent with the burial of large amounts of water-accessible surface for each step. ΔH°_3 is relatively temperature-independent and very unfavorable (~80 kcal/mol), consistent with the unstacking of ~13 base pairs of duplex DNA in forming the open complex.

M-AM-K1

SPONTANEOUS OPENING OF CYCLIC NUCLEOTIDE-GATED CHANNELS SUPPORTS AN ALLOSTERIC MODEL OF ACTIVATION
((G.R. Tibbs, E.H. Goulding, B.G. Leypold, D. T. Liu & S.A. Siegelbaum)) Center for Neurobiology & Behavior, Columbia University, NY, NY 10032

Chimeric constructs of bovine photoreceptor (RET) and catfish olfactory (OLF) cyclic nucleotide-gated (CNG) channels suggest that a domain extending from the middle of the amino terminus through the S2-S3 loop (N-S2) determines the free energy change of channel activation (*Goulding et al., 1994, Nature 372, 369-374*), with the RET N-S2 domain rendering channels harder to open than OLF. According to an allosteric model, the N-S2 domain should determine the spontaneous (ligand independent) open probability (s.o.p.) with constructs that include the OLF N-S2 exhibiting a higher s.o.p. than RET N-S2 containing channels. Equilibrium estimates of s.o.p. were determined by recording spontaneous single channel activity. OLF and OLF N-S2 containing channels have a s.o.p. of approximately $2*10^{-3}$ whereas RET N-S2 channels have a s.o.p. of approximately 10^{-5}. A point mutation (R559Q RET) in the ligand binding site RTAN sequence causes a 25 fold increase in the $K_{1/2}$ for activation by cGMP without altering the s.o.p. or maximal open probability in the presence of cGMP arguing that the s.o.p. is not due to residual cGMP. These data show that 1. A symmetrical allosteric model is appropriate to describe CNG channel gating 2. The free energy difference between open and closed states of the channel may be determined by the N-S2 domain 3. R559 makes a bond (at least -1.9kCal/mol) with cGMP that is involved in initial ligand binding 4. Activation involves no change in the interaction between R559 and cGMP.

M-AM-K2

CA-CALMODULIN BINDING TO cGMP-GATED CHANNELS: AFFINITY, STOICHIOMETRY, AND BINDING SITE DENSITY.
((Paul J. Bauer)) Institut für Biologische Informationsverarbeitung, Forschungszentrum Jülich, D-52425 Jülich, Germany.

Ca-calmodulin (Ca-CaM) binds to β-subunits of rod cGMP-gated channels thereby reducing the cGMP affinity (Hsu & Molday, Nature **361**, 1993, 76). I examined the Ca-CaM binding by investigating the influence of Ca-CaM on the Ca-efflux from bovine ROS membrane vesicles. If rod outer segment (ROS) membranes were washed at virtually zero Ca (1mM EDTA), the K_m of the dose-response curve was shifted by about 15μM to higher cGMP concentrations upon addition of Ca-CaM. No influence of Ca-CaM on the Ca-flux was observed with ROS membranes which were washed in 0.1 mM Ca. Compared with EDTA-washed membranes, the dose-response curves for channel activation were again shifted by about 15μM to higher cGMP-concentrations. Due to buffering effects, the half-maximal reduction of the Ca-flux by Ca-CaM increased with increasing vesicle concentration. Extrapolation to infinite dilution yielded a K_m-value for Ca-CaM binding of 1.01±0.20nM and a Hill coefficient of 1.36±0.15. Quantitative evaluation of the Ca-CaM buffering effect showed that one Ca-CaM binding site per 720 molecules of rhodopsin is present in ROS. Based on this value, a density of 560 Ca-CaM binding sites/μm^2 is estimated for ROS plasma membranes, - twice as high as the density of cGMP-gated channels (Bauer & Drechsler, J. Physiol. **451**, 1992, 109). The data suggest (**a**), that there is a Ca-binding regulatory protein of the channel in ROS, and (**b**), that two β-subunits are associated with each channel in rod photoreceptors.

Supported by DFG Ba 721/1-1

M-AM-K3

INHIBITORS OF CYCLIC-GMP SYNTHESIS AND DEGRADATION AFFECT LIGHT-INDUCED EXCITATION IN *DROSOPHILA* RETINAL PHOTORECEPTORS.
((Joan E. Haab, Farhood Farjah, Peter M. O'Day)) Institute of Neuroscience, University of Oregon, Eugene OR.

Visual excitation in photoreceptors from *Drosophila* retina is mediated by polyphosphoinositide (PI) signalling pathway. However exogenously added cyclic-GMP analog 8-Br-cGMP can (i) induce dramatic enhancement of light-induced currents measured in whole-cell tight-seal voltage-clamp (i^{hv}) and (ii) induce a membrane current (i^{m}) that reverses near the light response reversal voltage.

To examine whether endogenous cGMP may be involved in excitation, we have studied the effects of cGMP metabolic inhibitors on i^{hv} and i^{m} (V_m=-70mV). We report that both ZAPRINAST [500μM] (inhib. of cGMP degradatory enzyme, cG-phosphodiesterase) and LY83583 [500μM] (inhib. of cGMP synthetic enzyme, guanylate cyclase) induced inward currents whose amplitudes depended on the intensity of a preceding light flash.

Additionally, ZAPRINAST reduced i^{hv} in an intensity-dependent manner, such that responses to the brightest stimuli were completely suppressed. In contrast, LY83583 induced a transient, but dramatic enhancement of i^{hv} that decayed in ~20 sec. Effects of both ZAPRINAST and LY83583 were incompletely reversible. The results suggest that cGMP metabolism influences PI-dependent excitation in an undetermined way. Supported by NIH EY09388 and NSF BNS92-10096.

M-AM-K4

USE OF CAGED INOSITOL TRISPHOSPHATE ($InsP_3$) AND CONFOCAL MICROSCOPY TO LOCALLY RELEASE Ca^{2+} IN *LIMULUS* VENTRAL PHOTORECEPTORS.
((Kyrill Ukhanov and Richard Payne)) Dept. of Zoology, University of Maryland, College Park, MD 20742

The use of caged $InsP_3$ combined with confocal microscopy may provide new insights into the spatio-temporal characteristics of the phototransduction machinery in invertebrate photoreceptors. The sensitivity of *Limulus* ventral photoreceptors to light was first decreased using the procedure of Faddis and Brown (1992; J.Gen.Physiol 100,547). Photoreceptors were treated with 40-200 mM hydroxylamine and then pressure injected with 1 mM fluo-3, 12 mM GDPβS and 1.6-16 mM caged $InsP_3$ dissolved in 100 mM KAsp, 10 mM HEPES, pH 7.0. Following this treatment, the latent period of the photoreceptor's response to saturating flashes from the UV or 488 nm laser spot was prolonged to 50 ms, allowing the release of caged compounds before the beginning of the normal light response. All of the experiments were performed on a Zeiss 410 laser confocal microscope. Fluo-3 was excited by 488 nm laser light. Short (20-50 ms) superimposed flashes from the UV laser (364 nm) were used to photolyze caged $InsP_3$. Ca-release occurred within 15 ms of the onset of the UV flash when the laser spot was located in the most sensitive area of the R-lobe. Detection of the $InsP_3$-induced Ca rise led the electrical response by 1-4 ms. The averaged latency of the photoreceptor depolarization was 23±5 ms and that of the Ca rise was 21±6 ms. The response to caged $InsP_3$ was very sensitive to the location of the stimulating laser spot. When released distant from the rim of the R-lobe, $InsP_3$ was still able to induce fast Ca-release without significant effect on the electrical response. 10 mM of caged ATP was used as a control and showed no effect on the electrical response or light-induced Ca release.

M-AM-K5

KINETICS OF DIVALENT CATION BLOCKAGE OF LIGHT-DEPENDENT K CHANNELS: REQUIREMENT FOR AN OPEN PORE.
((Enrico Nasi and Maria del Pilar Gomez)) Department of Physiology Boston University School of Medicine and Marine Biological Laboratory Woods Hole, MA. (Spon. by R. Stephens)

The I-V relation for the light-dependent K conductance of hyperpolarizing *Pecten* photoreceptors rectifies outwardly, because of voltage-dependent block by extracellular Ca and Mg, similar to vertebrate rods. The blockage is sufficiently slow to permit the resolution of light-activated single-channel currents under physiological ionic conditions, at least at positive voltages. If the membrane is depolarized during illumination, the kinetics of the whole-cell light-dependent current exhibit an instantaneous jump, due to the increase in driving force on K ions, followed by a relaxation (τ_u~8-20 ms). This relaxation is not evident in the absence of divalent cations, and reflects the depolarization-induced relief of the block. The onset of the blockage was measured using elevated $[K]_o$ (50 mM), which ensures a sizable driving force during voltage steps in the hyperpolarizing direction. In this case, in addition to an instantaneous inward current proportional to ΔV_m, a relaxation to a smaller plateau becomes progressively more prominent as the step is made more negative; its time constant is inversely related to the size of the voltage step (τ_b~10-30 ms) and reflects the equilibration of the blocking site occupancy. In order to determine whether divalent cation block requires an open pore, we compared the photocurrent at different steady holding voltages: the kinetics become faster with hyperpolarization, but this effect is eliminated by removal of extracellular Ca and Mg. Moreover, the photocurrent amplitude is unaffected by voltage steps terminated before light stimulation with a temporal lag shorter than τ_b or τ_u. These observations indicate that channels must open in order for divalent cations to access the blocking site. Supportedby NIH grant RO1 EY-07559.

M-AM-K6

THE STOICHIOMETRY OF CYCLIC NUCLEOTIDE-GATED ION CHANNELS.
((D.T. Liu, G.R. Tibbs, & S.A. Siegelbaum)) Center for Neurobiology & Behavior, Columbia University, NY, NY 10032

Cyclic nucleotide-gated (CNG) ion channels are oligomeric structures containing at least two subunits. However, the total number of subunits per functional channel is unknown. To determine the subunit stoichiometry of CNG ion channels, we have coexpressed bovine retinal channels (RET) with a chimeric retinal channel containing the catfish olfactory channel P region (RO133). RO133 and RET show identical gating with cyclic nucleotides (Goulding et al., Nature 364:61-64, 1993). When expressed alone, RET subunits form a channel with a conductance of 30pS, while the RO133 subunits form a channel with a larger conductance of 85pS (-120mV, pH9.0). Assuming that RET and RO133 assemble to form heteromultimers and the conductance levels of heteromultimers are determined only by the subunit composition, the total number of conductance levels should be equal to the number of subunits plus one. When cRNAs of both RO133 and RET are injected in *Xenopus* oocytes, intermediate conductances are indeed observed in an excised inside-out patch with multiple channels. Single channel recordings reveal six conductance levels which would indicate a pentameric structure. However, dimer constructs reveal that two of these conductance levels are from channels with the same subunit composition (2xRO133:2xRET) but distinct orientations (similar subunits next to each other vs. similar subunits across from each other). Thus, the data demonstrate that 1. cyclic nucleotide-gated ion channels are tetrameric like the related voltage-gated potassium ion channels and 2. the orientation of pore regions affects the conductance of the channel.

M-AM-K7

MODULATION OF CONE PHOTORECEPTOR cGMP-GATED CHANNELS
((L.W. Haynes and S.C. Stotz)) Dept. of Medical Physiology and Neuroscience Research Group, University of Calgary, Calgary, AB, T2N 4N1, Canada

Inside-out patches containing cGMP-gated channels were excised from catfish rod or cone outer segments and the net cGMP-dependent currents elicited by saturating and sub-saturating concentrations of cGMP at ±30 mV were measured. The $K_{\frac{1}{2}}$ and the Hill coefficient were estimated by fitting with the Hill equation. At +30 mV, $K_{\frac{1}{2}}$ was 28 ± 5 μM (n = 17) and 51 ± 19 μM (n = 21) for the rod and cone channels, respectively. The lower affinity of cone channels is therefore not a species difference. In patches where data for both voltages were obtained, there was a significant increase in $K_{\frac{1}{2}}$ at −30 mV (rods: 12 ± 11%, n = 14; cones: 23 ± 13%, n = 5). For both types of channel, the Hill coefficient was ~2.3 and voltage-independent. Variability in $K_{\frac{1}{2}}$ was not due to cGMP hydrolysis since currents evoked by 8-Br-cGMP showed similar variability ($K_{\frac{1}{2}}$ = 10.4 ± 7.0 μM, n_H = 1.9 ± 0.6). Calcium-calmodulin decreased $K_{\frac{1}{2}}$ in rods by ~2 fold (n = 5), but had no effect upon cones (n = 14). This effect was independent of the initial value of $K_{\frac{1}{2}}$. These results indicate that the affinity of the cone channel for its ligand cannot be modulated by calmodulin during the photoresponse as has been proposed for the rod channel. In cones, ATP + IBMX produced a decrease in $K_{\frac{1}{2}}$ followed by an increase, suggesting an endogenous membrane-bound kinase acting upon at least two sites on the channel. Both the NO-generating agent sodium nitroprusside and IP_3 failed to alter $K_{\frac{1}{2}}$. Diacylglycerol agents are being investigated.

M-AM-K8

NMR EVIDENCE FOR CALCIUM-INDUCED EXTRUSION OF THE MYRISTOYL GROUP OF RECOVERIN.
((J.B. Ames, T. Tanaka, M. Ikura, and L. Stryer)) Dept. of Neurobiology, Stanford Univ., Stanford, CA 94305 and Ontario Cancer Institute, Univ. of Toronto, Toronto, Ontario, Canada M4X 1K9.

Recoverin, a new member of the EF-hand superfamily, serves as a Ca^{2+} sensor in vision. A myristoyl or related N-acyl group covalently attached to the N-terminus of recoverin enables it to translocate to disc membranes when the Ca^{2+} level is elevated. Ca^{2+}-bound recoverin prolongs the lifetime of rhodopsin by blocking its phosphorylation. The NMR solution structure of Ca^{2+}-free, myristoylated recoverin shows that the myristoyl group is sequestered in a deep hydrophobic pocket (Tanaka et al., *Nature* 376, 444). We report here NMR studies designed to answer two questions: (1) Does the binding of Ca^{2+} to recoverin induce the extrusion of the myristoyl group, or does it remain sequestered? (2) What is the effect of Ca^{2+}-binding on the hydrophobic core of the protein? ^1H-^{13}C shift correlation NMR spectra of recoverin containing a ^{13}C-labeled myristoyl group probe the effect of Ca^{2+} on the environment of the attached myristoyl group. In the Ca^{2+}-free state, each pair of methylene protons bonded to carbon atoms 2, 3, 11, 12 of the myristoyl group gives rise to two peaks. The splittings indicate that the myristoyl group interacts with the protein in the Ca^{2+}-free state. By contrast, only one peak is seen for each pair of methylene protons in the Ca^{2+}-bound state, indicating that the myristoyl group is located in an isotropic environment in this form. ^1H-^{13}C shift correlation NMR of ^{13}C-labeled recoverin also probes resonances of methyl groups in the hydrophobic core. The spectrum of Ca^{2+}-bound myristoylated recoverin is different from that of Ca^{2+}-free form but similar to that of Ca^{2+}-bound unmyristoylated recoverin. Hence, the myristoyl group interacts little with the hydrophobic core of recoverin in the Ca^{2+}-bound state. These NMR data demonstrate that the binding of Ca^{2+} to recoverin induces the extrusion of its myristoyl group into the solvent, which would enable it to interact with a lipid bilayer or a hydrophobic site of a target protein.

ION MOTIVE ATPases II

M-AM-L1

AMINO ACIDS LOCATED IN THE AMINO TERMINAL END OF THE RAT Na-PUMP α-SUBUNIT ARE ESSENTIAL FOR THE STIMULATION BY PROTEIN KINASE C.
((Carlos H. Pedemonte, Thomas A. Pressley* and Mustafa F. Lokhandwala)) College of Pharmacy, University of Houston, Houston, TX and *Dept. of Physiology, Texas Tech Univ., Health Sciences Center, Lubbock, TX

The molecular mechanisms involved in regulation of renal sodium metabolism are not clearly understood. The Na-pump, located in the basolateral membrane of the tubule epithelial cells, provides the driving force for the translocation of sodium from the lumen of the renal tubules to the blood supply. Several studies suggest that regulation of the Na-pump activity involves phosphorylation of the α-subunit by protein kinases. We have expressed the α-subunit of the rat Na-pump in opposum kidney (OK) cells and determined the effect of protein kinase C (PKC) on ouabain-sensitive potassium transport, a measure of Na-pump activity. Activation of PKC by the phorbol ester, phorbol 12-myristate 13-acetate, increased the ouabain-sensitive potassium transport of the transfected OK cells. Recent studies have implicated the amino terminus of the α-subunit as the target for phosphorylation by PKC. To test this possibility, we expressed a mutant α-subunit which lacks the first 31 amino acids of the wild-type protein. This truncated form was also capable of supporting ouabain-sensitive potassium transport, yet the activity of the mutant was not stimulated by phorbol ester. These results suggest that PKC stimulates directly the Na-pump activity containing the transfected α-subunit and that one or more amino acids within the α-subunit's amino terminus are involved in this stimulation.

M-AM-L2

SECONDARY STRUCTURE PREDICTION OF α- AND β-SUBUNITS OF Na^+,K^+-ATPase DERIVED FROM β-GALACTOSIDASE FUSION PROTEINS EXPRESSD IN YEAST.
(Bernd Fiedler and Georgios Scheiner-Bobis) Inst. Biochemistry and Endocrinology, JLU-Giessen, 35398 Giessen, Germany.

The intention of the work is to establish a secondary structure model for the Na^+,K^+-ATPase. The bacterial enzyme β-galactosidase was fused to the C-termini of truncated α- and β-subunits of Na^+,K^+-ATPase. Fusions were generated at Arg^{60}, Glu^{116}, Ala^{247}, Leu^{311}, Ala^{444}, Ala^{789}, Met^{809}, Asp^{884}, Ile^{946} and Arg^{972} of the sheep α_1-subunit and at Pro^{236} of the dog β-subunit. All fusion proteins are expressed in yeast as revealed by western analysis. Activity measurements of the reporter enzyme with X-Gal, C12FDG or ONPG demonstrate that only intracellular fusion sites lead to active β-galactosidase. This fact was also confirmed by indirect immunofluorescence microscopy with cells expressing the various hybrid proteins. The data suggest that the α-subunit of the Na^+,K^+-ATPase consists of ten membrane-spanning domains. They also indicate that the hydrophilic loop between the seventh and eighth membrane domains might be hidden in the membrane plane and surrounded by the transmembrane domains of the α- and β-subunits. Pro^{236} of the β-subunit is located on the extracellular surface, corresponding to a model with one transmembrane segment.

Supported through the Deutsche Forschungsgemeinschaft, SFB249.

M-AM-L3

MAPPING THE EXTRACELLULAR PORTION OF NA,K-ATPASE.
((S.Lutsenko, S.Daoud, J.H.Kaplan)). Oregon Health Sciences University, Dept. Biochemistry and Molecular Biology, Portland, OR, 97201

Na,K-ATPase in right-side-out oriented vesicles has been stabilized in two different conformations (phosphorylated, MgPi-form and K-bound form) and then treated with different chemical probes: Cys-directed 4-acetamido-4'-maleimidyl stilbene-2,2' disulfonic acid (SDSM), carboxyl-directed 4-(diazomethyl)-7-diethylaminocoumarin (DEAC) and Lys-directed 7-diethylamino coumarin-3-carboxylic acid succinimidyl ester (DEACSE). Effects on ATPase activity, incorporation into the α-subunit and potassium protection against modification have been characterized. Prior labeling of the extracellular Cys residues with SDSM decreases incorporation of another Cys-directed, fluorescent reagent CPM (7-diethylamino-3-(4'-maleimidyl)-4 methylcoumarin. The difference in labeling with these two reagents has been used to identify SDSM-accessible segments of the α-subunit of Na,K-ATPase. After isolation, labeled α-subunit has been digested by trypsin and tryptic peptides were separated on a Tricine gel and SDSM-labeled peptides identified by N-terminal amino-acid sequence analysis. The major peptide (2.5 kDa), which begins with NSFQQGM... contains a single Cys residue, which corresponds to Cys 964 of the α-subunit. Cys 964 is more accessible to modification with membrane-impermeable SDSM, when Na,K-ATPase is in Mg,P-form and less in K-form. Labeling of this Cys residue with uncharged CPM-reagent is not conformationally-dependent. These data indicate that Cys 964 is located at the extracellular portion of Na-pump very close to the membrane surface.
Supported by NIH GM39500 and HL 30315 to JHK.

M-AM-L4

MUTATIONS IN THE TRANSMEMBRANE DOMAIN OF Na^+,K^+ ATP ase α SUBUNIT THAT ALTER EXTERNAL K^+-DEPEND ACTIVATION KINETICS MODULATE OUABAIN INTERACTION WITH THE PUMP
((♥S. Yamamoto, *T. Kuntzweiler, ♥E. T. Wallick and ♥A. Yatani)) ♥Dept. of Pharmacol. & Cell Biophysics. and *Dep. of Mol. Genetics, Univ. of Cincinnati, Cincinnati, OH 45267

Using stable HeLa cells expressing wild-type and mutant cDNAs in combination with patch-clamp measurements of an outward Na^+ pump current (Ip), we have shown that mutations in the H1 domain of the Na^+,K^+ pump (NKA) α subunit at a site (C106) that determines cardiac glycoside affinity, also reduced the sensitivity of Ip to external K^+ (Yamamoto et al., 1995). This result suggested that variations in the pump's interaction with external cations might also affect the apparent sensitivity to ouabain. To test this possibility, we characterized the ouabain block of Ip in HeLa cells carrying a mutation at E327 in the H4, a site which has been suggested to play a role in a K^+-dependent conformational change of NKA. The functional role of this residue was studied by substituting the E→Q in a ouabain-resistant isoform (rat α2*). Both rat α2* and the mutant cells displayed marked external K^+-dependent Ip activation. However, the apparent affinity for K^+ was reduced from 1.2 to 8.6 mM by the E327Q mutation due to a slower activation rate. The cells expressing E327Q exhibited about 3-fold higher ouabain sensitivity. The apparent affinity of E327Q cells for ouabain was not altered by increasing external K^+ from 5 to 20 mM. These results suggest that a mutation of residue E327 alters a conformational change that is normally induced by the binding of external K^+. (Supported by AHA93012860, NSFCAA and HL50613)

M-AM-L5

PEPTIDE ASSOCIATIONS BETWEEN THE α / ß-SUBUNITS OF THE GASTRIC H,K-ATPASE
((Edd C. Rabon, Michele Hoggatt and Naomi Horiba)) Tulane University Medical School and Veterans Adm., New Orleans, LA 70012

The gastric H,K-ATPase is organized as an α,ß-heterodimer of the catalytic α-subunit and a WGA-reactive, glycosylated ß-subunit. Catalytic activity is present within a monomer of the heterodimer in solutions of the ATPase prepared in the nonionic detergent, $C_{12}E_8$. To delimited regions of the α- subunit that are associated with the ß-subunit, WGA affinity chromatography was used to purify $C_{12}E_8$ solutions of α-subunit, tryptic peptides copurifying with the ß-subunit. Several peptides purified by WGA chromatography were resolved by tricine SDS PAGE and submitted for sequence analysis. 3 peptides of M_r: 10.2, 7.8 and 6.4 kDa were resolved from tryptic digests obtained in the absence of K^+. Analysis of these peptides identified N-terminal sequences for LVNE (M7), GTPE (M1) and NIPE (M5), respectively. A second set of peptides was purified from a similar protocol utilizing tryptic proteolysis in a medium containing K^+. N terminal sequences of GTPE (M1) and NAAD (M5), were identified from the M_r; 7.1 kDa peptide and the sequence SIAY (M5) was identified in the M_r; 6.4 kDa peptide. These data demonstrate that extracytoplasmic loops of the α-subunit bounded by M1/M2, M5/M6 and M7/M8 domains are associated with the ß-subunit. This diversity suggests that extensive extracytoplasmic interactions rather that a single extracytoplasmic domain stabilizes the association of the gastric H,K-ATPase α/ß-heterodimer. NIH DK34286 and VA Merit support.

M-AM-L6

INTRODUCTION OF CYSTEINE RESIDUES INTO THE Ca^{2+} BINDING DOMAIN OF SERCA1. ((William J. Rice and David H. MacLennan)) Banting and Best Department of Medical Research, University of Toronto, Toronto, Ontario, Canada M5G 1L6

Structure/function relationships in the Ca^{2+} ATPase of skeletal muscle sarcoplasmic reticulum (SERCA1) have been analyzed extensively by site-specific mutagenesis. Six residues, located in transmembrane helices M4, M5, M6 and M8 have been implicated in Ca^{2+} binding. Mutagenesis of all residues in M4, M5, M6 and M8 has revealed a "patch" highly sensitive to mutation in M4, M5, and M6, but not in M8. These observations suggest that the "patches" face each other, making up the two Ca^{2+} binding sites. However, modelling of the Ca^{2+} binding domain will require information about the precise orientation of the different transmembrane helices with respect to each other. The relative orientation of transmembrane sequences in several bacterial transmembrane receptor proteins has been determined by the introduction of cysteines into the transmembrane domain followed by testing for the formation of interhelical disulfide crosslinks (1,2,3). We are adapting this strategy to the determination of the orientation of transmembrane helices M4, M5, M6 and M8 in SERCA1. We have replaced all six cysteines, predicted to be located in the transmembrane domain, with either alanine or serine. This mutant SERCA1 retained wild type Ca^{2+} affinity and 40% of normal Ca^{2+} uptake activity. Cysteine residues are being introduced two at a time into this mutant and the mutants are being tested for disulfide links. (Supported by National Institutes of Health, U.S.A.)
Ref. 1. Lynch, B.A. and Koshland, D. E. Jr. *PNAS* **88**, 10402-10406 (1991). 2. Pakula, A.A. and Simon, M.I. *PNAS* **89**, 4144-4148 (1992). 3. Lee, G.F. *et al. J. Biol. Chem.* **269**, 29920-29927 (1994).

M-AM-L7

EXPRESSION AND CHARACTERIZATION OF PMR1, A NOVEL Ca^{2+} PUMP IN YEAST GOLGI. ((A.Sorin and R. Rao)) Department of Physiology, The Johns Hopkins School of Medicine, Baltimore, MD 21205.

PMR1 has been cloned from the yeast *Saccharomyces cerevisiae* on the basis of homology with the plasma membrane H^+-ATPase (Rudolph *et al.*, 1989). Amino acid sequence analysis indicates that PMR1 is a Ca^{2+} pump, and is a member of the ubiquitous family of E_1E_2- or P-type ATPases that mediate the transfer of cations across membranes in bacteria, plants and animals. Yeast is a suitable expression system for structure-function studies on the Ca^{2+}-ATPase because it is readily amenable to biochemical and genetic manipulation. Initial goals of our study have been to obtain maximal quantities of PMR1, while minimizing background interference from other ATPases. Because constitutive overproduction of PMR1 is lethal, we use the strong and inducible heat shock promoter to direct expression of *PMR1* from a multicopy plasmid, after sufficient cell density is achieved. Yeast lysates are separated on a sucrose density gradient and fractions assayed for organellar markers. We show that PMR1 comigrates with Golgi and transports ^{45}Ca into isolated Golgi vesicles. Interestingly, another Ca^{2+} uptake activity is up-regulated in a PMR1 null mutant, suggesting a compensatory mechanism for Ca^{2+} homeostasis. Analysis of an isogenic set of yeast strains indicates that a second Ca^{2+} pump, PMC1, recently localized to yeast vacuoles (Cunningham and Fink, 1994), is involved in the compensation since a *Δpmr1Δpmc1* double mutant exhibits drastically reduced calcium uptake activity. However, the induced Ca^{2+}-ATPase activity we observe in the *Δpmr1* mutant localizes to the endoplasmic reticulum instead of the vacuole, pointing to a role for PMR1 in sorting of PMC1 to the vacuole.

M-AM-L8

AMINOPHOSPHOLIPID TRANSPORT AND PS STIMULATED Mg^{2+}-ATPASE ACTIVITIES IN MURINE ERYTHROCYTES. ((D. L. Daleke, E. W. Weber, and M. J. Wilson)) Department of Biochemistry and Molecular Biology, Indiana University School of Medicine, Bloomington, IN 47405.

Phospholipid asymmetry is maintained in the erythrocyte plasma membrane by active transport of aminophospholipids from the outer to the cytofacial monolayer. Although the protein responsible for this activity has yet to be positively identified, a Mg^{2+}-ATPase has been purified from human erythrocytes with many of the same characteristics as the transporter. It is stimulated by phosphatidylserine (PS) and inhibited by vanadate, calcium, and sulfhydryl reagents. Here we compare the rates of transport and PS stimulated Mg^{2+}-ATPase activity in human and mouse erythrocytes. Mouse erythrocytes transport dilauroylphosphatidylserine eight-fold faster than human erythrocytes using a cell morphology assay. Factors that influence PS transport in human erythrocytes also affect transport in murine erythrocytes. Transport activity is specific for amine-containing phospholipids, is unaffected by lipid acyl chain length or protease treatment, and is inhibited by vanadate, low temperatures (1 °C), and sulfhydryl oxidizing and alkylating agents. The energy of activation of transport was two-fold lower in mouse erythrocytes (8 kcal mol^{-1} v. 19 kcal mol^{-1}). PS-stimulated, vanadate-sensitive Mg^{2+}-ATPase activity was increased twelve fold in mouse erythrocyte membranes (52.9 nmoles Pi min^{-1} mg^{-1}) compared to human erythrocyte membranes (4.5 nmoles Pi min^{-1} mg^{-1}). Accelerated aminophospholipid transport may be due to increased specific acitivity of the Mg^{2+}-ATPase or to an increased density of tranporters in murine erythrocytes.

M-AM-L9

PHOSPHOLAMBAN CONSTRUCTS WITH DELETED OR ALTERED CYTOPLASMIC DOMAINS ARE POTENT INHIBITORS OF THE Ca^{2+} PUMP. ((Yoshihiro Kimura and David H. MacLennan)) Banting and Best Department of Medical Research, University of Toronto, Toronto, Ontario, Canada M5G 1L6

Phospholamban (PLN) inhibits the Ca^{2+} ATPase of cardiac sarcoplasmic reticulum (SERCA2) by lowering its apparent affinity for Ca^{2+} (K_{Ca}). Inhibition is believed to result from protein-protein interactions. In earlier studies, we defined the residues in the cytoplasmic domains of PLN and SERCA2 that are critical to the interaction between PLN and SERCA2 coexpressed in heterologous cell culture. In current experiments, we expressed SERCA2 with a variety of PLN constructs in which the NH_2-terminal cytoplasmic domains were either deleted or replaced. Deletions include domain 1a (residues 1-20), domain 1b (residues 21-30) or both domains 1a and 1b. Replacements of domains 1a and 1b were with well known epitopes (HA, Myc or Flag epitopes). Domain II (residues 31-52) alone lowered K_{Ca} about 0.15 pCa units. By comparison, PLN lowered K_{Ca} by 0.3 pCa units. All three epitope-labelled domain II constructs lowered K_{Ca}, the HA construct lowering K_{Ca} by 0.6 pCa units. The domain 1b-deleted construct shifted K_{Ca} by at least 1 pCa units and inhibition was not released by phosphorylation of the retained domain 1a. The constructs did not uncouple Ca^{2+} ATPase from Ca^{2+} transport. All domain II constructs inhibited SERCA3, which does not interact with PLN. We propose that there are two inhibitory interaction sites between PLN and SERCA2, one in cytoplasmic domains and one in transmembrane domains. We also propose that these two sites regulate each other through long range interactions. (Supported by the Human Frontiers Science Program Organization, The Heart and Stroke of Ontario and the Pharmaceutical Roundtable, Heart and Stroke Foundation of Canada).

M-AM-M1

MEMBRANE CONFORMATION OF THE TH9 HELIX OF THE ISOLATED TRANSMEMBRANE DOMAIN OF DIPHTHERIA TOXIN: A SITE-DIRECTED SPIN-LABELING STUDY. ((Kyoung Joon Oh[1], Hangjun Zhan[2], Can Cui[2], R. John Collier[2], and Wayne L. Hubbell[1])) [1]Jules Stein Eye Institute and Department of Chemistry & Biochemistry, University of California, Los Angeles, CA 90095; [2]Department of Microbiology and Molecular Genetics, Harvard Medical School, Boston, MA 02115.

A series of single cysteine substitution mutants of the diphtheria toxin transmembrane (T) domain were prepared and selectively spin-labeled at the consecutive residues from 356 to 376 on the TH9 helix. The electron paramagnetic resonance spectra of the mutants in solution at pH 8 show a periodicity in the nitroxide mobility consistent with the amphipathic nature of the TH9 helix in the X-ray structure. Upon membrane binding at pH 4.3, a major reorganization of the tertiary structure is detected in which residues previously immobilized in the protein interior become more mobile and exposed to the hydrophobic interior of the bilayer. In this state, the accessibilities of the nitroxide side chains to collision with polar (NiEDDA) and non-polar (O_2) reagents are periodic with sequence position, indicating that a helical structure is maintained. The oscillations in NiEDDA and O_2 accessibility are 180° out of phase with each other, demonstrating that one face of the helix is in contact with water and the other with the hydrophobic interior of the bilayer. These data are consistent with either an amphipathic helix lying on the bilayer surface, or an aqueous-filled transmembrane pore involving TH9. Results of experiments designed to distinguish these models will be presented.

M-AM-M2

PROBING THE STRUCTURE OF THE DIPHTHERIA TOXIN CHANNEL WITH METHANETHIOSULFONATE REAGENTS ((P. D. Huynh*, H. Zhan#, J. A. Mindell*, R. J. Collier#, and A. Finkelstein*)) #Harvard Medical School; *Albert Einstein College of Medicine. (Spon. by X.-Q. Qiu)

The T-domain of diphtheria toxin forms ion-conducting channels in lipid membranes. We have previously shown that 61 amino acids (residues 322-382) of this domain is sufficient to form channels indistinguishable from those of whole toxin. This segment forms an α-helical hairpin in aqueous solution, and is believed to retain this structure in membranes, with its tip exposed to the *trans* side of the membrane. To test this model we introduced cysteine at 24 positions (residues 342-365), one at a time by site-directed mutagenesis, to encompass the hairpin tip, and measured single channel properties in planar bilayers. The addition of a methanethiosulfonate (MTS) reagent to either side of the membrane induced a step change in the single channel conductance of a mutant channel within a fraction of a second to a few minutes after the channel opened, depending on the position of the cysteine. We interpret such step changes to result from one MTS molecule reacting with a cysteine residue lining the ion-conducting pathway. We report that 12 residues around the hairpin tip (347-359 except 349) responded to MTS, whereas residues flanking this region (342-346 and 360-365) did not. Qualitatively, cysteine residues at the tip of the hairpin reacted much faster with *trans* than with *cis* MTS; as the cysteine position was moved away from the tip of the hairpin the difference in these reaction rates diminished, consistent with the hairpin tip residing on the *trans* side.

M-AM-M3

PROGRESS TOWARDS THE X-RAY CRYSTAL STRUCTURE OF COLICIN IA. ((M.C. Wiener, D.M. Freymann, P. Ghosh, J. Finer-Moore, R.M. Stroud)) Dept. of Biochemistry & Biophysics, University of California, San Francisco, 94143-0448.

The formation of ion-permeable channels in target cell membranes is a general mechanism of cytotoxicity. The process involves secretion of a soluble protein which inserts into the plasma membrane of the target cell and forms pores. The *Escherichia coli* toxins, colicins, are a well-characterized example of this functional class of proteins. Ion-channel-forming colicins are multi-domain proteins. Essentially, there are three domains which function, respectively, to i) bind to a receptor on the outer membrane of susceptible bacteria, ii) translocate across the outer membrane, and iii) bind to the inner membrane and form a pore in the presence of the transmembrane voltage. We are determining the structure of the soluble form of an intact colicin, colicin Ia, which contains all three domains. A low-resolution structure of colicin Ia has been determined by our laboratory [Ghosh et al. (Nature Structural Biology, **1**, 597-604, 1994)]. We have subsequently extended resolution by using cryocrystallographic methods, and obtained isomorphous derivatives by reaction of mercurials with three different single-cysteine colicin mutants (wild-type colicin has no cysteines). Through iterative cycles of model-building, phase-combination, and solvent-flattening, the electron density maps are being interpreted. Our current structure ("in-progess") will be described.

M-AM-M4

STRUCTURE AND ACTION OF COLICIN IA. ((R.M. Stroud, M.C. Wiener and J.S. Finer-Moore)) Dept. of Biochemistry & Biophysics, UCSF, San Francisco, CA 94143-0448.

New developments have led to higher resolution phasing to 2.8Å resolution for crystals of full-length colicin Ia. The structure shows the disposition of 3 domains corresponding to the translocation, receptor binding and channel-forming regions. Channel recording measurements and proteolysis have shown which regions are involved in physiological channel formation of the voltage-gated channels. The location and conformation of the loop containing the voltage sensor are discussed with respect to the mechanism of insertion into the bilayer following initial attachment. The initial attachment complex is described based on proteolytic sensitivities in association with the lipid bilayer and interpreted in terms of the three-dimensional structure of colicin Ia

M-AM-M5

THE LOCALE OF THE LOW pH INDUCED STRUCTURAL CHANGE TO THE INSERTION-COMPETENT STATE OF THE COLICIN E1 CHANNEL PEPTIDE. ((B. A. Steer & A.R. Merrill)), Guelph-Waterloo Centre for Graduate Work in Chemistry, Dept. of Chem. and Biochem., Univ. of Guelph, Guelph, ON, Canada, N1G 2W1.

Colicin E1 is a bactericidal and toxin-like protein secreted by strains of *E. coli* which carry a *ColE1* plasmid. It forms a dissipative and lethal ion channel in the cytoplasmic membrane of sensitive *E. coli* and other coliform bacteria. Colicin E1 is divided into three functional domains including a translocation, a receptor binding and a channel-forming domain. The isolated thermolytic colicin E1 channel peptide has a highly α-helical, compact solution structure. Detergent or low pH (≤ 4) induced activation of the channel peptide to its insertion-competent state is required for *in vitro* channel formation. The peptide's transformation to the insertion-competent state involves a significant structural change which results in an increase in the hydrophobic character of the peptide. Using eleven single Trp mutant peptides, the locale of the low pH induced structural change in the peptide upon activation to the insertion competent state was investigated by tryptophan fluorescence. The measurement of single tryptophan quantum yields at both pH 6.0 and 3.5 mapped the structural change to the peptide segment containing residues 413, 424 and 431. These results are in agreement with earlier results from our laboratory which also characterised the insertion-competent state using tryptophan fluorescence spectroscopic techniques and detected a conformational change in the peptide segment containing Trp-424 [supported by the Natural Sciences and Engineering Research Council of Canada (A.R.M.)].

M-AM-M6

ORIENTATION OF THE HYDROPHOBIC HAIRPIN IN THE COLICIN Ia CHANNEL. ((P. Kienker, X.-Q. Qiu, S. Nassi, S. Slatin, A. Finkelstein and K. Jakes)) Albert Einstein College of Medicine, Bronx, NY 10461

The channel-forming colicins are bacteriocidal proteins that form voltage-dependent channels in the inner membrane of target cells and in planar lipid bilayers. All such colicins examined have a solitary hydrophobic sequence of approximately 40 amino acids near the C-terminus. The role of this segment in the initial interaction of the protein with the membrane and in the subsequent formation of an ion channel remains unsettled. Here we present evidence that the hydrophobic segment of colicin Ia adopts a transmembrane orientation in both the open and closed states of the channel. We introduced a cysteine at residue 594, at the center of the hydrophobic segment, and biotinylated it with reagents that attach a biotin to the cysteine via a disulfide bond. We find that the biotin-binding protein, streptavidin, when added to the *trans* compartment, alters the kinetics of channel gating, and that this effect can be reversed with reducing agents capable of cleaving the disulfide bond to remove the biotin. Furthermore, *trans* streptavidin can prevent the decrease in colicin activity normally caused by perfusion of the *cis* compartment, presumably by anchoring the hydrophobic segment in a transmembrane orientation. These effects are observed whether the channels are exposed to *trans* streptavidin in the open or closed state, and even if the channels are only exposed to *trans* streptavidin before their initial opening. These results are consistent with a model of colicin action in which the hydrophobic segment forms a helical hairpin which inserts into the bilayer early in the protein-membrane interaction and remains oriented perpendicular to the plane of the membrane throughout the gating process.

M-AM-M7

ALTERNATE STRUCTURES FOR THE COLICIN Ia OPEN CHANNEL.

((S. Slatin, K. Jakes, X.-Q. Qiu, P. Kienker, and A. Finkelstein,)) Albert Einstein College of Medicine, Bronx NY 10461

The channel-forming colicins are bacteriocidal proteins that form voltage-dependent channels in the inner membrane of target cells and in planar lipid bilayers. The channel-forming domain of colicin Ia extends roughly from residue 451 to the C-terminus of the molecule at residue 626. Gating of the channel is associated with the movement from one side of the membrane to the other of a substantial part of the channel-forming domain. We report here that the upstream boundary of the translocated region can be experimentally manipulated without blocking the ability of the protein to form voltage-gated channels. We constructed a series of single-cysteine mutants and chemically attached a biotin to the introduced cysteine. For mutations anywhere in the translocated domain (residues 474-541), the open channel could be prevented from closing by exposure to the biotin-binding protein, streptavidin, on the *trans* side of the membrane. The effect of *cis* streptavidin on closed channels depended on the location of the mutation within the translocated domain. For mutations near the downstream end, *cis* streptavidin blocked channel opening, consistent with a simple two state model. However, for upstream mutations, such as L474C, binding by *cis* streptavidin did not block turn-on but shifted the voltage dependence and changed the single channel conductance. Thus, this identifies two distinct open states: one with residue 474 on the *cis* side of the membrane and one with 474 on the *trans* side. These results demonstrate that colicin Ia can form channels with a variety of alternative structures by utilizing different upstream transmembrane segments.

M-AM-M8

COLICIN E1 CHANNELS EXHIBIT SUBSTATES AND HETEROGENEITY.

((B.N. Deriy, W.A. Cramer[1], F.S. Cohen)) Dept of Physiology, Rush Medical College, Chicago, IL 60612 and Dept of Biol Sci, Purdue Univ, W. Lafayette, IN 47907[1] (Sponsor, D.R. Pepperberg).

The single channel properties of colicin E1, WT, and its C-terminal polypeptide, P190, were examined by patch clamping large vesicles bathed by 1 M KCl, pH 4.0 and found to be qualitatively similar, but quantitatively different. WT and p190 channels that appeared early in experiments had comparable conductances, ≈ 20 pS, that sometimes exhibited 10 pS conductance substates. With time, larger channels appeared with integral multiple conductances of the early ones. Bursting, more common for P190, could occur with activation voltages, with longer burst duration for larger than for smaller channels. If a bursting channel was deactivated with voltage, bursting continued and subconductance levels appeared, more common for P190. Larger deactivation voltages led to less bursting and faster closing. The time for a WT, but not P190, channel to close when deactivated increased with its open time when activated. In contrast, for both WT and P190, the closed deactivation time of a channel did not affect its latency until opening in response to an activation voltage. Large deactivation voltages ($\geq$ 150 mV) caused a reversal of voltage dependence, more pronounced for P190. Reversed channels opened with deactivation voltages and closed with activation voltages. We conclude that colicins continuously reconfigure within membranes. Supported by NIH GM47828 and GM18457.

M-AM-M9

STRUCTURE PREDICTION OF THE COLICIN E1 IMMUNITY PROTEIN.

((J. B. Heymann and W. A. Cramer)) Department of Biological Sciences, Purdue University, West Lafayette, IN 47907.

E. coli cells producing colicin E1 protect themselves from this channel-forming cytotoxin by also synthesizing a protective integral membrane protein, the immunity protein (ImmE1), that prevents the formation or operation of the channel. Direct interaction between ImmE1 and colicin E1 is inferred from the specificity of colicin-immunity protein pairs in general, and the identification of immunity bypass mutants of colicin E1. A predominant feature in ImmE1 and related proteins, ImmE1*, Imm10, ImmIa and ImmIb, is the presence of three *trans*-membrane helices, with the bilayer architecture constraining these helices to almost parallel interactions. Helical ends were defined using established topology and hydropathy analysis. A heuristic search for helical pair interaction preference including limited simulated annealing was conducted on pairs of ImmE1 helices to find the most likely interhelical interactions. The results suggest a 6-helix dimer, consistent with the SDS-resistant dimer seen in SDS-PAGE. A dimer model of ImmE1 was constructed including the extrahelical loops. A model for Imm10 was also constructed, because it displays activity against colicin E1. It is concluded that the most significant difference between ImmE1 and Imm10 is the bulky periplasmic loop of the former, which is proposed to render ImmE1 ineffective against colicin 10. Hydrophobic residues in the three trans-membrane helices conserved between ImmE1 and Imm10 and predicted to face the lipid bilayer are considered candidates for interaction with other proteins, including colicin E1 and the *tol* proteins at the colicin entry sites. (Supported by NIH GM-18475)

PHOTOSYNTHETIC REACTION CENTERS II

M-AM-N1

ENDOR STUDIES OF THE CATION RADICAL OF THE PRIMARY DONOR IN *HELIOBACTERIA* SUGGEST THAT $P_{798}^{+\bullet}$ IS A SYMMETRIC DIMER *

((J. Rautter, B. Bönigk, W. Lubitz)), Max-Volmer-Institut, TU Berlin, D-10623 Berlin, Germany; ((H.-C. Chiou, R. E. Blankenship)), Chem. and Biochem. Dept., Arizona State University, Tempe AZ 85287-1064, USA

The hyperfine couplings (hfc's) of $P_{798}^{+\bullet}$ were determined in membrane fragments of *Heliobacillus (Hc.) mobilis* and *Heliobacterium (H.) chlorum* using ENDOR spectroscopy. The nearly identical spectra reveal a highly conserved electronic structure of the primary donors in both heliobacteria. The extracted isotropic methyl hfc's are 1.8, 3.7 and 5.0 MHz. These are approximately one half of the related values obtained for the respective BChl cation radical. A simulation of the EPR signal of $P_{798}^{+\bullet}$ (linewidth ΔB_{pp} = 0.95 mT) using the complete set of hfc's from ENDOR shows that this species is a BChl*g* dimer and that the unpaired electron is symmetrically delocalized over the two dimer halves. This symmetric dimer state is consistent with the homodimeric structure of the heliobacterial RC.

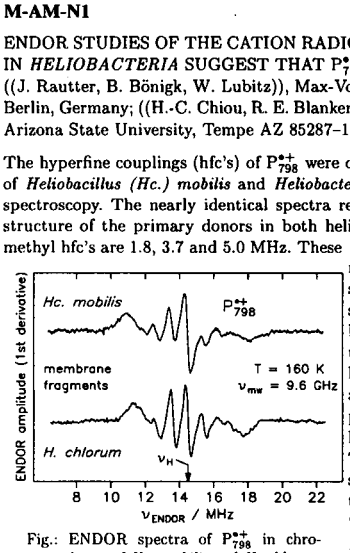

Fig.: ENDOR spectra of $P_{798}^{+\bullet}$ in chromatophores of *Hc. mobilis* and *H. chlorum*

* Supported by DFG (Sfb 312) and NSF.

M-AM-N2

THE PRIMARY ELECTRON DONOR, D, IN HETERODIMER HYDROGEN BOND MUTANTS: EPR/ENDOR ON A HIGH REDOX POTENTIAL D IN *RHODOBACTER SPHAEROIDES*

((M. Huber[#*], S. T. Krueger-Koplin[&], D. Davis[&], C.C. Schenck[&])) #* Institute of Organic Chemistry, FU Berlin, Takustr. 3, 14195 Berlin, FRG; & Department of Biochemistry, Colorado State University, USA

The electronic structure of D, a 'special pair' of bacteriochlorophylls (BChl) in bacterial photosynthesis, is investigated by EPR/ENDOR. In heterodimer mutants one of the BChl molecules of D is replaced by a bacteriopheophytin (BPhe), and in $D^{+\bullet}$, the photooxidized D, the unpaired electron is localized on the BChl [1]. Perturbations of $D^{+\bullet}$, i.e. $BChl^{-\bullet}$, due to hydrogen bonding are studied in HL (M202), where the BChl is at D_L, by removing the acetyl C=O hydrogen bond at ring I (HL (M202)/HF (L168)), or introducing a hydrogen bond at ring V (HL (M202)/LH (L131)). ENDOR reveals that spin density in ring III increases in the latter, and decreases in the former double mutant. The ENDOR spectra are in agreement with those given in [2].

In reaction centers (RC's) of HL (M202)/LH (L131) an additional radical is observed by EPR. The signal can be fitted with a powder pattern lineshape. The magnitude of the largest G- (G_x-) component ($G_x \approx 2.029$) suggests spin density on a sulfur atom, and G_z is close to G of the free electron, suggesting a π-type radical. It is tempting to speculate that the high oxidation potential of D in this mutant initiates radical reactions within the RC, e.g. with one of the Cys of Met residues close to D, leading to the radical observed. This may play a role in the lower photostability of the RC's of this mutant relative to wild type.

[1] M. Huber, et al. in: Reaction Centers of Photosynthetic Bacteria, M.-E. Michel-Beyerle (ed.), Springer Verlag, Berlin (1990), p. 219ff and *Biochim. Biophys. Acta* (1995), accepted

[2] J. Rautter, et al. *Biochemistry*, 34, 8130 (1995)

M-AM-N3

CAVITY MUTANTS INVOLVING RESIDUE L168 NEAR THE SPECIAL PAIR DIMER IN REACTION CENTERS OF *RB. SPHAEROIDES*. ((Laura J. Moore and Steven G. Boxer)) Chemistry Department, Stanford University, Stanford, CA 94305-5080.

Two cavity mutants of *Rb. sphaeroides* reaction centers (RCs) have been designed to probe the interaction between the protein and the special pair dimer (P). First, a single mutant in which His at L168 is replaced by Gly has been constructed. This mutation removes the hydrogen bond from the protein to the acetyl group of the P_L bacteriochlorophyll. The P band absorption spectrum of this mutant is similar to that of the mutant in which His is changed to Phe at L168; that is, it has an approximate 20 nm blue shift at 77K from that of wild type. However, the lineshape of the Stark spectrum in the cavity mutant is considerably different than that of both the His to Phe mutant and wild type. The second mutant adds the same cavity at L168 to a previously constructed mutant in which both axial histidine ligands to the special pair dimer (L173 and M202) have been replaced by glycine (Goldsmith and Boxer, *Biochemistry*, submitted). This triple mutant effectively removes all bonding connections of the special pair to the protein. Under normal isolation procedures these mutant reaction centers were isolated and were found to lack the P absorption band but retain relatively normal H and B absorption and Stark spectra. Both mutant RCs were also grown, isolated, or incubated in the presence of small exogenous ligands such as imidazole in an effort to incorporate these ligands into the cavities. This type of small ligand incorporation into cavities has been successful in both the axial mutants of RCs and a cavity mutant (His to Gly at residue 93) of myoglobin (DePillis *et .al*. (1994) *JACS*, **116**, 6981) The effect of the addition of these ligands on the redox, kinetic and spectroscopic properties of the special pair dimer will be discussed.

M-AM-N4

DETAILED MECHANISM OF EXCITATION ENERGY TRANSFER IN THE PHOTOSYNTHETIC REACTION CENTER ((T. Häberle, H. Lossau, G. Hartwich, A. Ogrodnik, H. Scheer[+] and M.E. Michel-Beyerle)) Institut für Physikalische Chemie, TU München, Lichtenbergstr. 4, D-85747 Garching. [+]Botanisches Institut der LMU München, Menzinger Str. 67, D-80638 München

In the reaction center (RC) from *Rhodobacter Sphaeroides* R26, where the monomeric bacteriochlorophyll (BChl) pigments have been replaced by 13^2-OH-Ni-bacteriochlorophyll (NiBChl), an ultrafast deactivation of the ^{1}NiBChl* state within 40 fs was inferred from femtosecond data [1] of the native RC and comparative studies of steady state absorption and fluorescence excitation spectra [2].

Recent fluorescence upconversion experiments on the Ni-RC with femtosecond time resolution revealed that the rise-time (75±20 fs) of the dimer fluorescence monitored at 940 nm is by a factor of two slower than the lifetime of ^{1}NiBChl* excited in the Q_y-transition. This observation implies that fast energy transfer populates an intermediate which decays with about ≈80 fs to the fluorescing dimer state.

Candidates for this intermediate are the upper excitonic component of the dimer ($^1P^*_+$) or vibrationally excited states thereof. Thus, the ultrashort lifetime of ^{1}NiBChl* allows the observation of relaxation-processes within the excited dimer on a 100 fs time scale. [1] Jia,Y., Jonas, D.M., Joo, T., Nagasawa, Y., Lang, M.J., and Fleming, G.R., J.Phys.Chem. 99 (1995) 6263 [2] Hartwich, G., Friese, M., Scheer, H., Ogrodnik, A., and Michel-Beyerle, M.E., Chem.Phys. 197 (1995) 423-434.

M-AM-N5

SLOW CHARGE SEPARATION IN MINORITY OF REACTION CENTERS CORRELATING WITH A BLUESHIFT OF THE LOWEST EXCITON BAND OF THE PRIMARY DONOR. (H. Lossau, G. Hartwich, A. Ogrodnik and M.E. Michel-Beyerle) Institut für Physikalische Chemie, TU München, Lichtenbergstr. 4, D-85747 Garching.

We have examined the dependence of the fluorescence decay pattern (40ps resolution) of the primary donor $^1P^*$ in the reaction center (RC) from *Rb. sphaeroides* R26 on quinone content and excitation wavelength. The fluorescence components in the 50ps to 1ns range (<5% of total amplitude) are almost unaffected by the quinone (Q_A) content, although this changes the $P^+H_A^-$ lifetime from ~17ns (Q_A-free RC) to ~ 130ps (Q_A-containing RC) at 85K. Thus, the fluorescence decay in this time window reflects slow charge separation of a minority of RC and cannot be due to recombination fluorescence of $P^+H_A^-$-states.

Excitation spectra of the 50ps to 1ns fluorescence components show a $^1P^*$-band being blue shifted as compared to the absorption spectrum. In contrast, the components faster than 40ps do not exhibit such a blue shift. Thus, in the above mentioned minority of RC slow primary charge separation proceeds from an energetically higher lying $^1P^*$-state.

M-AM-N6

THERMALLY ACTIVATED CHARGE SEPARATION IN THE MUTANT WM210 OF *RB. SPHAEROIDES* (A. Ogrodnik, M. Friese, P.Gast[+], A.J. Hoff[+], M.E. Michel-Beyerle, Inst. f. Physikalische Chemie, TU München, Lichtenbergstr.4 D-85747 Garching. [+]Huygens Laboratory, Niels Bohrweg 2, P.O. Box 9504, 2300 RA Leiden.

The effect of mutagenic replacement of the polar aminoacid residue tyrosine by the nonpolar tryptophan in the mutant WM210 of *Rb. sphaeroides* was studied in time resolved fluorescence. From the ns-delayed fluorescence an energy distribution of the radical pair state $P^+H^-_A$ with an average value of $\Delta G(^1P^*\text{-}P^+H^-_A)_{av}$≈0.16eV and a width 2σ=0.08eV was determined. The lifetime of $^1P^*$exhibits a multiple exponential decay revealing dispersed charge separation kinetics. At 280K and 85K the average lifetimes are $\langle\tau\rangle$=56ps and 366ps and their second moments $(\langle\tau^2\rangle\text{-}\langle\tau\rangle^2)^{1/2}$=70ps and 200ps, respectively. An Arrhenius plot of $\langle\tau\rangle$ yields an activation energy of 0.18eV in the temperature range 240K-280K, reflecting the shift of $P^+B^-_A$ beyond $^1P^*$. Extrapolation to 80K would yield a value $\langle\tau\rangle$=5ms. Instead the temperature dependence levels off and essentially becomes constant below 180K. At 80K the quantum yield of charge separation (i.e. of $P^+H^-_A$ formation) is 65%. Together with the average lifetime of 366ps this yields a time constant of $1/k_1$=560ps for charge separation and of 1ns for the competing loss process (internal conversion). We propose that below 180K temperature independent charge separation to $P^+H^-_A$ via the superexchange mechanism dominates. From the energetics derived above, one can estimate superexchange enhanced charge separation to $P^+H^-_A$ in native RCs not be much faster than 330ps assuming that no significant changes of the couplings between P and B and between B and H occur in the mutant. This is a factor of 100 slower than the time constant indeed observed in *Rb. sphaeroides* R26, thus supporting the formation $P^+B^-_A$ in the first charge separation step.

M-AM-N7

DIELECTRIC AND ENERGETIC RELAXATIONS OF REACTION CENTER ((Ben McMahon, Joachim D. Müller, Ben Marino, Peter Debrunner, Colin Wraight, & G. Ulrich Nienhaus)) Departments of Physics, Biophysics & Plant Biology, University of Illinois at Urbana-Champaign, IL 61801.

Charge separation in photosynthetic reaction center from *Rhodobacter Sphaeroides* is followed by conformational changes of the protein which occur on many different timescales. An understanding of these changes is required to explain the temperature dependence of the nonexponential rates of electron transfer. We present the time and temperature dependence of these conformational changes from 5 K to 300 K. The time and temperature dependent distribution of energies of the Q^-P^+ state is determined by fitting the nonexponential $Q_a \rightarrow P$ electron transfer kinetics to the spin boson model. This technique allows us to measure relaxations on the timescale of the reaction (60 ms) and slower, and to see the extent of heterogeneity of reaction center conformations. Dielectric relaxations are observed by monitoring electrochromic shifts in the optical absorbance spectrum of the chromophores, and are seen to extend over more than 10 decades in time. A model of this electron transfer reaction is presented which treats distributions, relaxations and fluctuations of protein structure in a unified way.

M-AM-N8

A DIFFERENCE FT-IR INVESTIGATION OF REDOX-ACTIVE TYROSINES D AND Z OF PHOTOSYSTEM II. ((Sunyoung Kim, Ned van Eps, and Bridgette A. Barry)) University of Minnesota, Department of Biochemistry, St. Paul, MN 55108-1022

There are two redox active tyrosine radicals in photosystem II (PSII): tyrosine 161 (Z) of the D1 polypeptide which participates in water oxidation reactions, and tyrosine 160 (D) of the D2 polypeptide, to which no function has been assigned. Although tyrosine D is not directly involved in the electron transfer events that leads to water oxidation, it is in complex charge equilibrium with the water-oxidizing complex. It has been shown to participate in slow redox reactions. With both spinach and *Synechocystis* 6803 PSII preparations, we have utilized Fourier-transform infrared (FT-IR) spectroscopy to acquire the vibrational difference spectrum associated with the oxidation of tyrosine D and Z. Isotopic shifts from model compounds are used to assign vibrational lines in these difference spectra. To identify amino acid side chains in the vicinity of tyrosines Z and D, we are employing isotopic labeling, site directed mutagenesis, and pH studies.